Crawford School of Public Policy

CAMA

Centre for Applied Macroeconomic Analysis

How Do Macroaggregates and Income Distribution Interact Dynamically? A Novel Structural Mixed Autoregression with Aggregate and Functional Variables

CAMA Working Paper 7/2025
February 2025

Yoosoon Chang
Indiana University
Centre for Applied Macroeconomic Analysis, ANU

Soyoung Kim
Seoul National University
Financial Services Commission of South Korea

Joon Y. Park
Indiana University

Keywords

monetary policy, income distribution, re-distributive effects, structural vector autoregression, functional time series

JEL Classification

E52, D31, C32

Abstract

This paper investigates the interactions between macroeconomic aggregates and income distribution by developing a structural VAR model with functional variables. With this novel empirical approach, we are able to identify and analyze the effects of various shocks to the income distribution on macro aggregates, as well as the effects of macroeconomic shocks on the income distribution. Our main findings are as follows: First, contractionary monetary pol-icy shocks reduce income inequality when focusing solely on the redistributive effects, without considering the negative impact on aggregate income levels. This improvement is achieved by reducing the number of low and high-income families while increasing the proportion of middle-income families. However, when the aggregate income shift is also taken into account, contractionary monetary policy shocks worsen income inequality. Second, shocks to the income distribution have a substantial effect on output fluctuations. For example, income distribution shocks identified to maximize future output levels have a significant and persistent positive effect on output, contributing up to 30% at long horizons and over 50% for the lowest income percentiles. However, alternative income distribution shocks identified to minimize the future Gini index do not have any significant negative effects on output. This finding, combined with the positive effect of output-maximizing income distribution shocks on equality, suggests that properly designed redistributive policies are not subject to the often-claimed trade-off between growth and equality. Moreover, variations in income distribution are primarily explained by shocks to the income distribution itself, rather than by aggregate shocks, including monetary shocks. This highlights the need for redistributive policies to substantially alter the income distribution and reduce inequality.

Address for correspondence:

(E) cama.admin@anu.edu.au

ISSN 2206-0332

How Do Macroaggregates and Income Distribution Interact Dynamically? A Novel Structural Mixed Autoregression with Aggregate and Functional Variables*

Yoosoon Chang† Soyoung Kim‡ Joon Y. Park§

January 29, 2025

Abstract

This paper investigates the interactions between macroeconomic aggregates and income distribution by developing a structural VAR model with functional variables. With this novel empirical approach, we are able to identify and analyze the effects of various shocks to the income distribution on macro aggregates, as well as the effects of macroeconomic shocks on the income distribution. Our main findings are as follows: First, contractionary monetary policy shocks reduce income inequality when focusing solely on the redistributive effects, without considering the negative impact on aggregate income levels. This improvement is achieved by reducing the number of low and high-income families while increasing the proportion of middle-income families. However, when the aggregate income shift is also taken into account, contractionary monetary policy shocks worsen income inequality. Second, shocks to the income distribution have a substantial effect on output fluctuations. For example, income distribution shocks identified to maximize future output levels have a significant and persistent positive effect on output, contributing up to 30% at long horizons and over 50% for the lowest income percentiles. However, alternative income distribution shocks identified to minimize the future Gini index do not have any significant negative effects on output. This finding, combined with the positive effect of output-maximizing income distribution shocks on equality, suggests that properly designed redistributive policies are not subject to the often-claimed trade-off between growth and equality. Moreover, variations in income distribution are primarily explained by shocks to the income distribution itself, rather than by aggregate shocks, including monetary shocks. This highlights the need for redistributive policies to substantially alter the income distribution and reduce inequality.

JEL Classification: E52, D31, C32

Keywords and phrases: monetary policy, income distribution, re-distributive effects, structural vector autoregression, functional time series

*The authors are grateful for comments and suggestions from Jae W. Sim and Ippei Fujiwara, from seminar participants at the Federal Reserve Board, University of Maryland, Cleveland FED, Korea Development Institute, Samsung Global Research, University of Illinois, Keio University, University of Kansas, Fundação Getulio Vargas, University of Wisconsin, and from participants of the 2022 Women in Econometrics Conference, the 2022 Midwest Econometrics Group Meetings, the 2023 SNDE Symposium, the 2023 SETA, the 2023 Stone-SNU Conference on Mobility and Inequality. This paper is part of the research activities at the Centre for Applied Macroeconomics at the BI Norwegian Business School. Our special thanks go to Changsik Kim for his help with obtaining cross-sectional income data, and also to Sangmyung Ha for excellent research assistance. All remaining errors are our own.

†Indiana University & CAMA, yoosoon@iu.edu.

‡Seoul National University & Financial Services Commission of South Korea, soyoungkim@snu.ac.kr.

§Indiana University, joon@iu.edu.

1 Introduction

The relationship between income distribution and aggregate macro variables has been discussed for a long time. A classic example is the relation between inequality and growth that has been studied both theoretically and empirically for several decades (Aghion (2000), Alesina and Rodrik (1994), Banerjee and Newman (1993), Forbes (2000), Islam (1995), Kaldor (1957), Kuznets (1955), Persson and Tabellini (1994)). In addition, some studies analyzed the relation between income distribution and a specific macroeconomic policy. For example, the effects of monetary policy on income distribution are investigated by various researchers in recent years (Amberg et al. (2022), Coibion et al. (2017), Mumtaz and Theophilopoulou (2017), Furceri et al. (2018), Holm et al. (2020)).

This paper develops a novel empirical framework to analyze the interactions between income distribution and aggregate macro variables. To utilize the entire income distributions, we use their densities as a functional variable in our model, introducing a structural mixed autoregression (structural MAR or SMAR) that combines a VAR and a functional autoregression. Statistical analysis of functional observations has been quite active in recent years – see monographs by Bosq (2000) and Ramsay and Silverman (2005), as well as notable works by Hall and Horowitz (2007), Hyndman and Ullah (2007), Park and Qian (2012), Hörmann and Kokoszka (2012), Aue et al. (2015), Hörmann et al. (2015), among many others. Based on the theory developed in Y. Chang et al. (2021b), we represent our functional variable as a finite-dimensional vector, which is integrated into the usual VAR for aggregate variables while allowing for contemporaneous as well as dynamic interactions.

Our research is related to several strands of literature. From a methodological perspective, our MAR model contributes towards a recently emerging literature that analyses the distributional effects of macroeconomic shocks (e.g., Chang et al., 2021a, 2022b, Inoue and Rossi, 2021, Meeks and Monti, 2022). Much of this literature utilizes existing methods in functional data analysis (see, e.g., Bosq (2000) and Paparoditis (2018) for foundational theory, and Ramsay and Silverman (2005, 2007), and Kokoszka and Reimherr (2017) for a non-technical review. For instance, Meeks and Monti (2022) estimate a New Keynesian Phillips curve where the inflation expectations distribution is used as an exogenous covariate using a functional principal component regression. Kokoszka et al. (2018) analyses the cross-section of returns using a functional regression model, thereby complementing the Fama–French approach based on portfolio construction.[1] Chang et al. (2022b) take a different approach and consider a functional autoregression where the inflation expectations distribution can be impacted by aggregate economic shocks. Inoue and Rossi (2021) consider a VAR in which aggregate series can be impacted by functional shocks. In contrast to these approaches, our MAR considers the joint dynamics of functional variables and aggregate time series in response to both functional and conventional shocks in a single framework. In this sense, our approach is similar to

[1] While the cross-sectional approach to returns is undoubtedly valuable for financial research, our paper's contribution lies in utilizing the mixed autoregression to uncover deeper insights into the nuanced effects of oil market dynamics on stock market behavior over time.

M.Chang et al. (2021a), who specify a nonlinear state-space model to capture the joint dynamics of aggregate macroeconomic time series and the earnings distribution. The key difference is that we treat the functional variables as observable as opposed to unobservable states. This means that we do not require the use of simulation-based estimation or filtering methods, but instead we can directly estimate the model parameters by the simple ordinary least squares. By doing so, we can identify both aggregate and functional shocks, and produce functional as well as conventional impulse response functions. In addition, we also develop and apply commonly used tools for VAR analysis, such as forecast error variance decomposition and historical decomposition, in our VAR with both aggregate and functional variables.

The representation of a functional variable as a finite-dimensional vector requires the choice of a basis for the function space, and we use the functional principal component (FPC) basis which by construction most effectively represents the fluctuation of a functional variable. The choice of basis is critically important, and we show in Appendix A that the functional principal component basis works very effectively and better than other common bases as a finite-dimensional representation of the income distribution. In a study conducted contemporaneously but independently of our research, M. Chang et al. (2022a) consider a state space model involving probability density as a functional variable. They specify that the loadings of a cubic spline basis employed to approximate density functions evolve as a VAR jointly with other scalar variables, and use a Bayesian approach to estimate the model by introducing an ad hoc relationship between the loadings obtained from approximated density functions and the density functions themselves.[2] In contrast, we let our functional variable defined as probability density be directly observed up to a negligible estimation error and use the data dependent functional principal component basis to approximate and include it in our VAR. As we show in Appendix A, it is more effective and precise to use our functional principal component basis to represent functional fluctuations in our model, rather than any other fixed basis including a cubic spline basis.[3]

To demonstrate usefulness of our framework, we construct a VAR model with functional variables and key macro variables such as output, the price level, and a monetary policy indicator. We first identify monetary policy shocks in the model by using a conventional method, e.g., Christiano et al. (1999), Christiano et al. (2005), and investigate the effects of monetary policy shocks on income distribution. Their influence is more nuanced than simply a mean shift or changes in dispersion. Contractionary monetary policy shocks worsen income inequality when the negative aggregate income shift is taken into account. However, when the aggregate income is preserved,

[2]They use log-density, while we use density itself, as a functional variable. An observed density is used to fit the data after demeaning, so we do not need to impose any non-negativity or unit integral restriction on density in our analysis. In the function space we analyze density, moments are defined nicely as inner products of density with polynomials. This allows us to compare the results using entire distribution with those relying only on moments. Moreover, the effective support of our observed density changes over time, and the log-transformation of our density is expected to unduly magnify the importance of its sparsely observed region.

[3]The existing theory for the finite-dimensional representation of a functional variable is only applicable for the principal component basis. To the best of the authors' knowledge, there is no existing theory showing the validity of the use of a fixed basis. Indeed, if the functional variable is nonstationary, the approximation based on any fixed basis fails as discussed in Chang et al. (2016).

contractionary monetary policy shocks have a positive re-distributive effect improving income inequality by reducing the number of low and high income people while increasing the number of middle income people. On the other hand, we also find that the contribution of monetary policy shocks to income distribution variation is relatively small, albeit significant. We will not find these results from the data unless we consider the entire income distribution together with aggregate variables. Modeling the whole distribution is therefore critical.[4]

We also identify two types of hypothetical structural shocks to income distributions – hypothetical growth-targeted and equity-targeted redistributive policy shocks. The former is identified as the shock to income distribution that has the largest positive effect on aggregate output ten years after the impact while the latter is identified as the income distribution shock that minimizes the Gini index ten years after the impact date. First, we find that hypothetical growth-targeted redistributive policy shocks have a huge and persistent positive effect on output fluctuations. The contribution of such shocks to the output fluctuations is approximately 30% at long horizons and over 50% for low-income percentiles. This finding suggests that properly-targeted redistributive policy shocks potentially have huge effects on output fluctuations. Second, we find that hypothetical growth-targeted redistributive policy shocks decrease the inequality substantially and persistently while hypothetical equity-targeted redistributive policy shocks do not have negative effects on output. This finding suggests that properly aimed redistributive policies are not subject to the often-claimed trade-off between growth and equality. Third, we find that variations in income distribution are primarily driven by shocks to the income distribution itself, rather than by aggregate shocks, including monetary policy shocks. This suggests that redistributive policies are necessary to significantly alter the income distribution and improve inequality.

The following section presents a detailed discussion of the data. A technical discussion of the MAR is the main focus of Section 3, which a general reader not interested in the technical details may skip. In Section 4, we discuss shocks to income distribution and our identification strategy for those shocks. Section 5 presents the main empirical results of the paper. Specifically, we present counterfactual responses from hypothetical unit impulses – i.e., impulse responses functions of aggregate economic variables and response surfaces of the income distribution that allow us to estimate effects from both aggregate shocks and income distribution shocks over the sample. Section 6 concludes. Appendices contain comparisons of the functional principal component basis described in Section 3 with alternative bases, alternate income distribution shocks, comparisons of the results of the SMAR with an SVAR that uses Gini index in place of the income distribution, robustness checks and other ancillary and supporting results.

[4] Amberg et al. (2022) found a similar result by using Swedish administrative individual-level data by investigating the effects on each quantile one-by-one. Compared to such a study, the current study provides a method to estimate the results on any properties of distribution in a single empirical framework.

Figure 1: Aggregate Macro Variables

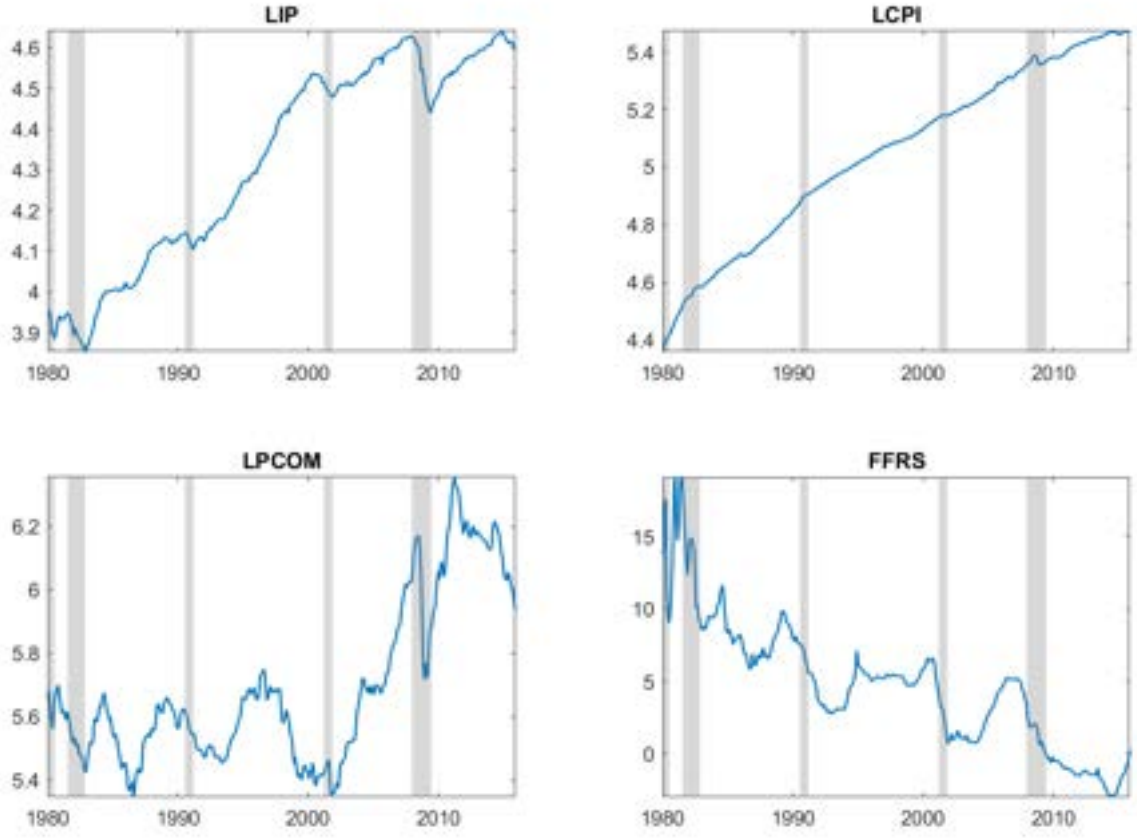

Notes: Plotted are log levels of Industrial Production (IP), Consumer Price Index (CPI) and commodity Price Index (PCOM), and Shadow Federal Funds Rates (FFRS). US recessions shaded in gray for reference.

2 Data

2.1 Aggregate Macro Variables

Figure 1 shows the aggregate variables that we use to represent macro economic activities. Plotted are the monthly observations, from January 1980 to December 2015, of the log levels of Industrial Production (IP), Consumer Price Index (CPI) and commodity Price Index (PCOM), and Shadow Federal Funds Rates (FFRS). We use shadow Federal Funds Rates to represent monetary policy stance near or at the zero lower bound[5].

The Figure 2 shows the Gini index at monthly frequency, as a measure of aggregate inequality. The blue line shows the time series of Gini index obtained from FRED, and the red line show the Gini index measured from disaggregate micro level data from the Consumer Expenditure (CEX) Survey, over the same sample period, January 1980 - December 2015, which will be explained in Section 2.2. Though they do not exactly overlap, they are highly correlated with a correlation coefficient 0.9984.

[5]We use shadow Federal Funds Rates constructed by Wu and Xia (2016).

Figure 2: Gini Index of Aggregate Inequality

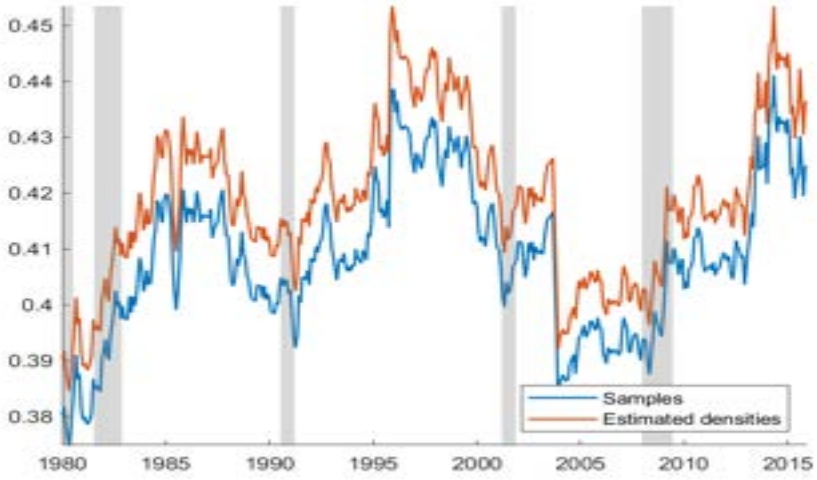

Notes: The blue line shows the time series of Gini index obtained from FRED, and the red line show the Gini index measured from disaggregate micro level data from the Consumer Expenditure Survey.

2.2 Disaggregate Income Data

We use the micro-level income data from Consumer Expenditure (CEX) Survey conducted by Bureau of Labor Statistics to construct time series of income distributions.[6] Specifically, we obtain monthly time series of cross-sectional income data from the CEX survey conducted by Bureau of Labor Statistics following Krueger and Perri (2006) which uses using the U.S. households monthly income data from the CEX survey series during the period from January 1980 to December 2015. The data span, from January 1980 to December 2015, is chosen primarily because we were able to obtain the cross-sectional income data at monthly frequency from the quarterly CEX survey. Details of the CEX survey income data and the construction income densities from them follow.

We obtain the time-series of cross-sectional income distributions using the U.S. households monthly income data obtained from the Consumer Expenditure Survey series[7]. The CEX survey consists of two surveys, Quarterly Interview Survey and Diary Survey, that provide continuous flow of information on buying habits, expenditures, income, and consumer unit (families and single consumers) characteristics of the US customers. The U.S. Census Bureau carries out the survey under contract with the Bureau of Labor Statistics. The CEX Survey is the only federal survey that provides information on complete range of consumer expenditures and incomes.

This data set spans 36 years and provides 432 monthly cross-sectional household observations with the number of households for each month ranging from 1,825 to 5,663. During the sample period, each household is included in the survey at most five times, and therefore the CEX survey provides pseudo panel data. In order to construct monthly household income, we follow the defini-

[6] Krueger and Perri (2006) use the Consumer Expenditure Survey (CEX) data to construct their monthly income data. Specifically, they define income as the sum of labor income (wages and salaries) and capital income (interest, dividends, and rents). They do not explicitly mention whether capital gains are included in their definition of income.

[7] It is formerly called the Survey of Consumer Expenditures

tions of income given by Krueger and Perri (2006), and aggregate the monthly values provided in Universal Classification Code (UCC) level for each month and year. See Krueger and Perri (2006) for detailed information. We then deflate the nominal income values by the monthly CPI for all urban households constructed with a base year which varies among 1982, 1983 and 1984. The CPI data used here are provided by the Bureau of Labor Statistics.

The CEX uses topcoding to change the values of the original data when they exceed some prescribed critical values, which are calculated for each variable containing sensitive information in accordance with the guidelines provided by the Census Disclosure Review Board. The critical values may vary year to year. Each observation that exceeds the critical value is replaced with a topcode value that represents the mean of all observations whose values exceed the critical value. Therefore, topcode values may also change over time and be applied at a different start point. In our analysis we drop all topcoded values of household income.[8] Following the sample selection criteria given in Krueger and Perri (2006), we exclude observations with possible measurement error or inconsistency problem.[9]

Figure 3 shows, on the left panel, the monthly time series of the densities of cross-sectionally demeaned incomes. At each time period, we use cross-sectionally demeaned monthly disaggregate income data to estimate the income density centered at zero, and track its mean using the monthly time series of aggregate income level.[10] The right panel shows the same densities of cross-sectionally demeaned incomes which are also demeaned over time. The temporally demeaned densities magnify the fluctuations in income distributions, which in turn allow us to focus on the distributional aspect of the income distribution.

3 Model and Methodology

In this section, we introduce the model and methodology used to study the interaction between the macroeconomic aggregates and income distributions. Our empirical analysis is based on a mixed autoregression (MAR), a mixture of vector autoregression and functional autoregression, which allow us to include functional variables, such as income distributions, as well as aggregate variables representing economic activities and policy variables in the model. We now discuss the MAR in detail and explain how to estimate it effectively.

[8] Dropping top-coded observations based on time-varying topcode values may potentially create some problems, for example when the number of excluded samples change over time. This is how Krueger and Perri (2006) handle this issue. Since we do not have a better alternate way of dealing with topcoded data, we follow their approach here.

[9] Krueger and Perri (2006) excludes all households that satisfy one of the eight exclusion criteria they provide in Appendix of their paper. We select the households with only the first five exclusion criteria to be able to include the households with weekly wages below half of the minimum wage, households classified as rural, and those households that did not complete the full set of four interviews but have complete income responses and have been interviewed five times. We relax these two exclusion restrictions to increase the number of observations across all income ranges each month. If we only consider households that meet all eight exclusion criteria, we have too few observations on the lower end of the income distribution for some periods. This leads to too many empty bins, which in turn makes our nonparametric density estimation more challenging.

[10] For kernel density estimation, we exclude the outliers on both ends at 1% for income distribution. Even after removing topcoded observations, the CEX income data still have outliers enough to cause the aforementioned empty bin problems. This is why we remove 0.5% of the observations at both left and right ends of the distribution.

Figure 3: Time Series of Income Distributions

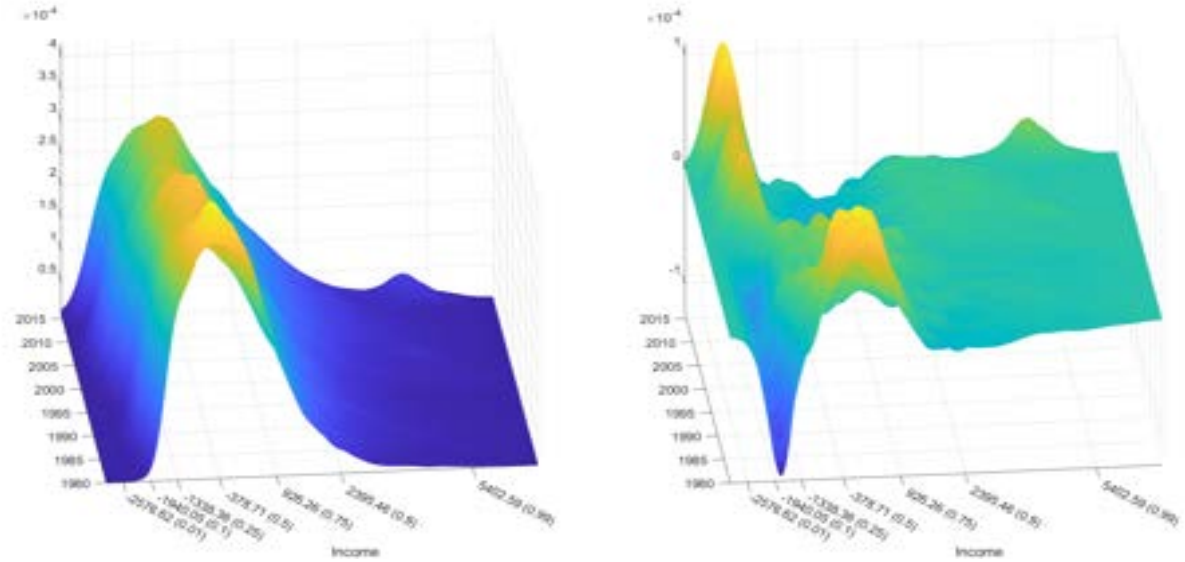

Notes: Left panel shows the monthly time series of the cross-sectionally demeaned densities estimated using the disaggregate income data from Consumer Expenditure Survey. Right panel shows the same densities demeaned over time. The horizontal income axis displays the quantile values of the demeaned income distribution at 1%, 10%, 25%, 50%, 75%, 90% and 99%. For example, 2395.46 (0.9) indicates the quantile value at the 90% level.

3.1 MAR

We denote by (x_t) the four-dimensional time series

$$x_t = (IP_t - \overline{IP}, CPI_t - \overline{CPI}, PCOM_t - \overline{PCOM}, FFRS_t - \overline{FFRS})'$$

defined for each t with the aggregate series (IP_t), (CPI_t), $(PCOM_t)$ and $(FFRS_t)$ introduced in Section 2 less their respective temporal means $\overline{IP}$, $\overline{CPI}$, $\overline{PCOM}$, and $\overline{FFRS}$. We denote by (f_t) the functional time series given by the cross-sectionally and temporally demeaned densities of the income distributions shown in the right panel of Figure 3.[11] Note that (f_t) represents purely distributional changes over time net of aggregate income fluctuations. $FFRS$ is included in the model to represent monetary policy stance. IP and CPI are the most important aggregate variables to represent macroeconomic conditions. $PCOM$ is included to represent inflationary pressure to which monetary policy reacts. See Sims (1992) and Christiano et al. (1999).

We then define (z_t) as $z_t = (x_t, f_t)$, which is assumed to follow an MAR given by

$$z_t = Az_{t-1} + \varepsilon_t, \tag{1}$$

where A is a bounded linear operator and (ε_t) is a functional error to be specified below. Let ℓ denote the number of aggregate variables, which is four in our model. Note that our MAR is defined

[11] In the paper, we use the density functions to represent income distributions. There are, of course, many other ways of representing income distributions. See Appendix D for detailed discussions on other choices and their relative advantages and disadvantages.

without the constant term. This is because we assume that all our variables, both the aggregate variables (x_t) and the functional variable (f_t), are demeaned a priori. This convention will be made throughout the paper. To define our MAR more precisely, we further let (f_t) be given as random elements taking values in a Hilbert space

$$H = \left\{ f : K \to R \,\middle|\, \int f(r)\, dr = 0, \int f(r)^2 dr < \infty \right\},$$

where K is a bounded subset of R and integrals are defined over K. Clearly, H is a Hilbert space, as a subspace of the usual Hilbert space of square integrable functions on K.

Now we may define (z_t) more formally as a time series of random elements in $R^\ell \oplus H$, which itself is a Hilbert space defined as the direct sum of R^ℓ and H. The new extended Hilbert space $R^\ell \oplus H$ is endowed with the inner product

$$\langle z, w \rangle = \langle x, y \rangle + \langle f, g \rangle$$

for all $z = (x, f)$ and $w = (y, g)$ with $x, y \in R^\ell$ and $f, g \in H$, where $\langle \cdot, \cdot \rangle$ is used as a generic notation for the inner product in R^ℓ, H, or $R^\ell \oplus H$ for notational brevity. The standard inner products in R^ℓ and H are given by

$$\langle x, y \rangle = x'y \quad \text{and} \quad \langle f, g \rangle = \int f(r) g(r) dr$$

respectively for all $x, y \in R^\ell$ and $f, g \in H$. We also use the same generic notation $\| \cdot \|$ for the norm induced by the inner product $\langle \cdot, \cdot \rangle$ in R^ℓ, H or $R^\ell \oplus H$, and therefore, $\|z\|^2 = \langle z, z \rangle = \langle x, x \rangle + \langle f, f \rangle = \|x\|^2 + \|f\|^2$ for all $z = (x, f) \in R^\ell \oplus H$.

We also need to introduce the notion of tensor product in H and $R^\ell \oplus H$. For $f, g \in H$, the tensor product $f \otimes g$ is defined as a linear operator on H satisfying

$$(f \otimes g)h = \langle h, g \rangle f$$

for all $h \in H$. We may define the tensor product $z \otimes w$ of $z = (x, f)$ and $w = (y, g)$ similarly as a linear operator on $R^\ell \oplus H$ given by

$$(z \otimes w)v = \langle v, w \rangle z = \big(c'y + \langle h, g \rangle\big)(x, f)$$

for all $v = (c, h) \in R^\ell \oplus H$. When $H = R^m$ and H becomes finite-dimensional, we have $f \otimes g = fg'$ and $z \otimes w = zw'$, and they become outer products of two vectors, in contrast to their inner products given by $\langle f, g \rangle = f'g$ and $\langle z, w \rangle = z'w$.

The autoregressive operator A in (1) is an element in the space $L(R^\ell \oplus H)$ of linear operators on $R^\ell \oplus H$ and may be written more explicitly as the matrix of operators

$$A = \begin{pmatrix} A_{RR} & A_{RH} \\ A_{HR} & A_{HH} \end{pmatrix},$$

where $A_{RR} : R^\ell \to R^\ell$, $A_{RH} : H \to R^\ell$, $A_{HR} : R^\ell \to H$, and $A_{HH} : H \to H$. If we let $w = Az$ for $z = (x, f)'$ and $w = (y, g)'$ with $x, y \in R^\ell$ and $f, g \in H$, we may represent A_{RR} as an $\ell \times \ell$ matrix such that $y = A_{RR}x$,

$$A_{RH} = \begin{pmatrix} \langle h_1, \cdot \rangle \\ \vdots \\ \langle h_\ell, \cdot \rangle \end{pmatrix} \quad \text{such that} \quad y = A_{RH} f = \begin{pmatrix} \langle h_1, f \rangle \\ \vdots \\ \langle h_\ell, f \rangle \end{pmatrix},$$

$$A_{HR} = \begin{pmatrix} k_1 & \cdots & k_\ell \end{pmatrix} \quad \text{such that} \quad g = A_{HR} x = \begin{pmatrix} k_1 & \cdots & k_\ell \end{pmatrix} x$$

for some $h_1, \ldots, h_\ell \in H$ and $k_1, \ldots, k_\ell \in H$, and A_{HH} is a bounded linear operator on H such that $g = A_{HH} f$.

The functional error (ε_t) in (1) is assumed to be white noise, such that we have $\mathbb{E}(\varepsilon_t) = 0$ and

$$\mathbb{E}(\varepsilon_t \otimes \varepsilon_s) = \begin{cases} \Omega & \text{for} \quad t = s \\ 0 & \quad\quad\; t \neq s \end{cases},$$

where $\mathbb{E}(\varepsilon_t \otimes \varepsilon_s)$ is the covariance operator of ε_t and ε_s defined as an operator on $R^\ell \oplus H$ such that $\langle z, \mathbb{E}(\varepsilon_t \otimes \varepsilon_s) w \rangle = \mathbb{E}\langle z, \varepsilon_t \rangle \langle w, \varepsilon_s \rangle$ for all $z, w \in R^\ell \oplus H$. In short, (ε_t) is a serially uncorrelated functional time series with mean zero and a common variance operator, which is simply a vector series of white noise in the finite-dimensional case.

3.2 Finite Dimensional Approximation and VAR Representation

In functional data analysis, functions are represented as finite-dimensional vectors in various ways. We encompass those approaches within a single framework, so that an approach to represent functions may be interpreted as a basis and truncation number. For instance, functions represented by long vectors consisting of their values in the ordinate corresponding to a selected grid of values in the abscissa may obviously be interpreted as their finite-dimensional representations using the basis (v_i) given by $v_i = \delta_{r_i}$, where δ_r is the Dirac delta function at $r \in R$. More generally, let (v_i) be an orthonormal basis of $R^\ell \oplus H$, and write $z \in R^\ell \oplus H$ as

$$z = \sum_{i=1}^{\infty} \langle v_i, z \rangle v_i,$$

which is approximated by

$$z \approx \sum_{i=1}^{n} \langle v_i, z \rangle v_i \tag{2}$$

for an appropriately chosen truncation number n.

Once we fix an orthonormal basis (v_i) of $R^\ell \oplus H$, we may represent the MAR in (1) as a finite-dimensional VAR. Our VAR representation closely follows that of Y. Chang et al. (2021b) and extends their VAR representation of functional autoregressions for functional time series (f_t) only

to mixed autoregressions for (z_t) that include ℓ-dimensional aggregate variables in addition to the functional variable (f_t).[12] Let $R^\ell \oplus V$ be the subspace of $R^\ell \oplus H$ spanned by a sub-basis $(v_i)_{i=1}^n$, and denote by P the Hilbert space projection on the subspace $R^\ell \oplus V$ so that $Pz = \sum_{i=1}^n \langle v_i, z\rangle v_i$. We approximate the MAR in (1) as

$$z_t = APz_{t-1} + A(1-P)z_{t-1} + \varepsilon_t \approx APz_{t-1} + \varepsilon_t, \tag{3}$$

where $1-P$ is an operator on $R^\ell \oplus H$ defined as $(1-P)z = z - Pz$ for all $z \in R^\ell \oplus H$. The approximation error $(A(1-P)z_{t-1})$ is asymptotically negligible under suitable regularity conditions and if we set $n \to \infty$ as $T \to \infty$ at an appropriate rate. The required conditions are not very stringent and expected to hold generally.

We now explain how to represent the approximate MAR in equation (3) as a finite-dimensional VAR. Define a mapping

$$\pi : z \mapsto \begin{pmatrix} \langle v_1, z\rangle \\ \vdots \\ \langle v_n, z\rangle \end{pmatrix} \tag{4}$$

and write

$$\pi(z) = [z] \tag{5}$$

for any $z \in R^\ell \oplus H$. Accordingly, let

$$\pi : A \mapsto \begin{pmatrix} \langle v_1, Av_1\rangle & \cdots & \langle v_1, Av_n\rangle \\ \vdots & \vdots & \vdots \\ \langle v_n, Av_1\rangle & \cdots & \langle v_n, Av_n\rangle \end{pmatrix} \tag{6}$$

be the corresponding mapping on A given by

$$\pi(A) = [A] \tag{7}$$

for any $A \in L(R^\ell \oplus H)$.

Using our notation in (5) and (7), we may approximate the MAR in (1) as

$$[z_t] = [A][z_{t-1}] + [\varepsilon_t], \tag{8}$$

a conventional n-dimensional VAR, which we refer to as the *approximate VAR* to our MAR. The approximate VAR in (8) is readily derived from the approximate MAR in (3), since we have $[APz] = [A][z]$ for any $z \in R^\ell \oplus H$ and $A \in L(R^\ell \oplus H)$, and $[z+w] = [z] + [w]$ for all $z, w \in R^\ell \oplus H$. The approximate MAR in (3) is therefore equivalent to the approximate VAR in (8), which implies that

[12] Our MAR extends the functional autoregressive model in Chang et al. (2021b) by adding aggregate time series. However, their theory is directly applicable for our MAR, since $R^\ell \oplus H$ may be viewed as an extended Hilbert space in a trivial sense. we use the approach developed by Chang et al. (2021b), which has some obvious advantages over other existing methods available for functional data analysis. This will be shown subsequently.

the original MAR in (1) may be analyzed by the approximate VAR in (8) for large n and T.

Our empirical analysis and statistical inference are based on the approximate VAR in (8). The validity of our procedure may be readily established following Y. Chang et al. (2021b), who show that the usual VAR methodologies and their sample and bootstrap asymptotic theories are generally applicable for the structural analysis of functional autoregressions based on approximate VARs like the one given in (8).

Although the π's in (4) and (6) are defined for any $z \in R^\ell \oplus H$ and $A \in L(R^\ell \oplus H)$, we interpret them as their restricted versions on $R^\ell \oplus V$ and $L(R^\ell \oplus V)$, respectively, whenever necessary. The restricted versions of π's are one-to-one, so that their inverses exist and are well defined. We may indeed easily show that

$$\pi^{-1}\big([z]\big) = Pz \quad \text{and} \quad \pi^{-1}\big([A]\big) = PAP.$$

Consequently, from the estimate $\widehat{[A]}$ of the autoregressive coefficient matrix $[A]$ and the fitted values $\big(\widehat{[\varepsilon_t]}\big)$ of the residuals $\big([\varepsilon_t]\big)$ in (8), we may easily obtain the corresponding estimate $\widehat{A}$ and the fitted functional residuals $\big(\widehat{\varepsilon}_t\big)$ as a linear operator on $R^\ell \oplus V$ and a functional time series taking values in $R^\ell \oplus V$ and hence in $R^\ell \oplus H$.

In fact, the π's in (4) and (6) are not just one-to-one mappings. They are *isometries*. For π in (4), we have

$$\|z\|^2 = x'x + \|f\|^2 = x'x + \sum_{i=1}^{m} \langle v_i, f\rangle^2 = \big\|[z]\big\|^2$$

for any $z = (x, f) \in R^\ell \oplus V$, where as before we use the generic notation $\|\cdot\|$ for the norms in $R^\ell \oplus V$ and R^n. Moreover, we have

$$\|\!|A|\!\|^2 = \operatorname{trace}(A'A) = \operatorname{trace}\big([A]'[A]\big) = \big\|\!\big|[A]\big|\!\big\|^2$$

for any Hilbert-Schmidt operator A on $R^\ell \oplus V$, where A' is the adjoint of the operator A, $[A]'$ is the transpose of the n-dimensional matrix $[A]$, and $\|\!|A|\!\|$ and $\|\!|[A]|\!\|$ denote the Hilbert-Schmidt norm of A and the Frobenius norm of $[A]$, respectively.

3.3 Choice of Basis: Non-Asymptotic Analysis

The VAR representation in (8) may be obtained for any orthonormal basis (v_i) of $R^\ell \oplus H$. The effectiveness of the resulting approximation, however, depends crucially on the choice of basis. We denote by (v_i^*) our particular choice of basis of $R^\ell \oplus H$, and show that it has some optimality properties and yields an efficient estimate of the functional operator A. To introduce (v_i^*) explicitly, we define $R^\ell \oplus H$ more explicitly as the Hilbert space generated by a basis defined as a union of a basis in R^ℓ and a basis in H. Specifically, we let $v_i^* = e_i$ for $i = 1, \ldots, \ell$, where (e_i) is the standard basis for R^ℓ, so that

$$x_t = \big(\langle v_1^*, z_t\rangle, \ldots, \langle v_\ell^*, z_t\rangle\big)'$$

for all t. Furthermore, define $v^*_{\ell+i} = e_i(\Gamma)$ for $i = 1, 2, \ldots$, where $e_i(\Gamma)$ denotes the eigenfunction associated with the i-th largest eigenvalue of the sample variance operator of (f_t)

$$\Gamma = \frac{1}{T}\sum_{t=1}^{T}(f_t \otimes f_t). \tag{9}$$

Note that $(e_i(\Gamma))$ is the (normalized) functional principal component (FPC) of (f_t), which is widely used in the functional data analysis literature including Bosq (2000), Ramsay and Silverman (2005), Hall and Horowitz (2007), and Park and Qian (2012), among many others. In the paper, we will refer to (v^*_i) as the *FPC basis*.[13] Our empirical analysis in the paper relies mainly on the VAR in (8) obtained using this basis.

Subsequently, we denote by $R^\ell \oplus V^*$ the subspace of $R^\ell \oplus H$ spanned by the sub-basis $(v^*_i)_{i=1}^n$, and by P^* the Hilbert space projection on $R^\ell \oplus V^*$. For comparison, we let $(v_i)_{i=1}^n$ be an arbitrary sub-basis in $R^\ell \oplus H$ with $v_i = e_i$ for $i = 1, \ldots, \ell$ spanning $R^\ell \oplus V$ and P be the Hilbert space projection on $R^\ell \oplus V$, so that the Hilbert space projection P^* on $R^\ell \oplus V^*$ spanned by $(v^*_i)_{i=1}^n$ may be regarded as a special case. Note that $(v^*_i)_{i=1}^\ell \equiv (v_i)_{i=1}^\ell$, since they both use the the standard basis for R^ℓ. We also let Π be the Hilbert space projection on V spanned by a sub-basis $(v_{\ell+i})_{i=1}^m$ in H with $m = n - \ell$, with Π^* as a special case when $(v^*_{\ell+i})_{i=1}^m$ is used as a sub-basis.

As in Y. Chang et al. (2021b), we define the functional R-squared as

$$\mathrm{FR}^2 = \frac{\sum_{t=1}^T \|\Pi f_t\|^2}{\sum_{t=1}^T \|f_t\|^2}$$

which represents the proportion of the total variation of (f_t) explained by its projection on V spanned by an arbitrary sub-basis $(v_{\ell+i})_{i=1}^m$. It follows that $\mathrm{FR}^2_* \geqslant \mathrm{FR}^2$, where we denote by FR^2_* the functional R-squared for the projection of (f_t) on V^* spanned by the sub-basis $(v^*_{\ell+i})_{i=1}^m$, which implies that the sub-basis $(v^*_{\ell+i})_{i=1}^m$ most effectively represents the temporal fluctuations of $(f_t)_{t=1}^T$. Because $\|Pz_t\|^2 = x'x + \|\Pi f_t\|^2$, we may also deduce that the basis $(v^*_i)_{i=1}^n$ represents the variations of (z_t) over time more effectively than any other basis $(v_i)_{i=1}^n$.

There are more advantages of choosing the FPC basis $(v^*_i)_{i=1}^n$ over any other basis $(v_i)_{i=1}^n$. The approximation of A given by P^*AP^* restricts A to the subspace $R^\ell \oplus V^*$ of $R^\ell \oplus H$, where (z_t) has the largest variation and consequently A is most strongly identified. In this sense, the basis (v^*_i) provides the most effective approximation of A among its alternate restrictions on an n-dimensional subspace $R^\ell \oplus V$ of $R^\ell \oplus H$. Finally, the use of $(v^*_i)_{i=1}^n$ makes the approximation error minimized, which means that we estimate the error variance most precisely if it is used.

Table A.1 and A.2 in Appendix A.2 report FR^2 statistics calculated using the FPC basis discussed here, as well as three other alternate basis, a histogram basis, a quantile basis, and an

[13] If a function is represented as a long vector, as is usually done in functional data analysis, the FPCA reduces to the principal component analysis (PCA). In our analysis, we represent the estimated densities of demeaned income levels as 1024-dimensional vectors to obtain FPCs. The dimension 1024 is non-consequential and does not affect our results unless it is set to be too small.

orthonormalized moment basis defined in Appendix A, for different values of the dimension m of the finite-dimensional approximation to (f_t). It is clear from the table that the FPC basis does a much better job of capturing variations in the demeaned income distributions, with just three basis functions capturing 96%. In contrast, the first three functions of the histogram basis capture 24%, the first three of the quantile basis capture 42%, and the first three moment basis capture only 17%. In particular, the mean of income distribution (first moment) captures only 9% of the variation in the income distribution. These results on FR^2 provide strong finite sample evidence for the superiority of the FPC basis over the others for any given number of bases.

We also present the integrated variances (IVARs) of the estimated A as further evidence in Table A.2 and Figure A.3. See Appendix A.3 for a detailed explanation of the IVAR. The IVARs of the three alternate basis are huge and grow rapidly as the number of bases m increases. In stark contrast, the IVARs of our FPC basis are much small and grow very slowly. Among the three alternate basis, the quantile basis has the smallest IVARs, which are still much greater than those of the FPC basis.

3.4 Reduced-Form Model Specification

We may generalize the first-order MAR in (1) to a p-th order MAR for any finite p, and consider

$$\begin{aligned} z_t &= A_1 z_{t-1} + \cdots + A_p z_{t-p} + \varepsilon_t \\ &= A_1 P z_{t-1} + \cdots + A_p P z_{t-p} + A_1(1-P) z_{t-1} + \cdots + A_p(1-P) z_{t-p} + \varepsilon_t \\ &\approx A_1 P z_{t-1} + \cdots + A_p P z_{t-p} + \varepsilon_t, \end{aligned} \tag{10}$$

whose corresponding approximate p-th order VAR is given by[14]

$$(z_t) \approx (A_1)(z_{t-1}) + \cdots + (A_p)(z_{t-p}) + (\varepsilon_t). \tag{11}$$

As is well known, a p-th order MAR and corresponding p-th order approximate VAR can be re-defined as a first-order MAR and corresponding approximate first-order approximate VAR in an extended space. Therefore, our interpretations and representations of the first-order MAR and the corresponding approximate VAR are applicable for p-th order MAR models.

Once we fix the truncation number $m = n - \ell$ and represent the functional variable in MAR as an m-dimensional vector, we may use standard lag selection procedures such as AIC and BIC to select the order of the approximate VAR, and ultimately the order of the underlying MAR. For our data, both the AIC and BIC select two lags with the choice of $m = 3$, so we set $p = 2$ for the subsequent empirical analysis.

[14] If FPCs are defined as factors, our VAR (8) may simply be viewed as a FAVAR. However, the factors in the VAR formulation of our approximated MAR are given by the inner products of our functional observations with their eigenfunctions, which are very different from the usual factors constructed from a panel and used in a FAVAR.

4 Identification

For our empirical study, we analyze a second-order MAR through the corresponding second-order approximate VAR in (11) with $p = 2$, which is given by

$$(z_t) \approx (A_1)(z_{t-1}) + (A_2)(z_{t-2}) + (\varepsilon_t). \tag{12}$$

For the subsequent structural analysis of our reduced-form approximate VAR (12), we write the error term as

$$(\varepsilon_t) = \left(\varepsilon_t^{IP}, \varepsilon_t^{CPI}, \varepsilon_t^{PCOM}, \varepsilon_t^{FFRS}, \varepsilon_t^{DIN_1}, \varepsilon_t^{DIN_2}, \varepsilon_t^{DIN_3}\right) \tag{13}$$

where (ε_t^{IP}), (ε_t^{CPI}), (ε_t^{PCOM}) and (ε_t^{FFRS}) are innovations to the aggregate variables (IP_t), (CPI_t), $(PCOM_t)$, and $(FFRS_t)$, respectively, and $(\varepsilon_t^{DIN_1})$, $(\varepsilon_t^{DIN_2})$ and $(\varepsilon_t^{DIN_3})$ are innovations to the three leading FPC loadings of the demeaned income distributions in our approximate VAR (12).

4.1 Structural Shocks

We define structural shocks (e_t) as

$$(\varepsilon_t) = Be_t \tag{14}$$

with their matrix coefficient B, which is also referred as the at-impact response matrix. The shocks (e_t) are usual structural shocks to be defined and identified. To identify the shocks in (14) of the approximate SVAR to our MAR, we introduce $m = 3$ functional shocks $(e_t^{DIN_1}, e_t^{DIN_2}, e_t^{DIN_3})$. Aggregate shocks (e_t^{IP}), (e_t^{CPI}), (e_t^{PCOM}), and (e_t^{FFRS}) are identified recursively à la Sims (1980), where contemporaneously more exogenous shocks are listed first. Following Christiano et al. (1996) and Christiano et al. (1999), (e_t^{FFRS}) is identified as monetary policy shocks.[15] We interpret these four aggregate shocks simply as unexpected changes in aggregate output, unexpected changes in aggregate prices, unexpected changes in commodity prices and unexpected changes in monetary policy, respectively. Three structural functional shocks $(e_t^{DIN_1})$, $(e_t^{DIN_2})$, $(e_t^{DIN_3})$ are also recursively identified. The recursive structure we impose for the three functional shocks is purely for convenience and strictly inconsequential. Moreover, we assume that aggregate shocks, including monetary policy shocks, are contemporaneously exogenous to three functional shocks. In this way, the functional shocks can be defined as pure functional shocks that are orthogonal to the aggregate shocks.

We let

$$e_t = \left(e_t^{IP}, e_t^{CPI}, e_t^{PCOM}, e_t^{DIN_1}, e_t^{DIN_2}, e_t^{DIN_3}\right), \tag{15}$$

which consists of four aggregate shocks and three functional shocks. Under our identifying restric-

[15] In this model, monetary policy authority is assumed to set monetary policy stance after observing current and lagged values of IP and CPI, two most important target variables of monetary policy, and $PCOM$, a variable representing inflationary pressure. Other aggregate shocks do not have clear structural interpretations.

tions, the matrix B is identified from the relationship

$$BB' = \Sigma,$$

where Σ is the estimated covariance matrix of (Be_t), such that $Be_t = (\varepsilon_t)$, for $t = 1, \ldots, T$.

We estimate the at-impact response matrix B, and use it to compute the aggregate structural shocks, (e_t^{IP}), (e_t^{CPI}), (e_t^{PCOM}), and (e_t^{FFRS}), and functional shocks, $(e_t^{DIN_1})$, $(e_t^{DIN_2})$ and $(e_t^{DIN_3})$.

The recursively identified functional shocks in (14), $(e_t^{DIN_1})$, $(e_t^{DIN_2})$ and $(e_t^{DIN_3})$, are not economically interpretable, and hence not a structural shock until we make meaningfully interpretable restrictions. For this reason, we may call them as semi-structural shocks. We subsequently use these estimated semi-structural functional shocks to identity an interpretable income distribution shock reflecting unexpected changes in income distributions. We illustrate how we may construct an interpretable structural income distribution shock below in 4.4.

4.2 Impulse Responses and Functional Impulse Responses

Each column of the coefficient matrix B provides at-impact responses of aggregate variables x_t and the m-dimensional vector (f_t) representing the demeaned density f_t of the income distribution to the corresponding recursively identified shock. Recall that (f) includes the loadings of the three leading leading FPCs of f_t. The responses of the ℓ aggregate variables in x_t and the m functional principal components (FPC) loadings in (f_t) to each aggregate shock in $(e_t^{IP}, e_t^{CPI}, e_t^{PCOM}, e_t^{FFRS})$ are obtained and interpreted as in the conventional SVAR models.

We define a functional impulse response h_k to be the response of the functional variable, income distribution (DIN), to the shock represented in the k^{th} column of (B) for $k = \ell + 1, \ldots, \ell + m$. Specifically, we let π be the isometry representing (f_t) as three dimensional vectors $\big((f_t)\big)$ and define

$$h_k = \pi^{-1}\left((B)_{\ell+1,k}, \ldots, (B)_{\ell+m,k}\right), \tag{16}$$

where $(B)_{a,b}$ denotes the (a,b)-th entry of (B).[16] We call (h_k) the *functional impulse response function* of DIN to a shock k of interest. Note that π^{-1} recovers functions from m-dimensional vectors.

For a graphical presentation of these functional responses, see the impulse response functions obtained from our data reported in Figure 6 in the following section. The four panels in the bottom row show the functional responses of the income distribution to the four aggregate shocks at-impact and over the next twelve month horizons. The impulse responses there are presented as a surface in a three-dimensional space, giving at each horizon a line in two dimensional space as for the conventional impulse response functions, of the income distribution to each aggregate structural shock. At each horizon, we therefore have a function (a line) instead of a number as the response to the given shock.

[16] Note that although the π's in (4) and (6) are defined for any z in $R^\ell \oplus H$ and for any linear operator in $R^\ell \oplus H$, we can interpret them as their restricted versions on $R^\ell \oplus V$ whenever necessary.

4.3 Variance Decomposition and Historical Decomposition

Using the estimates of the parameters (A_1) and (A_2) from the reduced-from approximate VAR (12), the estimate of the at-impact response matrix (B) from the structural VAR in (14), we may easily obtain the variance decomposition and historical decomposition of both macro aggregates and income distribution as in the standard finite dimensional VAR models. We may then use the essential isometry π^{-1} to take our results obtained with the finite $(\ell + m)$-dimensional vectors $(x_t, (f_t))$ in the vector space $R^{\ell+m}$ and interpret our results in the function space H of our original functional variables (x_t, f_t).

4.4 Structural Functional Shock Identification

As discussed earlier, the three semi-structural functional shocks are not individually identified in any structural sense.[17] These shocks are therefore not yet economically interpretable, and we need to identify interpretable structural shocks as linear combinations of these preliminary semi-structural functional shocks, $(e_t^{DIN_1})$, $(e_t^{DIN_2})$ and $(e_t^{DIN_3})$. We may indeed identify various shocks to income distributions by imposing additional identifying restrictions which provide a set of weights w_1, w_2, w_3 that can be used to combine the three functional shocks driving dynamics of income distributions.[18]

4.4.1 Output Maximizing Income Distribution Shock

Changes in income distribution can impact aggregate output levels. To explore the maximum effect on output that changes in income distribution may have, we identify the income distribution shock that maximizes aggregate output. Specifically, we determine the shock that induces the most positive cumulative response in aggregate output over a 10-year period by finding the linear combination of three functional shocks to income distributions that results in the highest positive cumulative impact on aggregate output.

We naturally refer to this shock as the *output-maximizing* income distribution shock, or simply the *YM shock*. Such shocks may arise from various events, including redistributive policy actions aimed at maximizing aggregate output. A redistributive policy designed to boost output could result in an income distribution shock like the YM shock. In this context, it may also be described as a 'hypothetical growth-targeted redistributive policy shock.' By analyzing the effects of the YM shock, we can infer the types of income distribution shocks that would most effectively increase output, providing valuable insights for designing growth-targeted redistributive policies.

Specifically, we define the YM shock as

$$e_t^{DIN*} = w_1^* e_t^{DIN_1} + w_2^* e_t^{DIN_2} + w_3^* e_t^{DIN_3},$$

[17] This problem of the lack of identification in functional shocks arises in all MAR models unless we set $m = 1$. In practice, this is rarely the case, since we would normally choose $m > 1$ in most MAR models to represent richer dynamics in functional time series.

[18] To be proper weights, w_1, w_2 and w_3 need to satisfy $w_1^2 + w_2^2 + w_3^2 = 1$.

where the weights w_1^*, w_2^*, and w_3^* are chosen to maximize the positive cumulative effect on output by the target year. To obtain $w^* = (w_1^*, w_2^*, w_3^*)'$, we let τ_1, τ_2, and τ_3 represent the cumulative responses of (Y_t) over 10 years following the shock impact date for the functional shocks $e_t^{DIN_1}$, $e_t^{DIN_2}$, and $e_t^{DIN_3}$, respectively. We then define

$$\tau(w) = w_1\tau_1 + w_2\tau_2 + w_3\tau_3$$

with $w = (w_1, w_2, w_3)'$. The optimal weights $w^* = (w_1^*, w_2^*, w_3^*)'$ are the maximizers of $\tau(w)$ subject to the constraint $w_1^2 + w_2^2 + w_3^2 = 1$. These weights are given by

$$w_k^* = \frac{\tau_k}{\sqrt{\tau_1^2 + \tau_2^2 + \tau_3^2}}$$

for $k = 1, 2, 3$.

In our empirical study with $m = 3$, we identify the YM shock using the weights $w^* = (w_1^*, w_2^*, w_3^*) = (-0.01, 0.99, 0.12)$, normalized by its norm $\|w^*\|$ to ensure that the identified structural income distribution shock also has the same unit variance as other structural shocks.

Figure 4 illustrates the response of the income distribution to the output-maximizing YM shock. The left panel displays the at-impact response of the entire demeaned income distribution as a functional impulse response, with the y-axis indicating the size of response and the x-axis representing quantile values of the demeaned income distribution at 1%, 10%, 25%, 50%, 75%, 90% and 99%, respectively.

The right panel shows the cumulative response of the income distribution one year after the impact date, obtained by adding the cumulative distributional response to the pre-shock income distribution. The top histogram summarizes this cumulative response across income decile groups, while the bottom histogram does so across income quintile groups. In these histograms, the x-axis represents the deciles (top) or quintiles (bottom) of the pre-shock income distribution. The blue bars show the original decile (or quintile) proportions before the shock, with each bar covering 10% (or 20%) of the pre-shock income distribution. The red bars indicate the changes in these proportions one year after the shock.

We can infer the distributional consequences of the YM income distribution shocks as follows: The YM shock affects the income distribution in contrasting ways for the top and bottom income groups. It significantly decreases the income of the poorest group in the bottom decile while modestly increasing the incomes of the richest in the top two decile groups. Additionally, the shock has varying effects on the middle-income groups: it raises the income of the lower-middle groups in the 2nd to 5th deciles but reduces the income of the upper-middle groups in the 6th to 8th deciles.

4.4.2 Inequality Minimizing Income Distribution Shock

Reducing income inequality has been a key policy objective. To explore how different income distribution shocks can achieve this, we identify an income distribution shock that minimizes income

Figure 4: At-impact Response of Income Distribution to YM Shock

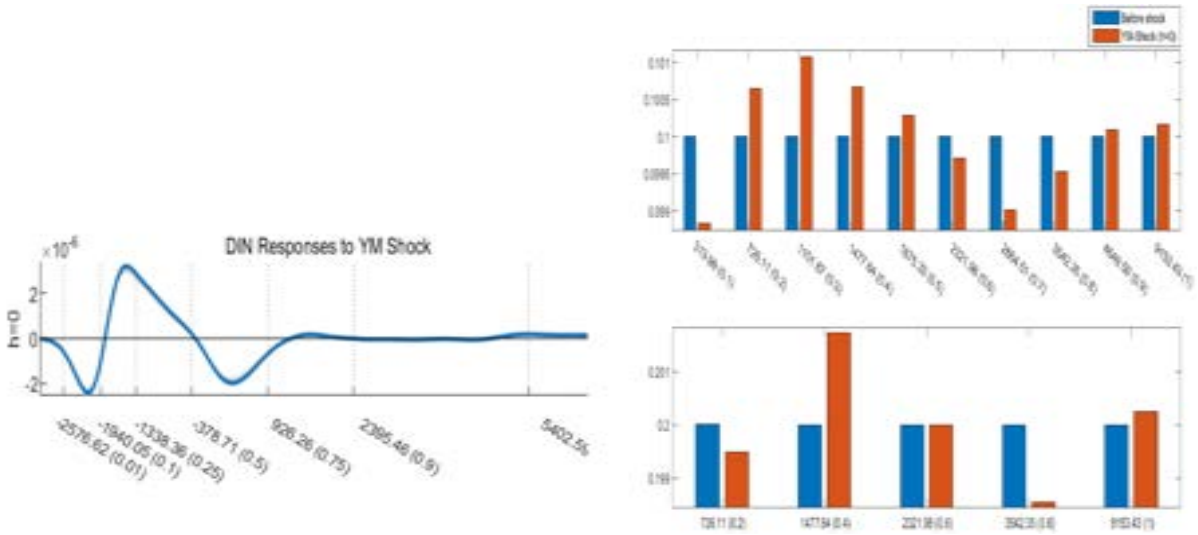

Notes: The left panel presents the at-impact impulse responses of the income distribution to the output-maximizing YM shock. It displays the response of the entire demeaned income distribution as a functional impulse response, with the y-axis showing the response and the x-axis indicating quantile values of the pre-shock demeaned income distribution at 1%, 10%, 25%, 50%, 75%, 90% and 99%. Shaded bands represent the 68% and 90% confidence intervals. The histograms on the right present cumulative responses of the income distribution one year after the impact. The top and bottom histograms summarize the cumulative responses, respectively, across decile and quintile income groups. The x-axis of the top (bottom) histogram represents the deciles (quintiles) of the pre-shock income distribution. In the top (bottom) histogram, the blue bars represent the pre-shock decile (quintile) proportions, with each bar covering 10% (20%) of the pre-shock income distribution, while the red bars show the changes in these proportions one year after the shock.

inequality. Specifically, we determine the shock that has the most negative cumulative effect on income inequality over a target period, such as 10 years after the impact date, as measured by the Gini index[19].

We identify this shock using a procedure similar to the one described in Section 4.4.1 for the YM shock. This involves finding the linear combination of three semi-structural functional shocks that results in the largest reduction in the Gini index. We refer to this income distribution shock as the *inequality-minimizing* or *GM shock*. Such a shock could arise from redistributive policy actions aimed at reducing income inequality or targeting equity. In this context, it may also be described as a hypothetical "equity-targeted redistributive policy shock." Analyzing the GM shock provides insights into the macroeconomic implications of equity-focused redistributive policies.

In our empirical study with $m = 3$, the weights $w^* = (w_1^*, w_2^*, w_3^*)$ for the GM shoc, which induces the most negative cumulative response of the Gini index 10 years after the impact, are (0.57, 0.24, -0.78).

Figure 5 shows the changes in the income distribution resulting from the inequality-minimizing GM shock at impact. In contrast to the growth-targeted YM shock, the equity-targeted GM shock substantially decreases the number of people in both the top decile and the bottom decile income groups. Furthermore, the GM shock affects the middle-income groups differently compared to the YM shock: it decreases the number of people in the lower-middle groups (2nd to 5th deciles) but substantially increases the number of people in the upper-middle groups (6th to 9th deciles).

5 Empirical Results

We investigate interactions between aggregate macro variables and income distribution by using the mixed autoregression (MAR) introduced in Section 3 in a structural form. In our MAR framework, impulse responses of the entire income distribution to each aggregate shock can be traced. Moreover, meaningfully interpretable distributional shocks can be defined using the functional shocks driving the income distributions. The new tools will then enable us to quantify and analyze not only the effects of aggregate shocks on the income distribution but also the effects of the income distributional shocks on macro aggregates in a novel way. Consequently, we can answer various policy questions which require an understanding of distributional effects of aggregate shocks. In particular, we study how monetary policy shocks affect income distribution, and also how shocks to income distribution affect key macro variables. We demonstrate in detail how we implement our procedure to quantify the distributional effects of contractionary monetary policy shocks, and how two interpretable income distribution shocks, YM and GM shocks, affect macro aggregates and income inequality.

Figure 6 presents impulse response functions of four scalar aggregate variables, IP, CPI, $PCOM$, $FFRS$, and impulse response surfaces of the functional variable DIN over 10 years (120

[19] Other commonly used inequality measures, such as the inter-quartile range, inter-decile range, top 10%, bottom 10%, among others, may also be used.

Figure 5: Changes in Income Distribution by Inequality-Minimizing GM shock

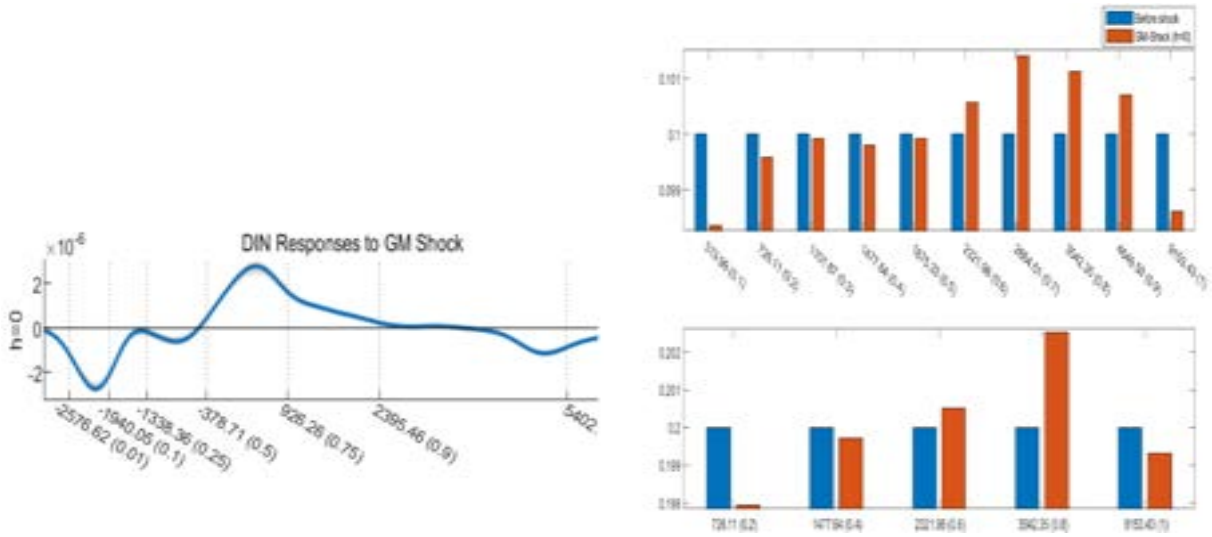

Notes: The left panel presents the at-impact impulse responses of the income distribution to the inequality minimizing GM shock. It displays the functional impulse response of the entire demeaned income distribution, with the y-axis indicating the response and the x-axis representing the quantile values at 1%, 10%, 25%, 50%, 75%, 90% and 99% from the pre-shock demeaned income distribution. Shaded bands represent the 68% and 90% confidence intervals. The right panel displays the cumulative response of the income distribution one year after the shock, with the top histogram summarizing it across income decile groups and the bottom histogram across income quintile groups. The x-axis of each histogram shows deciles (top) or quintiles (bottom) of the income distribution before the shock. In both histograms, blue bars represent the original proportions before the shock, while red bars illustrate the changes one year after the shock.

months). The top-left (4x4) block presents the standard IRFs of aggregate variables to aggregate shocks. The last row presents 3D response surfaces of the entire income distribution. Each surface presents the response of the income distribution to a shock at each horizon, which is a function over the entire income range. Each response surface presented in the bottom row plots probability densities in the z-axis, along the horizons in the x-axis as in the conventional response functions presented for the aggregate variables in the top four rows, and over the ranges of demeaned income levels in the y-axis.[20] For example, the surface in the (5,4)-panel shows impulse responses of the entire income distribution to monetary policy shocks. On the other hand, in the last column of Figure 6, each row presents the responses of each variable to the YM shock. Impulse responses of aggregate variables are reported with 68% and 90% probability bands that are signified, respectively, by darker and lighter shades.

5.1 Effects of Monetary Policy Shocks

Figure 7 presents the fourth column of Figure 6, which shows the impulse responses to monetary policy shock, under FFRS. The left column displays IRFs of the aggregate variables and impulse response surface of the income distribution to contractionary monetary policy shocks. The three-

[20]The unit on the z-axis, *density* or *probability density*, does not have a specific unit of measurement in the traditional sense, as it represents the likelihood of the income levels falling within a particular range rather than a direct measurement.

Figure 6: **Impulse Response Functions and Surfaces**

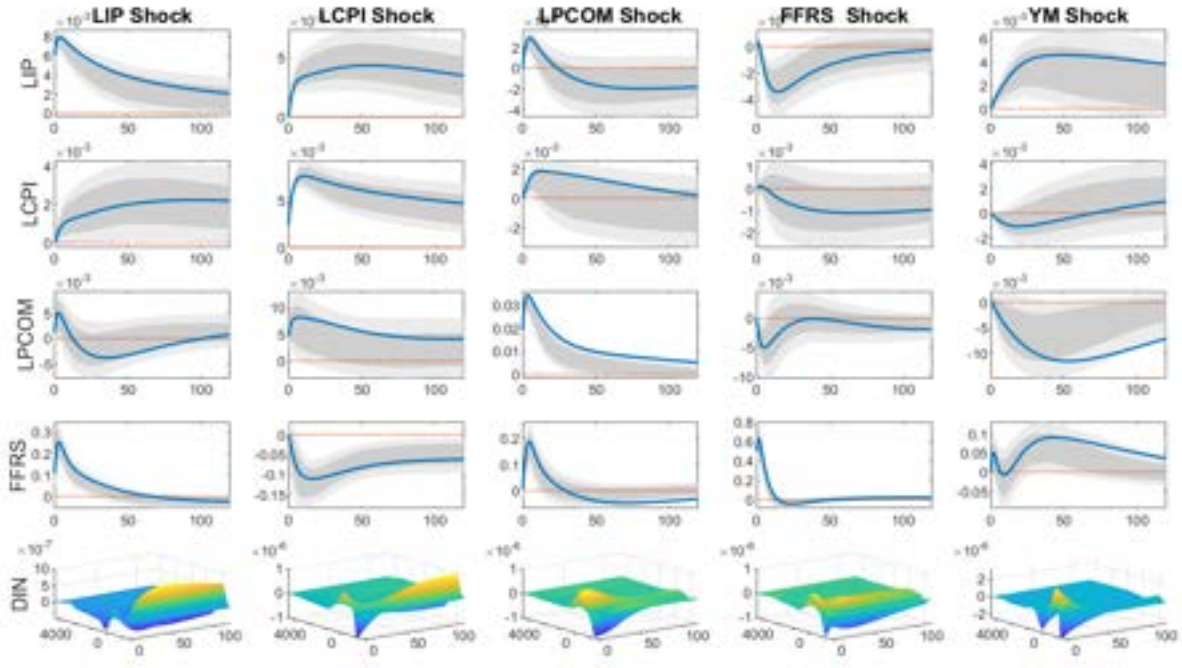

Notes: Presented are impulse response functions of aggregate variables, IP, CPI, $PCOM$, $FFRS$, and impulse response *surfaces* of the functional variable DIN over 10 years (120 months). The top-left (4x4) block presents the standard IRFs of aggregate variables to aggregate shocks. The last row presents 3D response surfaces of the entire income distribution. Each surface presents the response of the income distribution to a shock at each horizon, which is a function over the entire income range. Each response surface presented in the bottom row plots probability densities in the z-axis, along the horizons in the x-axis, and over the ranges of demeaned income levels in the y-axis. The last column presents the responses of each variable to the YM shock. Impulse responses of aggregate variables are reported with 68% and 90% probability bands that are signified, respectively, by darker and lighter shades.

dimensional response surface in the bottom row is sliced at the horizons $h = 0, 12, 24, 60$ and 120 months, with the resulting two-dimensional slices, representing the functional impulse responses of the income distribution, shown on the right.

In Figure 7, we observe that output declines temporarily and the price level declines persistently in response to the FFRS shocks, which is the expected effect of monetary policy shocks. More interestingly, we see markedly different responses in income distribution across income levels. The effects of the contractionary monetary policy shock are clearly heterogeneous for different income groups.

Note that the impulse responses of the DIN presented in Figure 7 show only the distributional effects, without accounting for any changes in the mean level. Specifically, the negative impact of the FFRS shocks on aggregate output (or income), reported in the top-left panel of Figure 7, is not reflected in the DIN responses. Therefore, to precisely quantify the effects of FFRS shocks on the income distribution, we need to consider both the shifts in the mean of the income distribution implied by changes in aggregate income (IP)[21] and the pure distributional changes implied by

[21] To calculate the shift in mean of the income distribution, we determine the response of aggregate output (log

Figure 7: Impulse Response Functions and Surfaces to Contractionary Monetary Policy Shocks

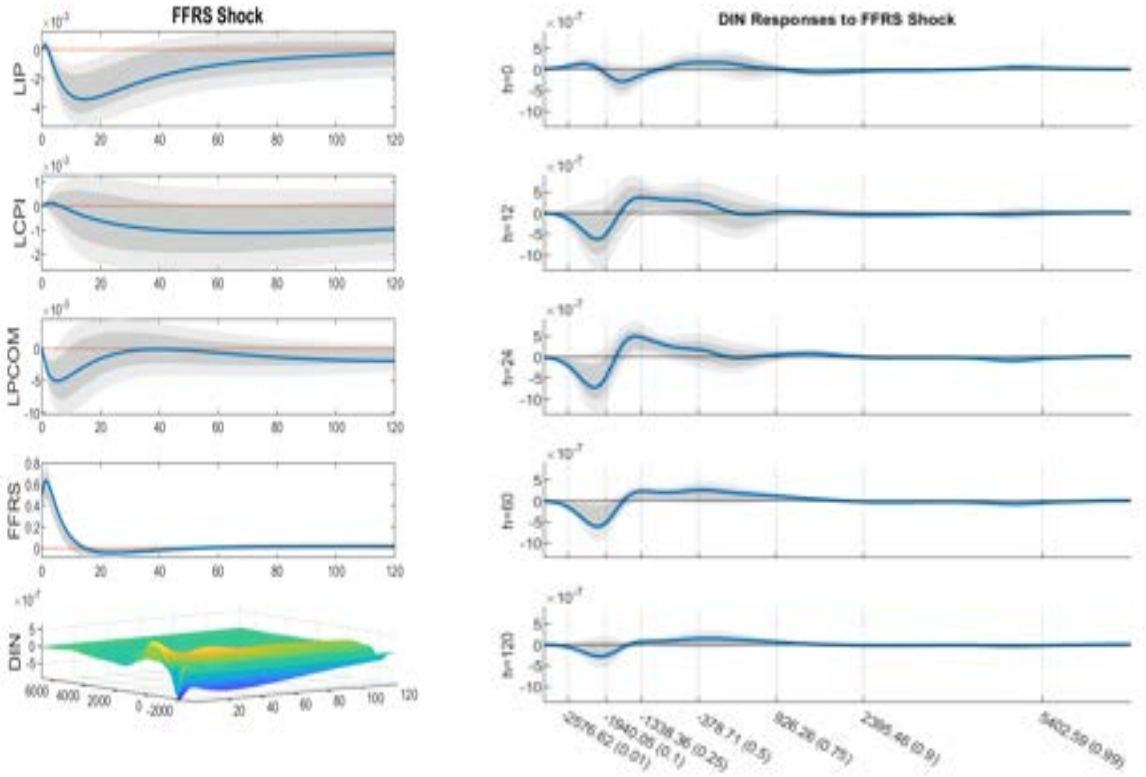

Notes: On the left are IRFs of the aggregate variables and impulse response surface of the income distribution to contractionary monetary policy shocks. On the right, the functional impulse responses of the demeaned income distribution - two dimensional slices of the response surface - are shown for the horizons $h = 0, 12, 24, 60$ and 120 months, with the y-axis indicating the response and the x-axis representing quantile values (1%, 10%, 25%, 50%, 75%, 90% and 99%). Shaded bands represent the 68% and 90% confidence intervals.

the responses of the (cross-sectionally demeaned) income distribution (DIN) to FFRS shocks. By combining these two effects, pure distributional effects and aggregate effects, we can quantify the redistributive effects of the monetary policy shock on the income distribution.

Figure 8 presents the DIN responses to contractionary monetary policy shocks one year after the impact in histograms. The top (bottom) panel on the left shows how the income distribution changes *without* the mean shift for decile (quintile) income groups. Similarly, the top (bottom) panel on the right shows those obtained *with* the mean shift for decile (quintile) income groups.

Figure 9 and Figure 10 present, respectively, without and with the mean shift, responses of income distribution to the contractionary monetary policy shock with the 90% confidence intervals in histograms for quintile income groups at four different horizons together–at-impact ($h = 0$, top-left), $h = 12$ months, (top-right), $h = 24$ months (bottom-left) and $h = 60$ months (bottom-right) after the impact. Shifts in the mean level of income distribution due to the contractionary monetary

industrial production, IP) to the FFRS shocks, since the difference in log IP is approximately the percentage change in IP. From the IRF matrix, we infer that the percentage change in the mean of income distribution implied by IRFs of aggregate income (IP) is 0% at impact, -0.1056% at $h = 60$, and -0.0264% at $h = 120$.

Figure 8: Distributional Effects of Contractionary Monetary Policy Shocks

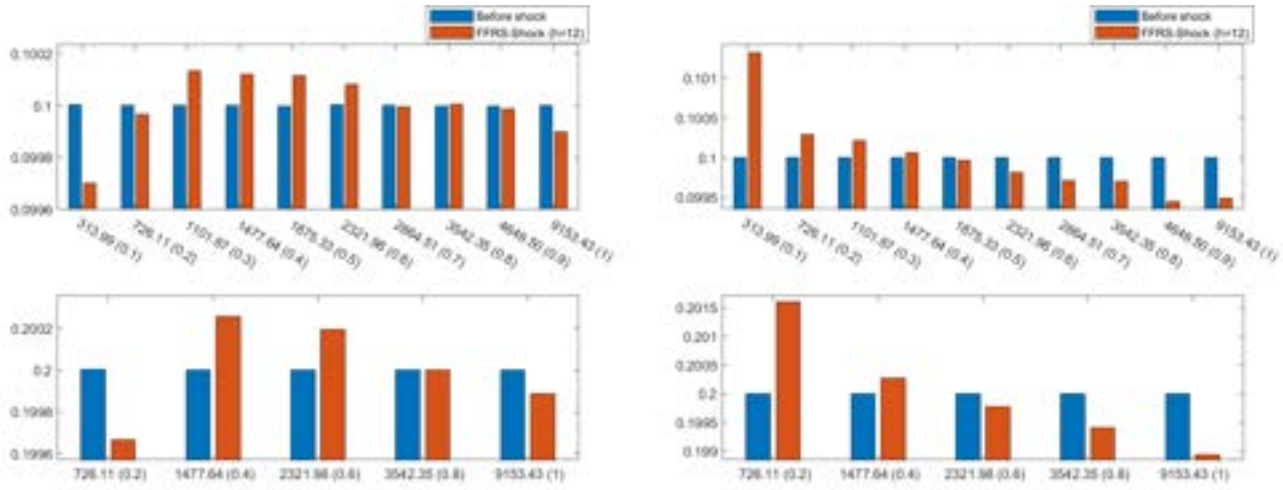

Notes: Presented are the DIN responses to contractionary monetary policy shocks one year after the impact in histograms. The top (bottom) panel on the left shows how the income distribution changes *without* the mean shift for decile (quintile) income groups. Similarly, the top (bottom) panel on the right shows those obtained *with* the mean shift for decile (quintile) income groups.

policy shock are measured by the changes in aggregated income due to the FFRS shock shown in the top-left panel of Figure 7.

To see more explicitly how the monetary policy tightening affects inequality, we also present in Figure 11, the impulse response functions of the Gini index computed from the income distribution, *without* the mean shift (left) and *with* the mean shift (right). Shaded bands represent the 68% and 90% confidence intervals.

When the mean shift in the income distribution is not taken into account, contractionary monetary policy shocks lead to a substantial decrease in the proportions of low income groups (the bottom 10% and 20%, with a particularly significant reduction in the poorest 10% group). These shocks also increase the proportion of the middle-income group (from the bottom 30% to 60%) and decrease the proportions of high-income groups (the top 10% and 20%). This suggests that monetary policy may play a positive role in reducing income inequality. This pure distributional effect is clearly illustrated by the impulse response function of the Gini Index computed from the counterfactual income distribution responses, which shows a sharp decrease from the impact date and remains persistently low even after 10 years.

We observe markedly different effects of monetary policy on income inequality when considering changes in aggregate income. The path of changes in the aggregate income level is shown in the top-left panel of Figure 7, which tracks changes in the mean level of the income distribution. In response to contractionary monetary policy shocks, aggregate output decreases, implying that the income levels of all workers decrease by the same amount, in addition to the pure distributional effect discussed earlier. This reduction diminishes the relative income share of low-income workers, leading to an increase in the Gini Index, thereby worsening inequality. The right panel of Figure 11

Figure 9: DIN Responses to Contractionary Monetary Policy Shock without Mean Shift

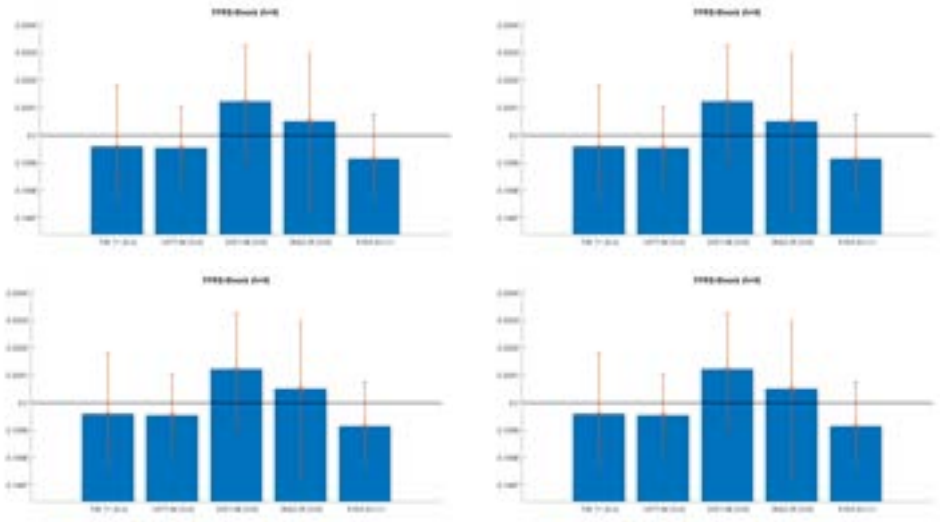

Notes: Responses of the income distribution to contractionary monetary policy shocks in histograms for quintile income groups at-impact ($h = 0$, top-left), $h = 12$ months, (top-right), $h = 24$ months (bottom-left) and $h = 60$ months (bottom-right) after the impact. The numbers on the horizontal axis are the quintile values obtained from the pre-shock income distribution. The black horizontal line signifies the benchmark 20% line, and the vertical line at the top center of each bar represents the 90% confidence interval. Mean shift by the aggregate output is *not* considered.

Figure 10: DIN Responses to Contractionary Monetary Policy Shock with Mean Shift

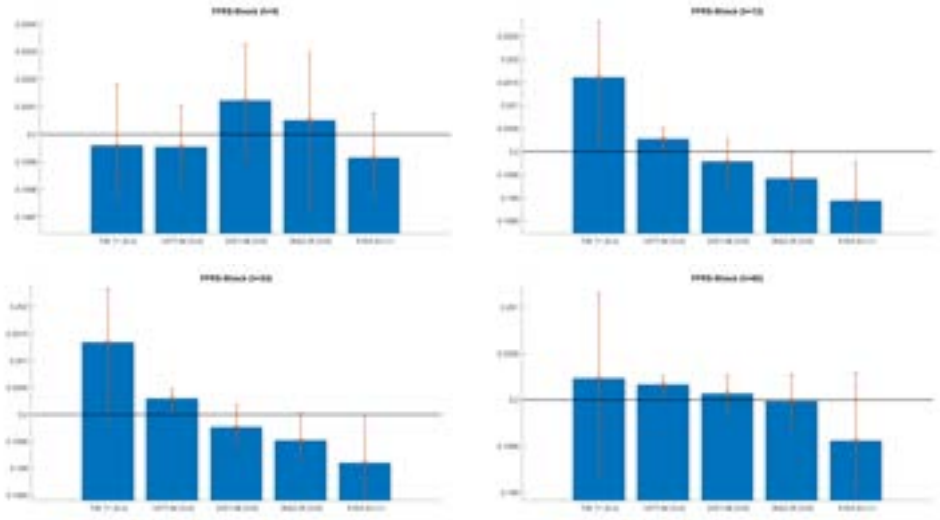

Notes: Responses of the income distribution to contractionary monetary policy shocks in histograms for quintile income groups at-impact ($h = 0$, top-left), $h = 12$ months, (top-right), $h = 24$ months (bottom-left) and $h = 60$ months (bottom-right) after the impact. The numbers on the horizontal axis are the quintile values obtained from the pre-shock income distribution. The black horizontal line signifies the benchmark 20% line, and the vertical line at the top center of each bar represents the 90% confidence interval. Mean shift by the aggregate output is considered.

Figure 11: IRFs of Gini Index to Contractionary Monetary Policy Shocks with $m = 2$

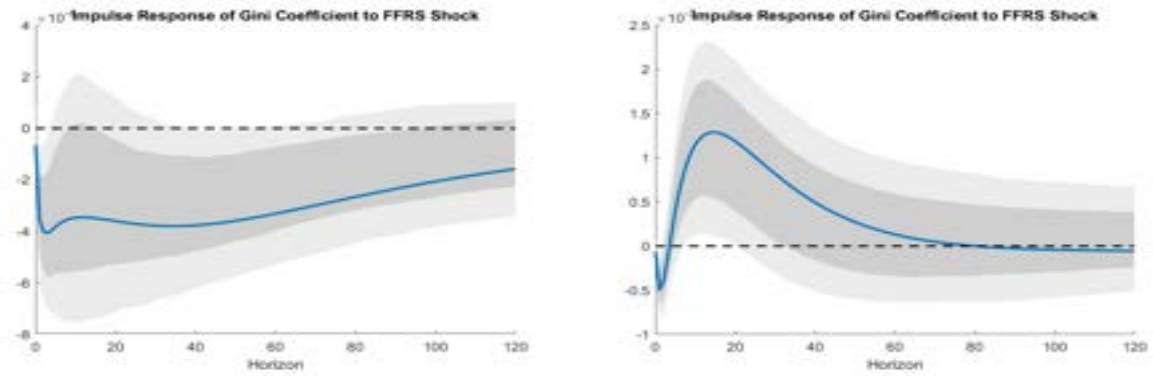

Notes: Presented are the impulse response functions of the Gini index computed from the income distribution over a 10-year horizon, *without* the mean shift (left) and *with* the mean shift (right). Shaded bands represent the 68% and 90% confidence intervals.

illustrates the trajectory of the Gini index in response to contractionary monetary policy: the Gini index initially declines but begins to increase in a few months, peaking around 1.5 years after the impact, and remains elevated for up to 6 years. Initially, the pure distributional effect dominates, causing the Gini index to decline, but as aggregate output decreases, the aggregate effect takes over, resulting in a gradual rise in the Gini index over time.

Figure 12 presents the forecast error variance decomposition (FEVD) of the variables in the MAR model attributable to four aggregate structural shocks ($e_t^{IP}, e_t^{CPI}, e_t^{PCOM}, e_t^{FFRS}$) and one income distribution (DIN) shock (e_t^{DIN}) which is constructed simply as the sum of the three independent semi-structural functional shocks ($e_t^{DIN_1}, e_t^{DIN_2}, e_t^{DIN_3}$) driving the time series of income distribution (DIN). We call the one dimensional income distribution shock (e_t^{DIN}) as *DIN shock*. Each shock's contribution is color-coded, with the color codes provided in the legend box at the bottom of the figure. The four panels in the first row show the FEVDs for four aggregate variables. The four panels in the second row and the first panel in the third row present the FEVDs for the proportions of the population at income levels around the 1st, 25th, 50th, 75th, and 99th percentiles of the most recent income distribution, December 2015.[22] The remaining three panels in the third row present the FEVDs for the bottom 25%, middle 50%, and top 25% income groups defined using the historical average income distribution. FFRS shocks affect low-income groups more than high-income groups; however, the contribution of FFRS shocks to income distribution variations is limited in all cases (less than 10%). For the FEVDs presented here and in the subsequent historical decompositions, we focus solely on the contribution of monetary policy shocks and defer the analysis of other shocks to Section 5.2.

We perform historical decompositions (HD) attributable to four aggregate shocks and one income distribution shock, YM shock. The results on HDs for four aggregate variables (IP, CPI, $PCOM$, $FFRS$) are presented in Figure 13. To discuss impacts of shocks on income inequality, we also

[22]These percentile values from the *demeaned* income distribution in December 2015 are, respectively, -$2,576.62 (1st), -$1,338.36 (25th), -$378.71 (50th), $926.26 (75th), and $5,402.59 (99th).

Figure 12: **Variance Decomposition from MAR with DIN Shock**

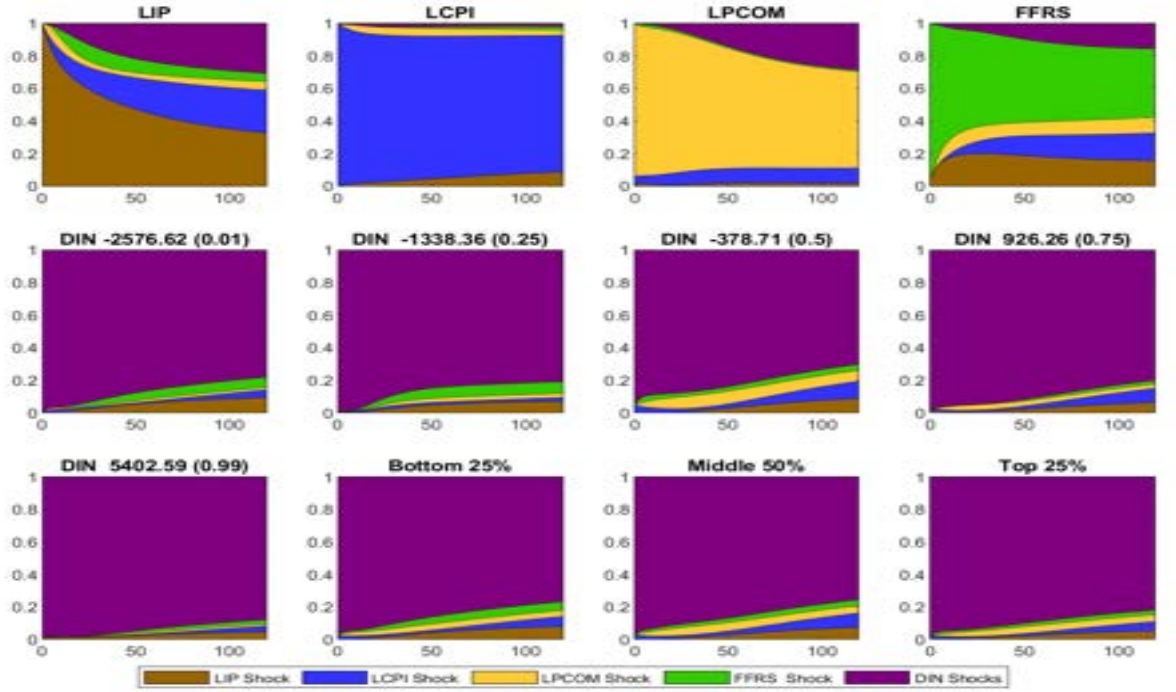

Notes: Presented are the forecast error variance decomposition (FEVD) of the variables in the MAR model attributable to four aggregate shocks and one income distribution shock. Each shock's contribution is color-coded, with the color codes provided in the legend box at the bottom of the figure. The four panels in the first row show the FEVDs for four aggregate variables. The four panels in the second row and the first panel in the third row present the FEVDs for the proportions of the population at income levels around the 1st, 25th, 50th, 75th, and 99th percentiles of the most recent income distribution, December 2015. The remaining three panels in the third row present the FEVDs for the bottom 25%, middle 50%, and top 25% income groups, defined using the historical average income distribution.

consider three benchmark income groups – bottom 25%, middle 50% and top 25%, defined with the 25th, 50th and 75th percentiles of the historical average income distribution. We then examine whether a given shock increases or decreases proportions of the population in the given group relative to the corresponding benchmark proportions. Figure 14 presents the HDs for the proportions of the population in three income groups (bottom 25%, middle 50% and top 25%), defined using the historical average income distribution. The contribution from each shock is signified by a color-coded bar, and the color codes are given in the legend box at the bottom of the figure.

We observe that monetary policy shocks have minimal effect on the evolution of the income distributions of all three groups. The role of monetary policy shocks in explaining the evolution of income distribution for each income group is even smaller than their role in explaining aggregate output (IP) fluctuations, which is relatively small. Considering our earlier findings from the impulse response analysis and variance decompositions, monetary policy shocks appear to play a minimal role in the rising income inequality observed in the US during our sample period. This is a new finding that cannot be obtained from conventional aggregate VAR analysis and shows the potential for our analysis to explore further distributional implications of monetary policy.

Figure 13: **Historical Decomposition of Aggregate Variables from MAR with YM Shock**

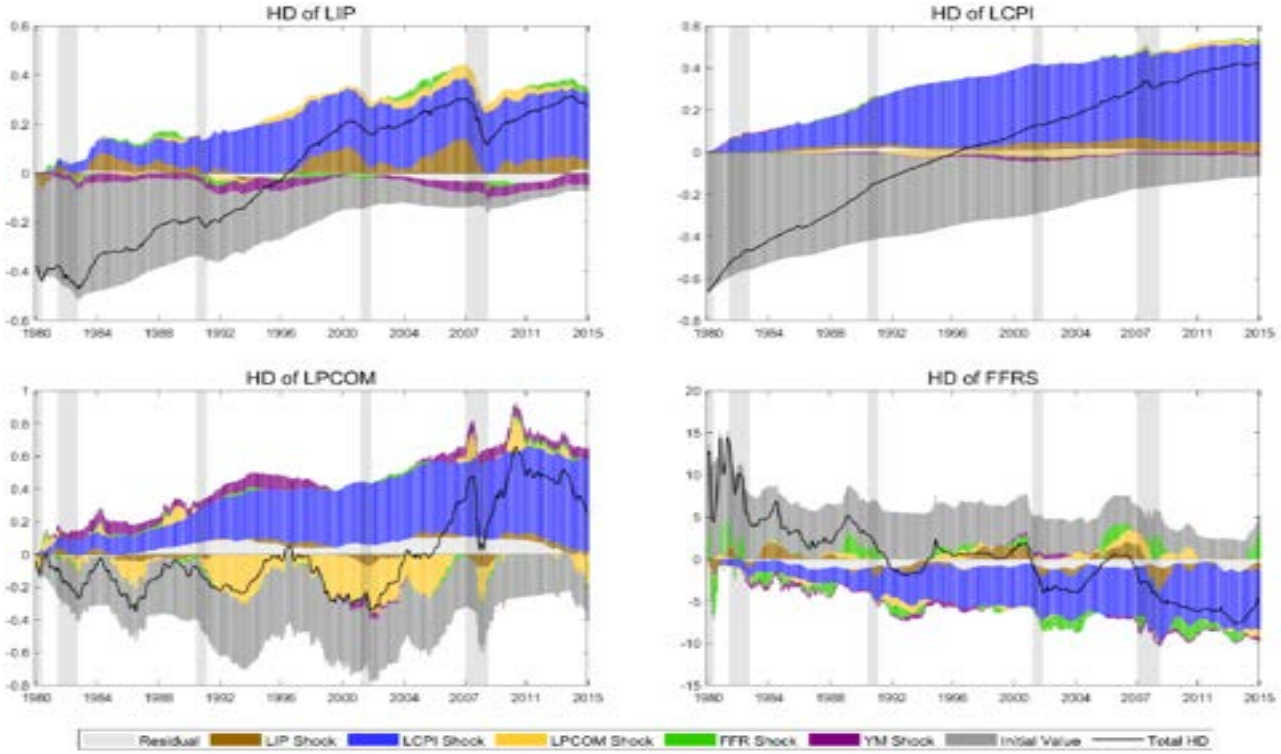

Figure 14: **Historical Decomposition of Income Distribution from MAR with YM Shock**

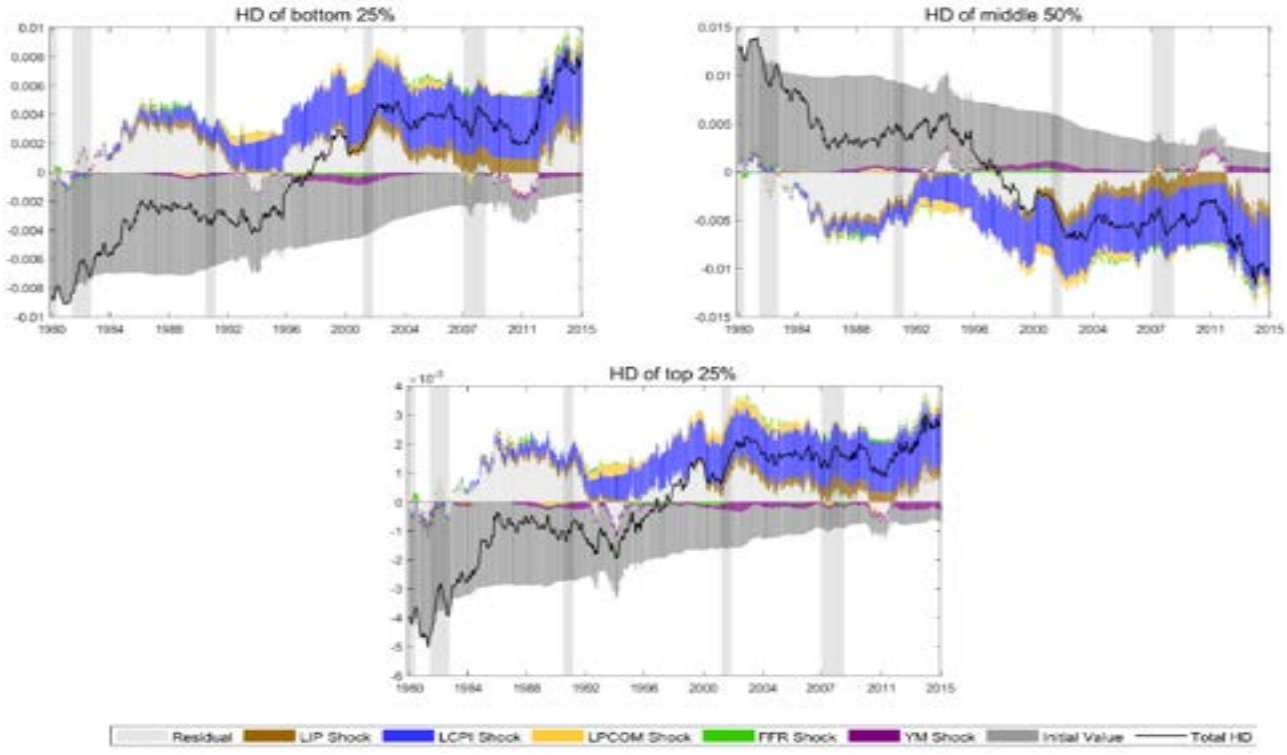

Figure 15: Impulse Response Functions and Surfaces to YM Shocks

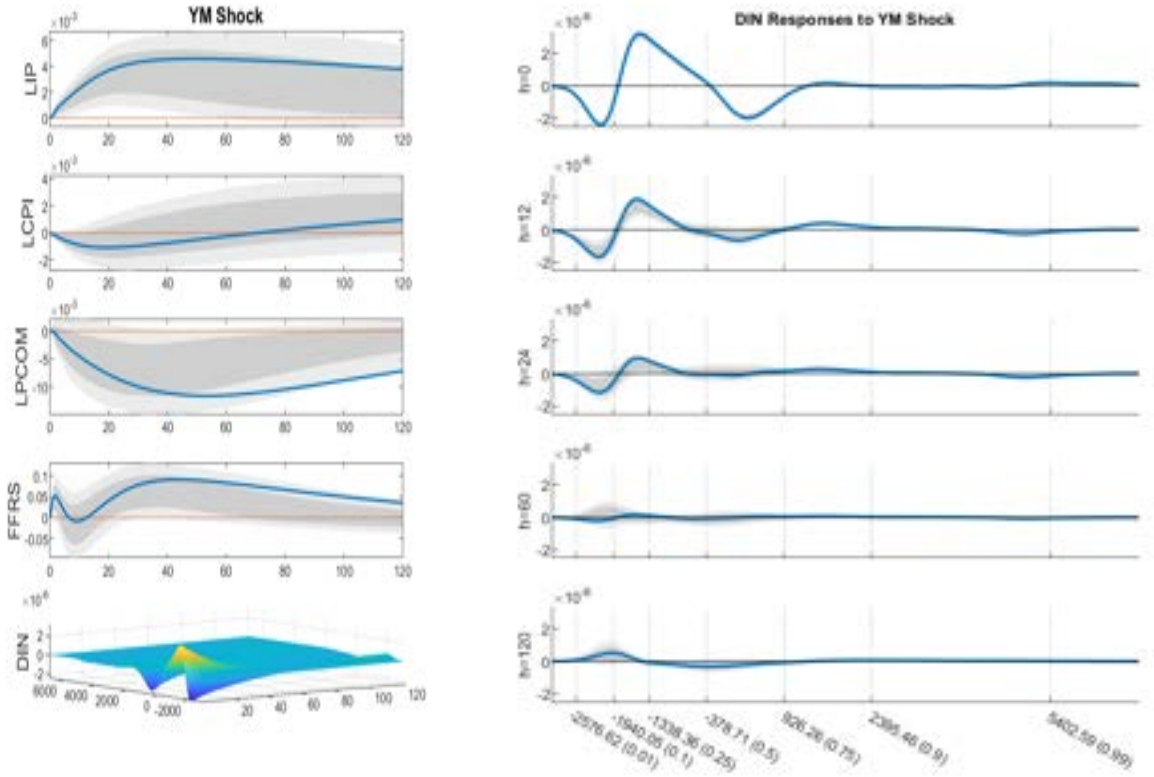

Notes: Presented on the left are IRFs of the aggregate variables and impulse response surfaces of the income distribution to output-maximizing YM shock. On the right, presented are the functional impulse response functions - two dimensional slices of the response surface - are shown for the horizons $h = 0, 12, 24, 60$ and 120 months, with the y-axis indicating the response and the x-axis representing quantile values (1%, 10%, 25%, 50%, 75%, 90% and 99%). Shaded bands represent the 68% and 90% confidence intervals.

5.2 Effects of Output-Maximizing, Hypothetical Growth-Targeted Redistributive Policy Shocks

To study effects of shocks to income distribution on macroeconomy, we first consider the output-maximizing YM shock, or hypothetical 'growth-targeted redistributive policy' shocks, identified in Section 4.4.1 as a linear combination of the three semi-structural functional shocks driving the income distributions that maximizes the aggregate output ten years after the impact.

Figure 15 reports the fifth column of Figure 6 presenting the impulse responses to the YM shock. Presented on the left are IRFs of the aggregate variables and impulse response surface of the income distribution to the YM shock. On the right, presented are the two-dimensional slices of the three-dimensional DIN response surface at the bottom row for the horizons $h = 0, 12, 24, 60$ and 120 months.

Figure 16 and Figure 17 present, respectively, without and with the mean shift, responses of income distribution to the output-maximizing YM shock in histograms for quintile income groups at-impact ($h = 0$, top-left), $h = 12$ months, (top-right), $h = 24$ months (bottom-left) and $h = 60$

Figure 16: DIN Responses to Output-Maximizing YM Shock without Mean Shift

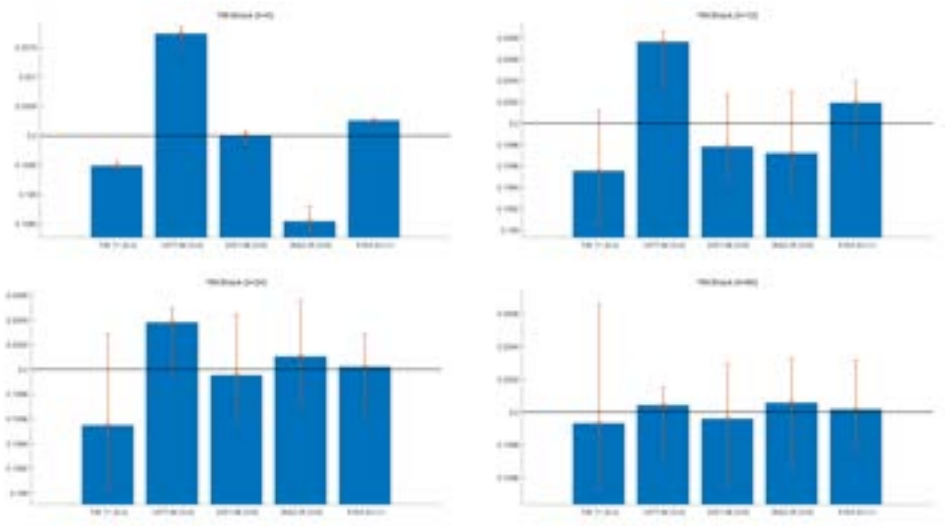

Notes: Responses of the income distribution to the output-maximizing YM shock in histograms for quintile income groups at-impact ($h = 0$, top-left), $h = 12$ months, (top-right), $h = 24$ months (bottom-left) and $h = 60$ months (bottom-right) after the impact. The numbers on the horizontal axis are the quintile values obtained from the pre-shock income distribution. The black horizontal line signifies the benchmark 20% line, and the vertical line at the top center of each bar represents the 90% confidence interval. Mean shift by the aggregate output is *not* considered.

months (bottom-right) after the impact. Shifts in the mean level of income distribution due to the YM shock are measured by the changes in aggregated income due to the YM shock shown in the top-left panel of Figure 15.

We first discuss effects of YM shocks on macro aggregate variables reflected in their impulse response functions presented in the first four panels in the left column of Figure 15. The most salient finding is that YM shocks increase output substantially. The size of output (IP) increase is much larger and persistent than that of monetary policy shocks shown in the top-left panel of Figure 7. This result suggests that distributional shocks can have a huge effect on aggregate output potentially, and a well-designed redistributive policy may have a substantial effect on output. Price (CPI) does not change much, but commodity prices ($PCOM$) decreases substantially and persistently. Fed funds rate ($FFRS$) increases in the medium run, which may be related to counter-cyclical and counter-inflation monetary policy actions.

Then, we infer the redistributive nature of the YM shocks by characterizing the income distribution changes to the YM shocks, without the mean-shift reflected in the aggregate output, from the right panels of Figure 15 and Figure 16. At-impact, the YM shock decreases the poorest decile income group and upper middle income groups in the fourth quintile group, while increasing the lower middle income groups in the second quintile and the richest in the top quintile group. The sharp drop in the poorest decile income group clearly contributes to reducing income inequality. Such inequality reducing, purely redistributive effect of the YM shock is not permanent and vanishes about 5 years after the impact date.

We discuss in detail the effect of YM shocks on income inequality. The left panel of Figure 18

Figure 17: DIN Responses to Output-Maximizing YM Shock with Mean Shift

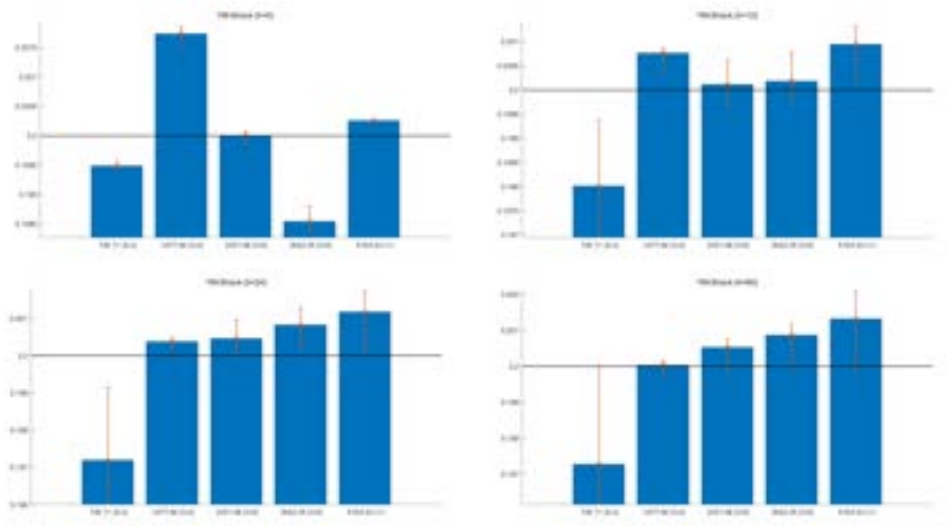

Notes: Responses of the income distribution to the output-maximizing YM shock in histograms for quintile income groups at-impact ($h = 0$, top-left), $h = 12$ months, (top-right), $h = 24$ months (bottom-left) and $h = 60$ months (bottom-right) after the impact. The numbers on the horizontal axis are the quintile values obtained from the pre-shock income distribution. The black horizontal line signifies the benchmark 20% line, and the vertical line at the top center of each bar represents the 90% confidence interval. Mean shift by the aggregate output is considered.

shows the IRFs of the Gini index obtained using the response of the income distribution to the YM shock without the mean shift reflected in the changes in the aggregate output. This is therefore the inequality implications of the hypothetical, purely redistributive YM shock discussed above. As noted earlier, changes in aggregate income due to the YM shock are significantly positive and persistent; see the top-left panel of Figure 15. Without taking into account the positive responses of the aggregate income, the significant initial decline in the Gini index diminishes and becomes insignificant after six years. On the other hand, when such positive and persistent mean shift is taken into account, income inequality decreases except in the very short-run. As shown in the right panel of Figure 18, the Gini index increases slightly at-impact, but quickly becomes negative and remains negative in the long run. Hence, the YM shock decreases the inequality substantially and persistently. As aggregate output increases, the income levels of all workers increase by the same amount, in addition to the pure distributional effects discussed above.[23] This increases the relative income share of low-income workers, which leads to a decrease in the Gini index. Therefore, by taking account of the aggregate output effect, in addition to the purely distributional effect, the reduction in the Gini index turns out to be greater. Moreover, the finding that the YM shocks increase both growth and equality suggests that properly aimed growth-targeted redistributive policies are not subject to the often-claimed trade-off between growth and equality.

We discuss how YM shocks contribute to the fluctuations of both aggregate variables and the

[23]There are more families in the upper quintiles with a positive aggregate mean shift than without, as shown in Figure 17 (with mean shift) and Figure 16 (without mean shift). This is because the income levels of all workers are higher when there is a positive mean shift compared to when there is no mean shift.

Figure 18: IRFs of Gini Index to YM Shock

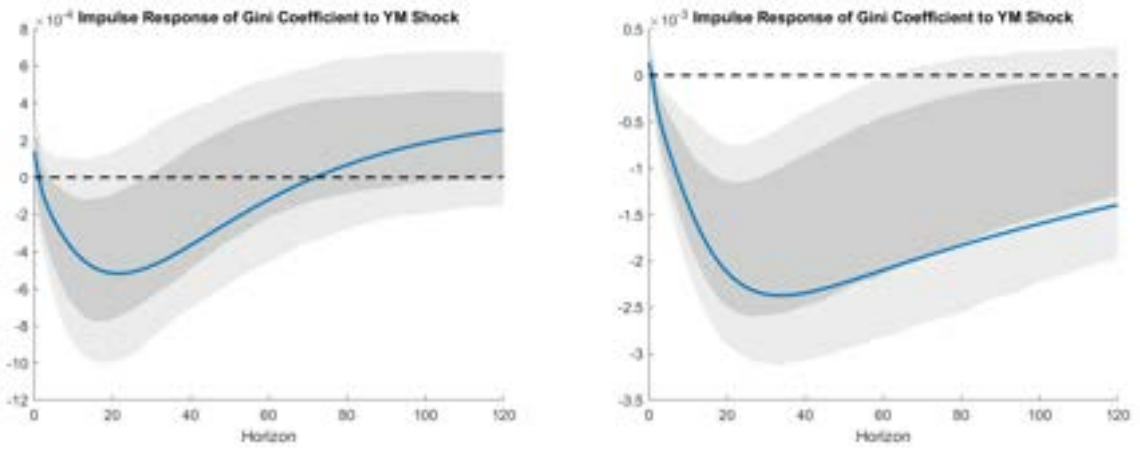

Notes: Impulse response functions of the Gini index to YM shock *without* the mean shift (on the left) and *with* the mean shift (on the right). Shaded bands represent the 68% and 90% confidence intervals.

income distribution. Figure 19 shows the forecast error variance decomposition obtained with four aggregate shocks and the output maximizing YM Shock which is a linear combination of the three DIN shocks satisfying our identifying restriction. Each shock is color-coded, and the color codes are given in the legend box at the bottom of each figure. The purple area shows the contribution to the forecast error variances of YM shocks while the sum of the purple and white areas show the total contribution of the income distribution (DIN) shocks, i.e., the sum of the contributions from the three independent functional shocks driving the dynamics of the income distribution. The total contributions from the three independent DIN shocks, which are given here as the combined areas of purple and white color areas, are the purple areas shown earlier in Figure 12.

he five panels, including the four panels in the second row and the first panel in the third row of Figure 19, present the variance decomposition of income levels in the small neighborhoods of the 1st, 25th, 50th, 75th, and 99th percentiles of the income distribution in the last period. The remaining three panels of the third row present the variance decomposition of incomes for the bottom 25%, middle 50%, and top 25% of the average income distribution. As shown in the second and third rows, the three DIN shocks explain most of the income distribution variations. We also observe that YM shocks substantially contribute to fluctuations in IP and $PCOM$. In particular, the contribution to IP is large, accounting for up to 30% in the long run. The contribution of YM shocks to IP is far greater than that of FFRS shocks, especially in the long run. In addition, YM shocks have a huge and persistent impact on the income distribution of the low-income group.

As discussed above, our empirical results from variance decompositions of aggregate variables and income distribution (DIN) indicate that DIN shocks matter for output, commodity prices, and interest rates, but not overall prices. They also show that YM shocks are relatively more influential for the poor than for the rich income groups. Most interestingly, the DIN shock accounts for the majority of variations in income distribution, making it the main driver of income distribution changes. In contrast, monetary policy shocks play a relatively minor role in explaining

Figure 19: **Variance Decomposition from MAR with YM Shock**

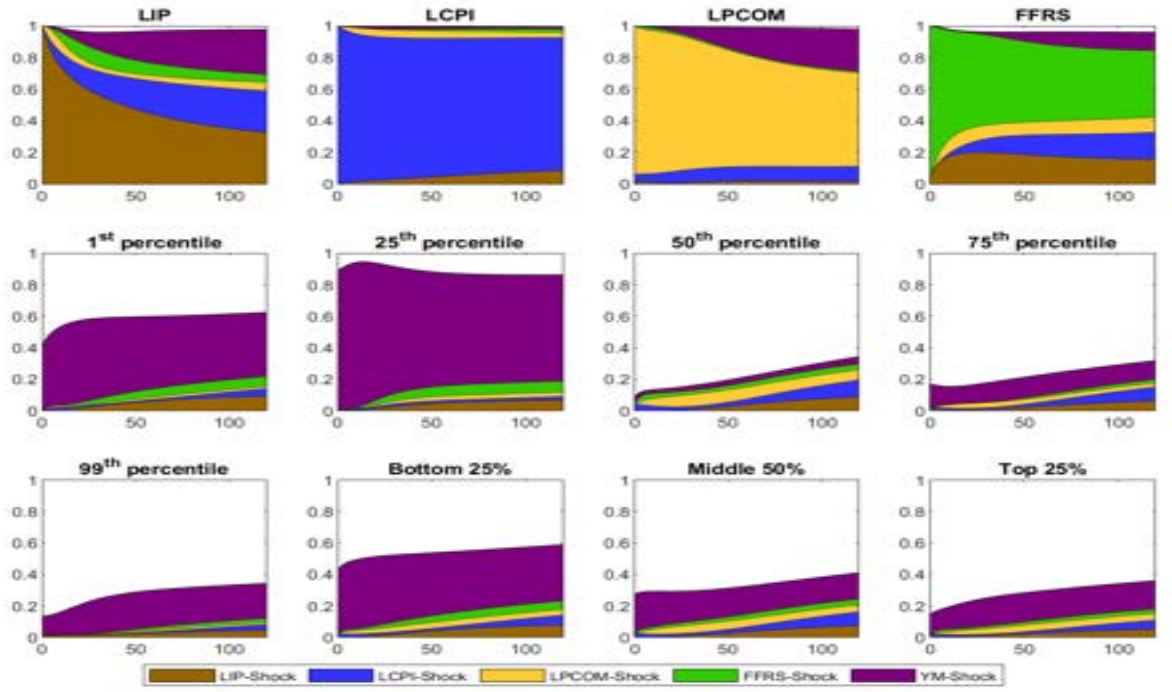

Notes: Presented are the forecast error variance decomposition (FEVD) of the variables in the MAR model attributable to four aggregate shocks and one distributional YM shock. Each shock's contribution is color-coded, with the color codes provided in the legend box at the bottom of the figure. The four panels in the first row show the FEVDs for four aggregate variables. The four panels in the second row and the first panel in the third row present the FEVDs for the proportions of the population at income levels around the 1st, 25th, 50th, 75th, and 99th percentiles of the most recent income distribution, December 2015. The remaining three panels in the third row present the FEVDs for the bottom 25%, middle 50%, and top 25% income groups, defined using the historical average income distribution.

these variations. These findings suggest that redistributive policies targeting income distribution directly, rather than macroeconomic policies targeting aggregate variables such as monetary policy, are necessary to substantially alter income distribution and improve inequality.

Next, we discuss historical decompositions (HD) obtained with the four aggregate shocks and the YM shock. Figure 13 presents the HDs of the aggregate variables in the MAR model attributable to four aggregate shocks and the distributional YM shock. We find that the YM shocks (signified by purple bars) tend to have a negative contribution to output level but a positive contribution to commodity prices throughout our sample period except for the early 2000s. The income distribution shock as a whole (purple and white bars combined) tends to contribute negatively to output level and $FFRS$ but positively to $PCOM$ level throughout the sample period. Interestingly, YM shocks and the income distribution shocks as a whole have negative contributions on output level in all recessions except for the one in the early 2000s.

In Figure 14, we also observe that YM shocks (purple bars) reduce the proportion of the bottom 25% and the top 25%, but increase that of the middle 50%, especially in the late 1990s and early 2000s, which likely reduces income inequality. Interestingly however, the income distribution shocks

excluding the YM shock (only white bars) have huge positive contributions to the proportions of the bottom 25% and the top 25% and equally large negative contribution to the proportion of the middle 50%, thereby increasing income inequality. Note that all three non-policy aggregate shocks also have worsened inequality throughout our sample period. Also note that among them the CPI shock has contributed most substantially and its impact is increasing. This result suggests that the YM shock, if it can be implemented with a growth-targeted redistributive policy, has a potential to mitigate the negative effects of aggregate shocks on income inequality discussed above.

5.3 Effects of Inequality-Minimizing, Hypothetical Equity-targeted Redistributive Policy Shocks

We now explore the effects of the GM shock identified as a linear combination of the three functional shocks that minimizes the Gini index ten years after the impact.

Figure 20 reports the impulse responses to the GM shock. Presented on the left are IRFs of the aggregate variables and impulse response surface of the income distribution to the GM shock. On the right, presented are the two-dimensional slices of the three-dimensional DIN response surface in the bottom row for the horizons $h = 0, 12, 24, 60$ and 120 months. In response to the GM shock, IP decreases in the short run and increases in the long run, but the responses tend to be insignificant. $PCOM$ and CPI tend to decrease but responses of CPI are insignificant. $FFRS$ increases and the short-run increase is significant. Figures 17 and 16 further present, respectively, with and without the mean shift, responses of income distribution to the output-maximizing growth-targeted YM shock in histograms for quintile income groups at-impact ($h = 0$, top-left), $h = 12$ months, (top-right), $h = 24$ months (bottom-left) and $h = 60$ months (bottom-right) after the impact. The mean shift in the income distribution is measured by the changes in aggregate output.

The inequality-minimizing GM Shock changes the income distribution in a distinctively different way compared to the growth-targeted YM shock, which is not surprising because two shocks have different natures. GM shocks decrease both the poorest group in the bottom quintile and the richest group in the top quintile, but tend to increase the middle income group in the remaining three middle quintiles. Such a change in income distribution naturally improves income inequality. Interestingly, this pattern of changes is found in both Figures 21 and 22, without and with the mean shift, respectively. Output responses are relatively small, so the results with and without the mean shift are similar.

Figure 23 shows the IRFs of the Gini index obtained using the response of the income distribution to the GM shock with the mean shift on the left panel and without the mean shift on the right panel. The results confirm that GM shocks reduce inequality. The Gini index decreases sharply initially, and this decline continues over time, although the rate of decrease slows. When the mean shift is taken into account, the decline in the Gini index becomes persistent, though insignificant, which can be attributed to the aggregate output responses. Aggregate output begins to increase five years after the impact and stays positive even after ten years, albeit not significantly, leading to an improvement of inequality in addition to the improvements from the distributional effects.

Figure 20: Impulse Response Functions and Surfaces to GM shocks

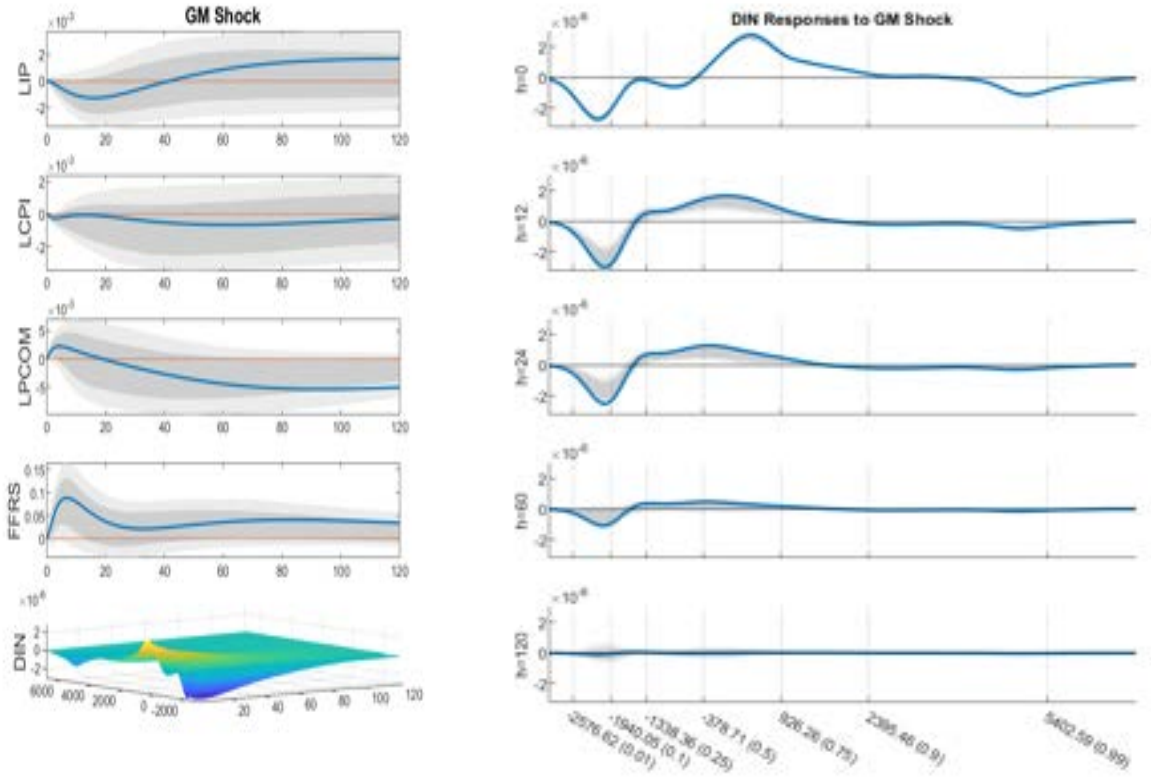

Notes: Presented on the left are IRFs of the aggregate variables and impulse response surfaces of the income distribution to inequality-minimizing GM shock. On the right, presented are the functional impulse response functions - two dimensional slices of the response surface - for the horizons $h = 0, 12, 24, 60$ and 120 months.

Figure 24 shows the forecast error variance decomposition for four aggregate shocks and the GM shock, which is a linear combination of the three DIN shocks satisfying the identifying restriction. We find that the GM shock contributes less to aggregate variables compared to YM shocks. However, GM shocks still account for variations in IP as much as FFRS shocks do and explain variations in $PCOM$ substantially more than FFRS shocks, particularly over longer horizons. Furthermore, GM shocks explain more than half of the variations at all income levels except around the 25th percentile.

The historical decompositions with the equity-targeted GM shock and four aggregate shocks are presented in Figures 25 and 26. From the historical decompositions of the aggregate variables presented in Figure 25, we find that GM shocks' effects have been a negative contribution to output starting from late 1980s, but a positive contribution to commodity prices throughout our sample period, especially from mid-1980s. As shown in Figure 26, the effects of GM shocks on the income distribution have been changing over time. Until the global financial crisis (GFC), GM shocks increase proportions of the bottom 25% and top 25%, but decrease the middle 50%, thereby worsening income inequality. During the GFC and its aftermath (until around 2012), the opposite happens, decreasing inequality. In recent years, GM shocks start increasing inequality again as in the pre-

Figure 21: DIN Responses to Inequality-Minimizing GM Shock without Mean Shift

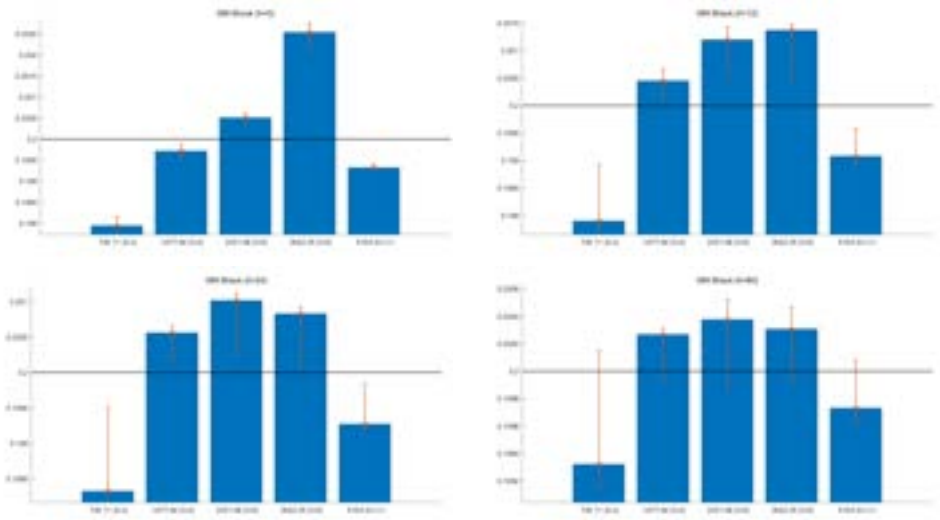

Notes: DIN responses to the inequality minimizing equity-targeted GM shock in histograms for quintile income groups at-impact ($h = 0$, top-left), $h = 12$ months, (top-right), $h = 24$ months (bottom-left) and $h = 60$ months (bottom-right) after the impact. Mean shift by the aggregate output is not considered when computing the changes in income distribution. The numbers on the horizontal axis are the quintile values obtained from the pre-shock income distribution. The black horizontal line signifies the benchmark 20% line, and the vertical line at the top center of each bar represents the 90% confidence interval.

Figure 22: DIN Responses to Inequality-Minimizing GM Shock with Mean Shift

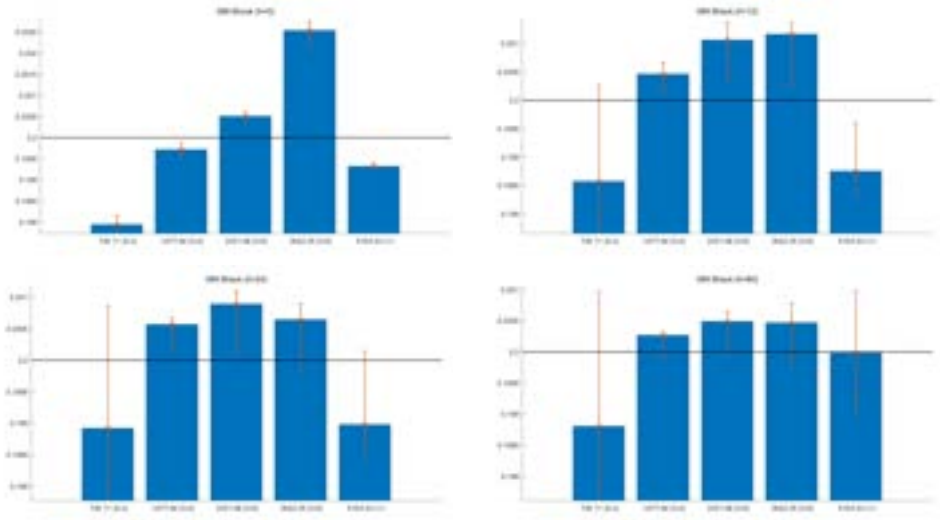

Notes: Responses to the inequality-minimizing equity-targeted GM shock of income distribution *with* the mean shift measured by the changes in aggregate output in histograms for quintile income groups at-impact ($h = 0$, top-left), $h = 12$ months, (top-right), $h = 24$ months (bottom-left) and $h = 60$ months (bottom-right) after the impact. The numbers on the horizontal axis are the quintile values obtained from the income distribution on the month the shock is given. The black horizontal line signifies the benchmark 20% line, and the vertical line at the top center of each bar represents the 90% confidence interval.

Figure 23: IRFs of Gini Index to GM Shock

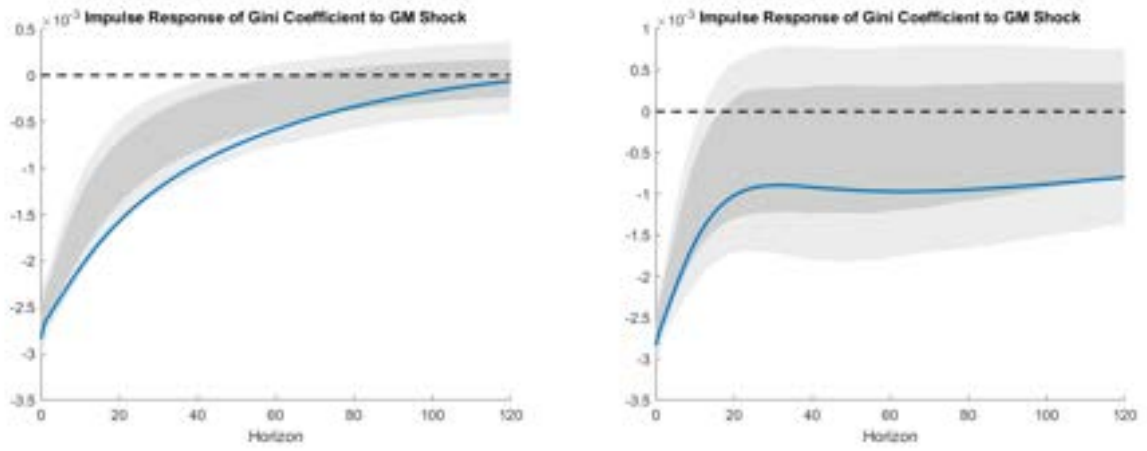

Notes: Impulse response functions of the Gini index to GM shock *without* the mean shift (on the left) and *with* the mean shift (on the right). Shaded bands represent the 68% and 90% confidence intervals.

GFC period. We also observe that GM shocks have contributed negatively to FFRS throughout our sample period.

5.4 Other Possible Income Distribution Shocks and Robustness Checks

In Appendix B, we explore two additional income distribution shocks. First, we examine an income distribution shock that maximizes monetary policy responses, as reflected in the cumulative changes in the shadow Fed funds rate over a five-year horizon. Details of this interest rate-maximizing shock, labeled as the *MP shock*, are provided in Appendix B.1. Second, we consider an income distribution shock that leads to maximal increases in the price level, as reflected in the cumulative changes in the consumer price index (CPI) five years after the impact. Further discussions on this price-maximizing shock, labeled as the *PM shock*, are presented in Appendix B.2. The identification of these shocks follows the same procedure used for the output-maximizing YM shock and the inequality-minimizing GM shock.

We examine the robustness of our benchmark results with respect to the number m of FPCs used to approximate income distributions in Appendix C.

The dimension m of our VAR is determined by the number of the FPCs used to approximate the demeaned density (w_t) with $w_t = (f_t - \overline{f})$. For the choice of m, we simply followed the convention in the literature, which is described in Section 3.2 of Hörmann and Kokoszka (2012) as by finding "a balance between retaining the relevant information in the sample, and the danger of working with the reciprocals of small eigenvalues." Our choice $m = 3$ was made as such. It is important to check the robustness of our results to the choice of m, and we find that our results are quite robust with respect to the choice of m as we show in this section.

We provide explicit evidence on the robustness of our results against the choice of m. We repeat the same analysis on our approximate VAR model with $m = 2$ and $m = 4$, i.e., using two and four

Figure 24: **Variance Decomposition from MAR with GM Shock**

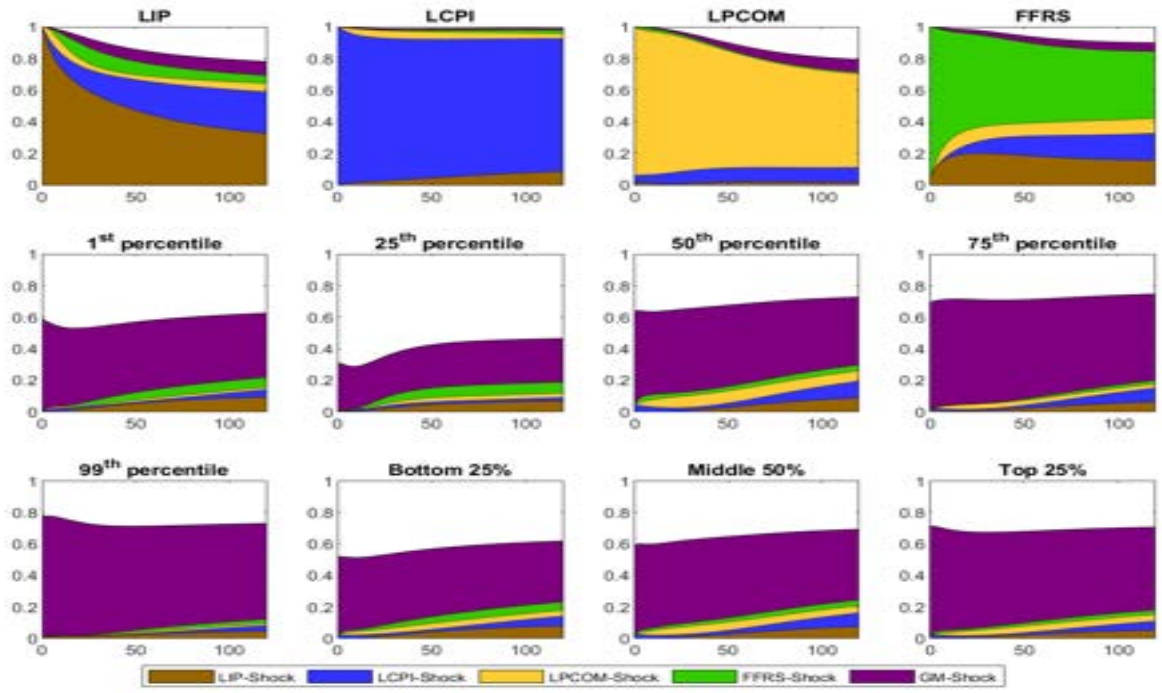

Notes: Presented are the forecast error variance decomposition (FEVD) of the variables in the MAR model attributable to four aggregate shocks and the distributional GM shock. Each shock's contribution is color-coded, with the color codes provided in the legend box at the bottom of them figure. The four panels in the first row present the FEVDs for four aggregate variables. The four panels in the second row and the first panel in the third row present the FEVDs for the proportion of people with income levels in the neighborhood around the first, 25th, 50th, 75th and 99the percentiles of the most recent income distribution, December 2015. The remaining three panels in the third row present the FEVDs for the bottom 25%, middle 50% and top 25% income groups, defined using the average income distribution.

Figure 25: **Historical Decomposition Aggregate Variables from MAR with GM Shock**

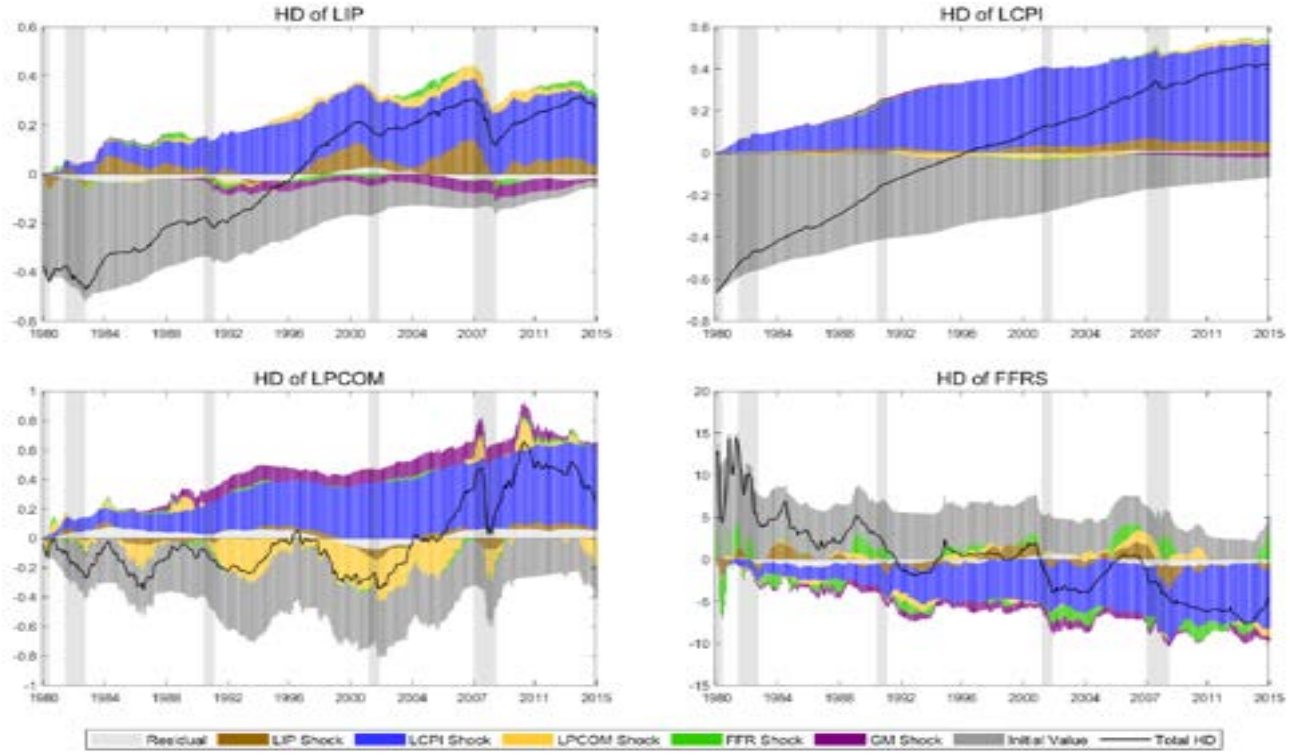

Figure 26: **Variance Decomposition of Income Distribution from MAR with GM Shock**

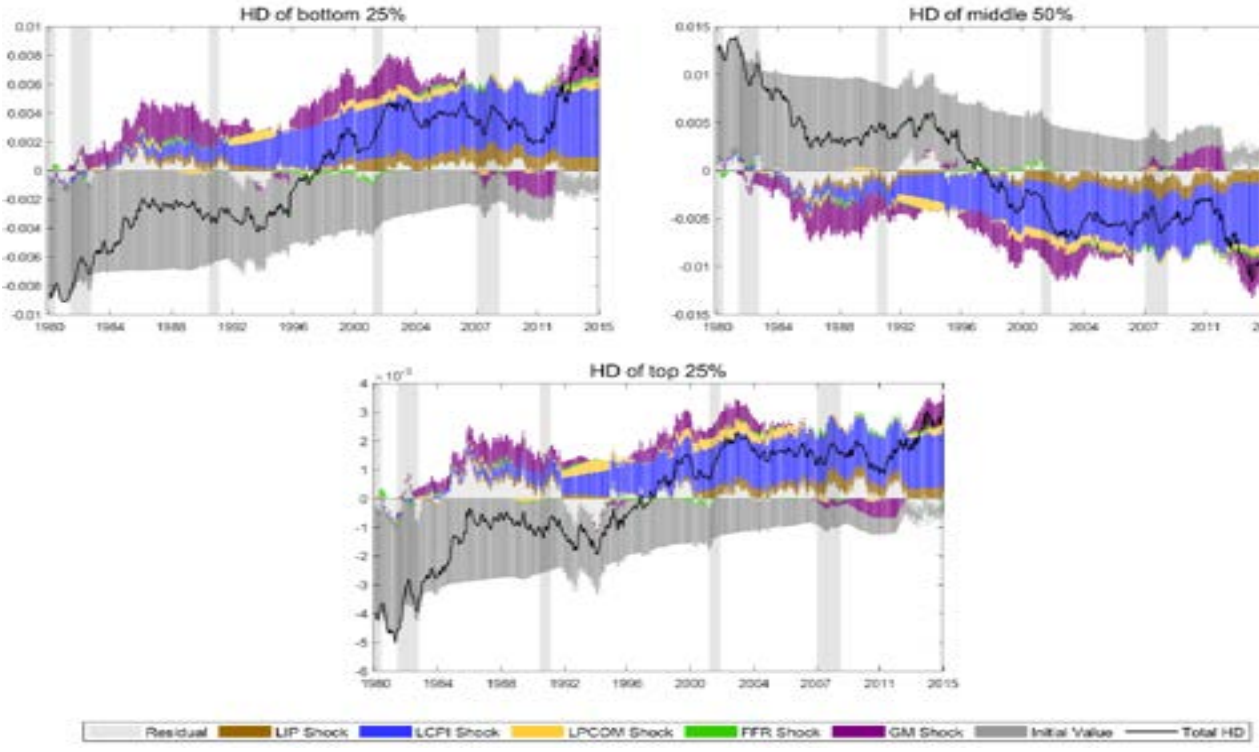

FPCs, instead of three FPCs. When $m = 3$ is chosen optimally, using $m = 2$ allows us to assess the bias incurred by omitting the third FPC. Conversely, using $m = 4$ helps evaluate the robustness of the benchmark results with $m = 3$ to the inclusion of an additional, unnecessary FPC component.

In Appendix C.1 and C.2 , we report key results obtained with two and four FPCs in sequel in the same format as the benchmark results presented in the main text for easy comparisons. As the results below show, all qualitative conclusions remain unchanged with only minor quantitative differences.

6 Conclusion

This paper develops a structural VAR model with functional variables to investigate the interactions between macroeconomic aggregates and income distribution. With this novel empirical approach, we are able to identify and analyze the effects of various shocks to the income distribution on macro aggregates, as well as the effects of macroeconomic shocks on the income distribution. In our empirical applications, we investigate the effects of monetary policy shocks on income distribution and the role of various hypothetical distributional shocks in business cycles. Our main empirical results are as follows. First, contractionary monetary policy shocks worsen inequality, but its role in explaining income inequality changes is relatively small. Second, properly aimed redistributive policies can have huge effects on output and income distribution my without creating the trade-off between growth and inequality.

As demonstrated in the paper, our empirical framework to approximate and analyze functional variables in standard models makes a significant push on methodological front for studying distributional effects of policies. Policymakers are becoming more interested in the distributional effects of their policies, as reflected clearly, for instance, in the recent statements by governors of Federal Reserve, which explicitly mentions their concerns on inequality.[24] As illustrated, our MAR methodology effectively quantifies the distributional effects of monetary policy shocks and identifies income distribution shocks that can be interpreted as outcomes of redistributive policies. This enables us to study their impacts on both macroeconomic variables and income distribution. Consequently, our

[24] Examples include:

- "The Fed provides this help by influencing interest rates. Although we work through financial markets, our goal is to help Main Street, not Wall Street... When the Federal Reserve's policies are effective, they improve the welfare of everyone who benefits from a stronger economy, most of all those who have been hit hardest by the recession and the slow recovery." (https://www.federalreserve.gov/newsevents/speech/yellen20140331a.htm)
- "It is no secret that the past few decades of widening inequality can be summed up as significant income and wealth gains for those at the very top and stagnant living standards for the majority. I think it is appropriate to ask whether this trend is compatible with values rooted in our nation's history, among them the high value Americans have traditionally placed on equality of opportunity." (https://www.federalreserve.gov/newsevents/speech/yellen20141017a.htm)
- "We view maximum employment as a broad and inclusive goal. Those who have historically been left behind stand the best chance of prospering in a strong economy with plentiful job opportunities. Our recent history highlights both the benefits of a strong economy and the severe costs of a weak one." (https://www.federalreserve.gov/newsevents/speech/powell20210503a.htm)

new functional approach has significant potential for widespread use in analyzing the distributional effects of macroeconomic and redistributive policies.

A similarly broad impact could be achieved in other settings where one is interested in describing the effects of aggregate shocks on a distribution of various economic variables such as expected inflation distributions, temperature anomaly distributions or on general functions such as yield curves and employment and labor force participation profiles across ages or occupations, to name a few. We therefore contribute to improving how economists solve and estimate models where distributions matter. Distributions matter when there is heterogeneity or generic uncertainty, which cannot be described only by a few moments or features of a distribution, which is often the case in real-world settings. These models, a prime example of which are the heterogeneous agent new Keynesian (HANK) models, are difficult to solve and estimate precisely because distributions introduce an infinite number of state variables. Our simple and efficient approach to functional data analysis therefore has promising potential to approximate infinite dimensional state variables in heterogenous agent models, estimate them using both macro and micro level data, and conduct counterfactual policy analysis.

References

Aghion, P. (2000). Schumpeterian growth theory and the dynamics of income inequality. Econometrica, 70(3):855–882.

Alesina, A. and Rodrik, D. (1994). Distributive politics and economic growth. Quarterly Journal of Economics, 109(2):465–490.

Amberg, N., Jansson, T., Klein, M., and Rogantini Picco, A. (2022). American economic review: Insights. American Economic Review: Insights, 4(3):289–304.

Aue, A., Norinho, D. D., and Hörmann, S. (2015). On the prediction of functional time series. Journal of the American Statistical Association, 110:378–392.

Banerjee, A. V. and Newman, A. F. (1993). Occupational choice and the process of development. Journal of Political Economy, 101:274–298.

Bosq, D. (2000). Linear Processes in Function Spaces. Springer-Verlag.

Chang, M., Chen, X., and Schorfheide, F. (2021a). Heterogeneity and aggregate fluctuations. Technical report, National Bureau of Economic Research. Working Paper 28853.

Chang, M., Chen, X., and Schorfheide, F. (2022a). Heterogeneity and aggregate fluctuations. Working Paper 28853, National Bureau of Economic Research. https://doi.org/10.3386/w28853.

Chang, Y., Gómez-Rodríguez, F., and Hong, M. G. H. (2022b). The Effects of Economic Shocks on Heterogeneous Inflation Expectations. International Monetary Fund.

Chang, Y., Kim, C., and Park, J. Y. (2016). Nonstationarity in time series of state densities. Journal of Econometrics, 192:152–167.

Chang, Y., Park, J. Y., and Pyun, D. (2021b). From functional autoregressions to vector autoregressions. Working Paper, Indiana University.

Christiano, L. J., Eichenbaum, M., and Evans, C. L. (1996). The effects of monetary policy shocks: Evidence from the flow of funds. Review of Economics and Statistics, 78:16–34.

Christiano, L. J., Eichenbaum, M., and Evans, C. L. (1999). Monetary policy shocks: What have we learned and to what end? In Taylor, J. B. and Woodford, M., editors, Handbook of Macroeconomics, volume 1, pages 65–148. Elsevier.

Christiano, L. J., Eichenbaum, M., and Evans, C. L. (2005). Nominal rigidities and the dynamic effects of a shock to monetary policy. Journal of Political Economy, 113:1–45.

Coibion, O., Gorodnichenko, Y., Kueng, L., and Silvia, J. (2017). Innocent bystanders? monetary policy and inequality. Journal of Monetary Economics, 88(C):70–89.

Forbes, K. (2000). A reassessment of the relationship between inequality and growth. American Economic Review, 90(4):869–887.

Furceri, D., Loungani, P., and Zdzienicka, A. (2018). The effects of monetary policy shocks on inequality. Journal of International Money and Finance, 85(C):168–186.

Hall, P. and Horowitz, J. L. (2007). Methodology and convergence rates for functional linear regression. Annals of Statistics, 35:70–91.

Holm, M., Paul, P., and Tischbirek, A. (2020). The transmission of monetary policy under the microscope. Journal of Political Economy. forthcoming.

Horta, E. and Ziegelmann, F. (2018). Dynamics of financial returns densities: A functional approach applied to the bovespa intraday index. International Journal of Forecasting, 34:75–88.

Hyndman, R. and Ullah, M. (2007). Robust forecasting of mortality and fertility rates: A functional data approach. Computational Statistics and Data Analysis, 51:4942–4956.

Hörmann, S., Kidziński, L., and Hallin, M. (2015). Dynamic functional principal components. Journal of the Royal Statistical Society: Series B (Statistical Methodology), 77:319–348.

Hörmann, S. and Kokoszka, P. (2012). Functional time series. In Handbook of Statistics: Time Series Analysis – Methods and Applications, pages 157–186. Elsevier, Amsterdam.

Inoue, A. and Rossi, B. (2021). A new approach to measuring economic policy shocks, with an application to conventional and unconventional monetary policy. Quantitative Economics, 12(4):1085–1138.

Islam, N. (1995). Growth empirics: A panel data approach. Quarterly Journal of Economics, 110(4):1127–1170.

Kaldor, N. (1957). A model of economic growth. Economic Journal, 67:591–624.

Kneip, A. and Utikal, K. J. (2001). Inference for density families using functional principal component analysis. Journal of the American Statistical Association, 96:519–542.

Kokoszka, P., Miao, H., Reimherr, M., and Taoufik, B. (2018). Dynamic functional regression with application to the cross-section of returns. Journal of Financial Econometrics, 16(3):461–485.

Kokoszka, P. and Reimherr, M. (2017). Introduction to Functional Data Analysis. CRC Press.

Krueger, D. and Perri, F. (2006). Does income inequality lead to consumption inequality? Evidence and theory. Review of Economic Studies, 73:163–193.

Kuznets, S. (1955). Economic growth and income inequality. American Economic Review, 45(1):1–28.

Meeks, R. and Monti, F. (2022). Heterogeneous beliefs and the Phillips curve. Available at SSRN.

Mumtaz, H. and Theophilopoulou, A. (2017). The impact of monetary policy on inequality in the uk. an empirical analysis. European Economic Review, 98(C):410–423.

Paparoditis, E. (2018). Sieve bootstrap for functional time series. Annals of Statistics, 46:3510–3538.

Park, J. Y. and Qian, J. (2012). Functional regression of continuous state distributions. Journal of Econometrics, 167:397–412.

Persson, T. and Tabellini, G. (1994). Is inequality harmful for growth. American Economic Review, 84(3):600–621.

Petersen, A. and Müller, H.-G. (2016). Functional data analysis for density functions by transformation to a Hilbert space. Annals of Statistics, 44:183–218.

Petersen, A., Zhang, C., and Kokoszka, P. (2022). Modeling probability density functions as data objects. Econometrics and Statistics, 21:159–178.

Ramsay, J. O. and Silverman, B. W. (2005). Functional Data Analysis. Springer.

Ramsay, J. O. and Silverman, B. W. (2007). Applied Functional Data Analysis: Methods and Case Studies. Springer.

Sims, C. A. (1980). Macroeconomics and reality. Econometrica, pages 1–48.

Sims, C. A. (1992). Interpreting the macroeconomic time series facts: The effects of monetary policy. European Economic Review, 36 (5):975–1000.

Wu, J. C. and Xia, F. D. (2016). Measuring the macroeconomic impact of monetary policy at the zero lower bound. Journal of Money, Credit and Banking, 48 (2-3):253–291.

Zhang, C., Kokoszka, P., and Petersen, A. (2022). Wasserstein autoregressive models for density time series. Journal of Time Series Analysis, 43:30–52.

Figure A.1: **Cumulative Scree Plot**

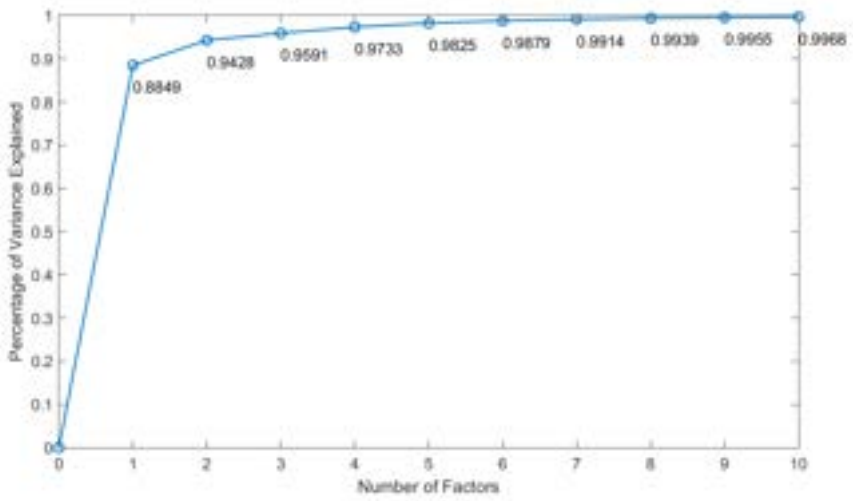

Appendix A Choice of Basis

In this appendix, we focus on details of the comparisons of the functional principal components basis that we employ in this paper and for which we advocate more generally to reasonable alternative bases. Let ℓ denote the number of aggregate variables, which is three in our model. To show how important it is in practice to choose a basis $(v_{\ell+i})$ for the functional variable (f_t), we compare estimators of A based on our basis $(v^*_{\ell+i})$ and other bases generically denoted by $(v_{\ell+i})$. As an alternative to our basis $(v^*_{\ell+i})$, we consider three other bases: a histogram basis given by indicators on a partition of the support of the demeaned income distributions, a quantile basis, and an orthonormalized moment basis. For this comparison, we set (f_t) to be functions defined on the interval $[-2971.58, 6899.39)$. Details of the four alternative bases follow. Note that all the bases are normalized so that $\|v_i\| = 1$.

A.1 Alternative Bases

Functional Principal Component (FPC) Basis. As described in the Section 3, we perform principal components analysis on the sample variance operator Γ of (f_t) given in equation (9), where $e_i(\Gamma)$ denotes the eigenfunction associated with its ith largest eigenvalue. Figure A.1 shows the cumulative scree plot with the first ten eigenvalues of the sample variance operator. The FPC basis is defined by basis function $v^*_{\ell+i}(r) = e_i(\Gamma)$ for $i = 1, \ldots, m$. This is the basis we use for our analysis.

Interval Basis. The interval basis $(v_{\ell+i})$ is given by

$$v_{\ell+i}(r) = \frac{1}{\sqrt{q_i - p_i}} 1\{p_i \leqslant r < q_i\},$$

where $\big([p_i, q_i)\big)$ is a partition of the common support $[p, q)$ with $p = -5.30$ and $q = 5.56$ of the densities (f_t) into m-sub-intervals.[25] Note that

$$\langle v_{\ell+i}, f_t \rangle = \frac{1}{\sqrt{q_i - p_i}} \int_{p_i}^{q_i} f_t(r) dr \approx \frac{1}{\sqrt{q_i - p_i}} \frac{1}{N} \sum_{j=1}^{N} 1\{p_i \leqslant r_{jt} < q_i\},$$

where (r_{jt}) are observations on the demeaned incomes available for cross-sections $j = 1, \ldots, N$ and time periods $t = 1, \ldots, T$,

If we set the length of the sub-intervals $\big([p_i, q_i)\big)$ in the partition to be the same across all $i = 1, \ldots, m$, we call the resulting interval basis $(v_{\ell+i})$ the *histogram basis*. In case that we define the sub-intervals $\big([p_i, q_i)\big)$, $i = 1, \ldots, m$, in the partition to be $(i/m) \times 100$ percentile of the empirical distribution of observations (r_{jt}) on the demeaned income levels for $j = 1, \ldots, N$ and $t = 1, \ldots, T$, the interval basis $(v_{\ell+i})$ is referred in particular to as the *quantile basis*.

Orthonormalized Moment Basis. The orthonormal moment basis $(v_{\ell+i})$ is obtained by the Gram-Schmidt orthogonalization procedure from the pre-basis defined as $u_i(r) = r^i$ for $i \geqslant 1$. We call (u_i) a moment basis because

$$\langle u_i, f_t \rangle = \int r^i f_t(r) dr \approx \frac{1}{N} \sum_{j=1}^{N} r_{jt}^i,$$

where as before (r_{jt}) denote observations on the demeaned incomes available for cross-sections $j = 1, \ldots, N$ and time periods $t = 1, \ldots, T$, and the collection $(\langle u_i, f_t \rangle)$ represents the i-th moments of the demeaned income distributions given by the densities (f_t) for $i \geqslant 1$.

A.2 Computation of FR^2 and Numerical Results

Table A.1 and Figure A.2 show, numerical results and their plots of the functional R-squared from the four sub-bases described above, namely, the FPC, histogram, quantile, and orthornormalized moment bases.

[25] Note that FR^2 is generally not strictly increasing in the number m of basis used for the interval basis, because the basis – i.e., the whole set of basis functions – is different for each n.

m	FPC Basis	Histogram Basis	Quantile Basis	Moment Basis
1	0.8849	0.0201	0.0126	0.0909
2	0.9428	0.0207	0.3314	0.1581
3	0.9591	0.2366	0.4157	0.1694
4	0.9733	0.4208	0.4484	0.2203
5	0.9825	0.3826	0.4674	0.2528
6	0.9879	0.3822	0.4777	0.3052
7	0.9914	0.4103	0.4862	0.3522
8	0.9939	0.4682	0.4944	0.3592
9	0.9955	0.5429	0.5029	0.4276
10	0.9968	0.6320	0.5115	0.5603

Table A.1: FR^2 for four choices of basis

Notes: Presented are numerical results of the functional R-squared computed with the four sub-bases considered for comparison, namely, the FPC, histogram, quantile, and orthornormalized moment bases. The four bases are described in Section A.1 and computation of FR^2 is described in Section A.2. In the first column, m denotes number of bases used.

Figure A.2: FR2 for four choices of basis

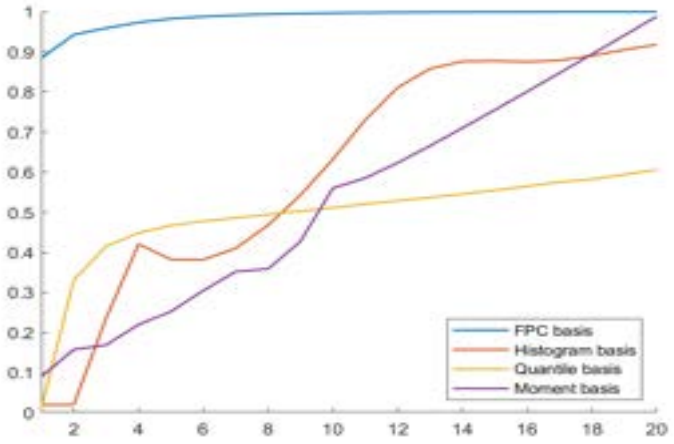

Notes: Presented are plots of the functional R-squared values computed with the four sub-bases considered for comparison, namely, the FPC, histogram, quantile, and orthornormalized moment bases. The four bases are described in Section A.1 and computation of FR^2 is described in Section A.2.

As noted in Section 3, the functional R-squared is defined by equation

$$\mathrm{FR}^2 = \frac{\sum_{t=1}^{T} \|\Pi f_t\|^2}{\sum_{t=1}^{T} \|f_t\|^2},$$

where Π is the Hilbert space projection on V spanned by a sub-basis $(v_{\ell+i})_{i=1}^{m}$.

The (normalized) FPC bases for H are given by the eigenfunctions $(v_i^*)_{i=1}^{T}$ of sample variance operator Γ in (9) associated with nonzero eigenvalues $(\lambda_i)_{i=1}^{T}$. If we let Π^* be the projection on the

subspace V^* spanned by $(v_i^*)_{i=1}^m$, it follows that

$$\sum_{t=1}^{T} \|\Pi f_t\|^2 = \sum_{i=1}^{m} \langle v_i^*, f_t \rangle^2 = T \sum_{i=1}^{m} \lambda_i$$

and

$$\sum_{t=1}^{T} \|f_t\|^2 = \sum_{i=1}^{T} \langle v_i^*, f_t \rangle^2 = T \sum_{i=1}^{T} \lambda_i,$$

since

$$\Pi^* f_t = \sum_{i=1}^{m} \langle v_i^*, f_t \rangle v_i^* \quad \text{and} \quad f_t = \sum_{i=1}^{T} \langle v_i^*, f_t \rangle v_i^*,$$

$\langle v_i^*, \Gamma v_i^* \rangle = \lambda_i$ for $i = 1, \ldots, T$ and $\langle v_i^*, \Gamma v_j^* \rangle = 0$ for all $i \neq j$. Note that

$$\lambda_i = \langle v_i^*, \Gamma v_i^* \rangle = \frac{1}{T} \sum_{t=1}^{T} \langle v_i^*, f_t \rangle^2$$

for $i = 1, \ldots, T$. Clearly, the choice of the basis (v_i) only affects $\sum_{t=1}^{T} \|\Pi f_t\|^2$, not $\sum_{t=1}^{T} \|f_t\|^2 = T \sum_{i=1}^{T} \lambda_i$.

Table A.1 and Figure A.2 show, numerical results and their plots of the functional R-squared from the four sub-bases described above, namely, the FPC, histogram, quantile, and orthornormalized moment bases. We note that FR2 may not strictly increasing in the number m of the basis used for the histogram basis, since the basis used is different for each case of m. For example, having just two indicator bases of equal length has higher FR2 than having three indicator bases of equal length. This happens because there is more variation in the functions between negative and positive values of the domain compared to the variation in the partition made by three intervals of equal length. The results are discussed in Section 3.

A.3 Computations of Integrated Variances and Numerical Results

As Table A.1 illustrates, we can make the FR^2 arbitrarily large for any given basis (v_i) simply by increasing the number of basis functions m. However, doing so comes at a cost. The variance of the estimator $\widehat{A}$ for the autoregressive operator A is expected to increase with m, and it can increase very sharply and become explosive even when m is moderately large. It is therefore prudent to investigate this rate of increase.

Below we discuss how we compute integrated variances (IVARs). Let $\widehat{A}_k$ be the estimator obtained from $\widehat{(A_k)}$ by $\widehat{A}_k = \pi^{-1}\big(\widehat{(A_k)}\big)$, which we may regard more explicitly as the estimator of $\overline{A}_k = \pi^{-1}\big((A_k)\big) = PA_kP$ for $k = 1$ or 2, and let

$$\widehat{A} = \begin{pmatrix} \widehat{A}_1 \\ \widehat{A}_2 \end{pmatrix} \quad \text{and} \quad \overline{A} = \begin{pmatrix} \overline{A}_1 \\ \overline{A}_2 \end{pmatrix},$$

which are operators from H to $H \times H$. Furthermore, we define

$$Q = \begin{pmatrix} P & 0 \\ 0 & P \end{pmatrix} \quad \text{and} \quad \Lambda = \frac{1}{T} \sum_{t=1}^{T} \left[\begin{pmatrix} z_t \\ z_{t-1} \end{pmatrix} \otimes \begin{pmatrix} z_t \\ z_{t-1} \end{pmatrix} \right]$$

for the MAR(2) model of Section 3. Here, P is the Hilbert space projection defined by $Pz = \sum_{i=1}^{n}\langle v_i, z\rangle v_i$ where z is defined as $(x, f)'$ with x being a ℓ-dimensional vector of aggregate variables. Now, (v_i) is the basis in the extended Hilbert space $R^l \times H$.

Then the MSE of $\widehat{A}$ is given by

$$\mathbb{E}\|\widehat{A} - \overline{A}\|^2 = \mathbb{E}\|\widehat{A} - \mathbb{E}\widehat{A}\|^2 + \|\mathbb{E}\widehat{A} - \overline{A}\|^2,$$

where $\|\cdot\|$ denotes the Hilbert-Schmidt norm in H. The MSE of $\widehat{A}$ is thus decomposed into the variance and the squared bias terms. The variance term of $\widehat{A}$, which is the integrated variance (IVAR), is approximately given by

$$(\operatorname{trace}\Omega)\big(\operatorname{trace}(Q\Lambda Q)^+\big),$$

where Ω is the variance operator of (ε_t) defined in Section 3, and $(Q\Lambda Q)^+$ is the inverse of the bounded linear operator $Q\Lambda Q$ restricted to the subspace $V \times V$ of $H \times H$. For the sake of completeness, the squared bias term of $\widehat{A}$ is approximately given by

$$\|A(1-Q)\Lambda Q(Q\Lambda Q)^+\|^2,$$

where A is defined from A_1 and A_2 similarly to $\widehat{A}$ and $\overline{A}$.

We also compute the variance of the functional variables (f_t) conditionally on the aggregate variables x_t. The inverse $(Q\Lambda Q)^+$ defined above may be written as

$$\Gamma = (Q\Lambda Q)^+ = \left(\frac{1}{T}\sum_{t=1}^{T}\left[\begin{pmatrix} x_t \\ (f)_t \\ x_{t-1} \\ (f)_{t-1}\end{pmatrix}\begin{pmatrix} x_t \\ (f)_t \\ x_{t-1} \\ (f)_{t-1}\end{pmatrix}'\right]\right)^+,$$

so that the conditional variance $\Gamma_{f\cdot x}$ of functional variables (f_t) on the aggregate variables x_t is given by

$$\Gamma_{f\cdot x} = \Gamma_{ff} - \Gamma_{fx}\Gamma_{xx}^{-1}\Gamma_{xf}$$

where Γ_{ff}, Γ_{fx} and Γ_{xx} denote, respectively, the unconditional variance of (f_t), covariance between (f_t) and x_t and variance of x_t.

Figure A.3 compares the conditional IVARs for the four choices of basis for the number m of bases upto 10. The actual values of IVARs for some cases are too huge to fit in the table cells, so we report the IVARs scaled by 10^{-8}.

Table A.1 and Figure A.2 show, numerical results and their plots of the functional R-squared from the four sub-bases described above, namely, the FPC, histogram, quantile, and orthornormalized moment bases. We note that FR2 may not strictly increasing in the number m of the basis used for the histogram basis, since the basis used is different for each case of m. For example, having just two indicator bases of equal length has higher FR2 than having three indicator bases of equal length. This happens because there is more variation in the functions between negative and positive values of the domain compared to the variation in the partition made by three intervals of equal length. The results are discussed in Section 3.

m	FPC Basis	Indicator Basis	Quantile Basis	Moment Basis
1	0.879	22.069	14.899	5.029
2	3.101	91.525	33.281	24.238
3	4.872	218.963	63.504	73.155
4	10.546	522.272	91.327	127.847
5	14.279	1234.047	124.681	246.410
6	18.923	2179.446	169.958	402.601
7	24.042	4372.095	238.313	720.407
8	34.486	7561.455	328.062	1138.031
9	43.466	16222.373	515.494	1831.119
10	60.725	32001.877	798.174	2798.105

Table A.2: Conditional Integrated Variances

Notes: Presented are numerical results of the variance factor, trace $(\Gamma_{f \cdot x})$, of the conditional integrated variance (IVARs) discussed in Section A.1 computed, for comparison, using four bases, namely, the FPC, histogram, quantile, and orthornormalized moment bases. The IVARs are computed for each basis with the given number m of basis functions, $m = 1, \ldots, 10$. The actual values of IVARs for some cases are too huge to fit in the table cells, so we report the IVARs scaled by 10^{-8}.

Figure A.3: Conditional Integrated Variances

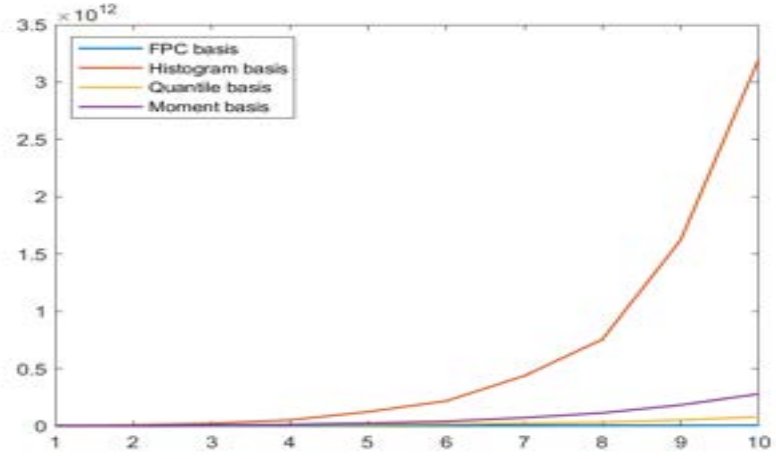

Notes: Plots of the variance factor, trace $(\Gamma_{f \cdot x})$, of the conditional integrated variance (IVARs) discussed in Section A.1 computed, for comparison, using four bases, namely, the FPC, histogram, quantile, and orthornormalized moment bases. The IVARs are computed for each basis with the given number m of basis functions, $m = 1, \ldots, 10$. Four lines show the plots of the IVARs computed using the four bases with m of bases, for $m = 1, \ldots, 10$, as shown in x-axis.

Figure B.1: Impulse Response Functions and Surfaces to MP-Shock

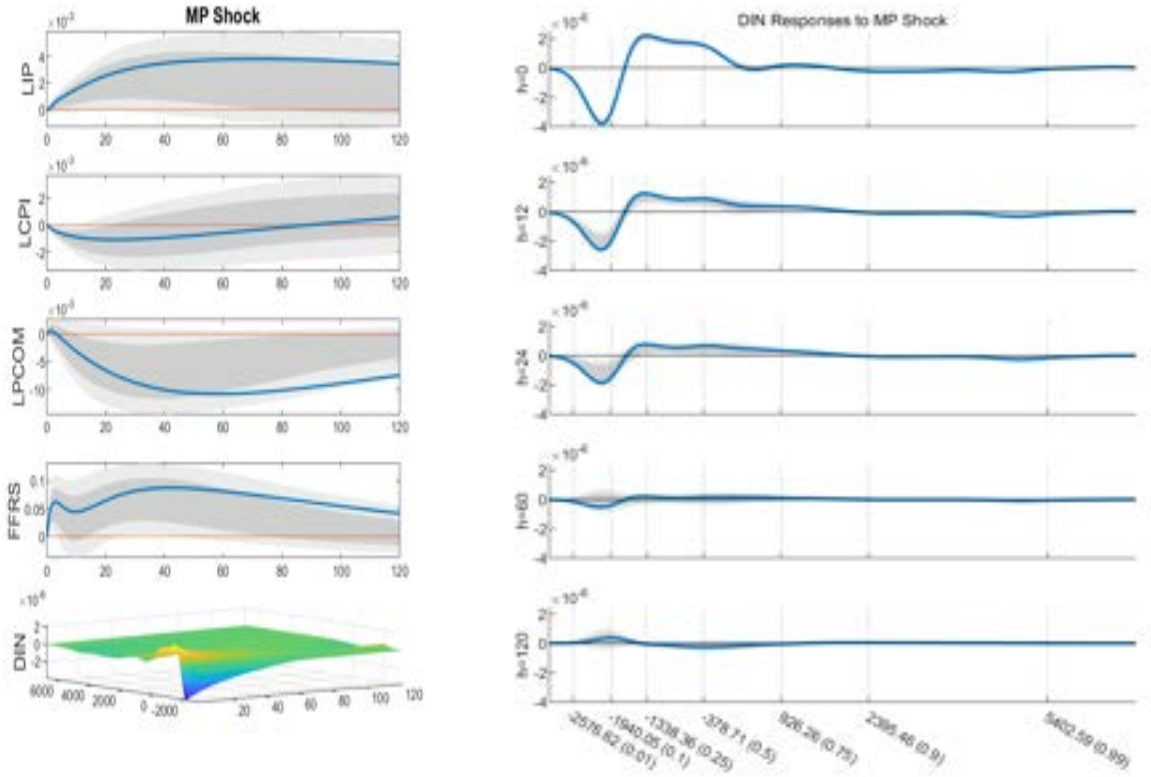

Notes: Presented on the left are IRFs of the aggregate variables and impulse response surfaces of the income distribution to interest rate-maximizing MP-shock. On the right, presented are the functional impulse response functions - two dimensional slices of the response surface - for the horizons $h = 0, 12, 24, 60$ and 120 months.

Appendix B Alternate Income Distribution Shocks

B.1 Interest Rate-Maximizing MP-Shock

We consider an income distribution shock that induces maximal monetary policy responses reflected in the changes in the FFRS. To identify this income distribution shock, we follow the same procedure used to construct the output maximizing YM shock and Gini index minimizing GM shock with a different target horizon. Since effects of monetary policies are considered temporary or short-run, we find the linear combination of the three functional income distribution shocks that leads to most positive cumulative changes in the Federal funds rate upto five years after the impact date. We consider five-year, instead of ten-year, horizons because monetary policy, used as a tool for stabilization over a business cycle horizon, does not tend to respond to the same direction for a long time. We refer this policy interest rate maximizing income distribution shock as *MP-shock*. In our empirical study, we find the weights for the combination to be $(0.54, 0.84, -0.03)$.

B.2 Price-Maximizing PM-Shock

We consider an income distribution shock that induces maximal price level increases reflected in the changes in the variable CPI. To identify this income distribution shock, we follow the same procedure used to construct the output maximizing YM shock and Gini index minimizing GM shock with a different target horizon. Since we would like to check the issue for a business cycle horizon,

Figure B.2: DIN Responses to Interest Rate-Maximizing MP-Shock

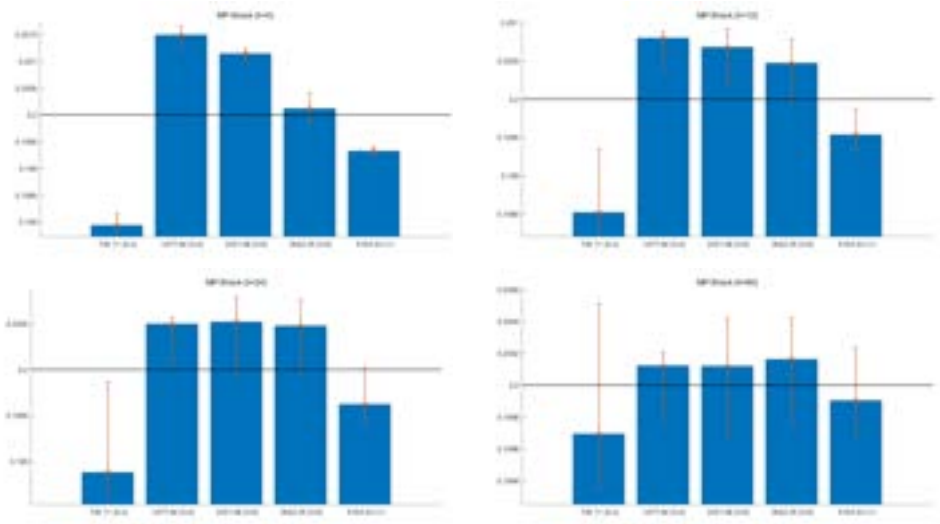

Notes: DIN responses to the FFR maximizing MP-shock in histograms for quintile income groups at-impact ($h = 0$, top-left), $h = 12$ months, (top-right), $h = 24$ months (bottom-left) and $h = 60$ months (bottom-right) after the impact. The numbers on the horizontal axis are the quintile values obtained from the income distribution on the month the shock is given. The black horizontal line signifies the benchmark 20% line, and the vertical line at the top center of each bar represents the 90% confidence interval. Mean shift by the aggregate output is not considered when computing the changes in income distribution.

Figure B.3: DIN Responses to Interest Rate-Maximizing MP-Shock with Mean Shift

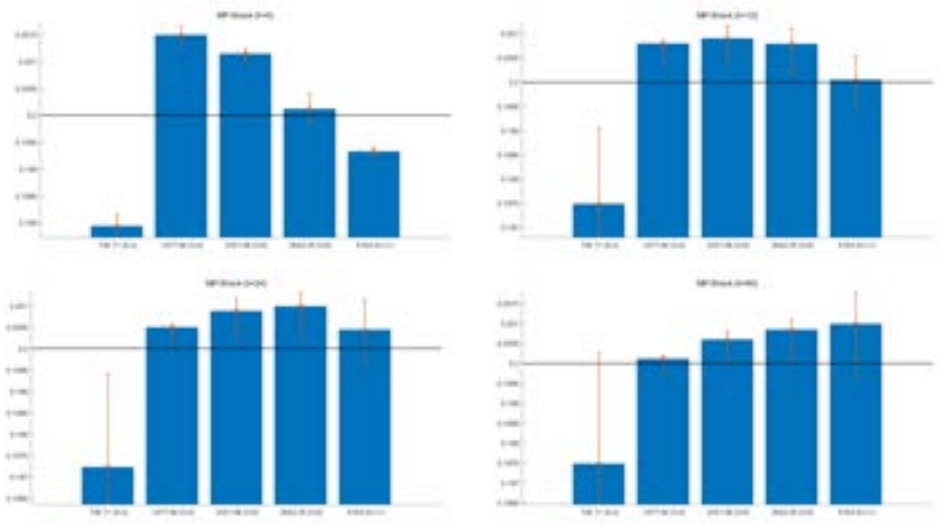

Notes: Responses to the FFR maximizing MP-shock of income distribution *with* the mean shift by the aggregate output in histograms for quintile income groups at-impact ($h = 0$, top-left), $h = 12$ months, (top-right), $h = 24$ months (bottom-left) and $h = 60$ months (bottom-right) after the impact. The numbers on the horizontal axis are the quintile values obtained from the income distribution on the month the shock is given. The black horizontal line signifies the benchmark 20% line, and the vertical line at the top center of each bar represents the 90% confidence interval. Mean shift by the aggregate output is taken into account.

Figure B.4: **Variance Decomposition from MAR with MP Shock**

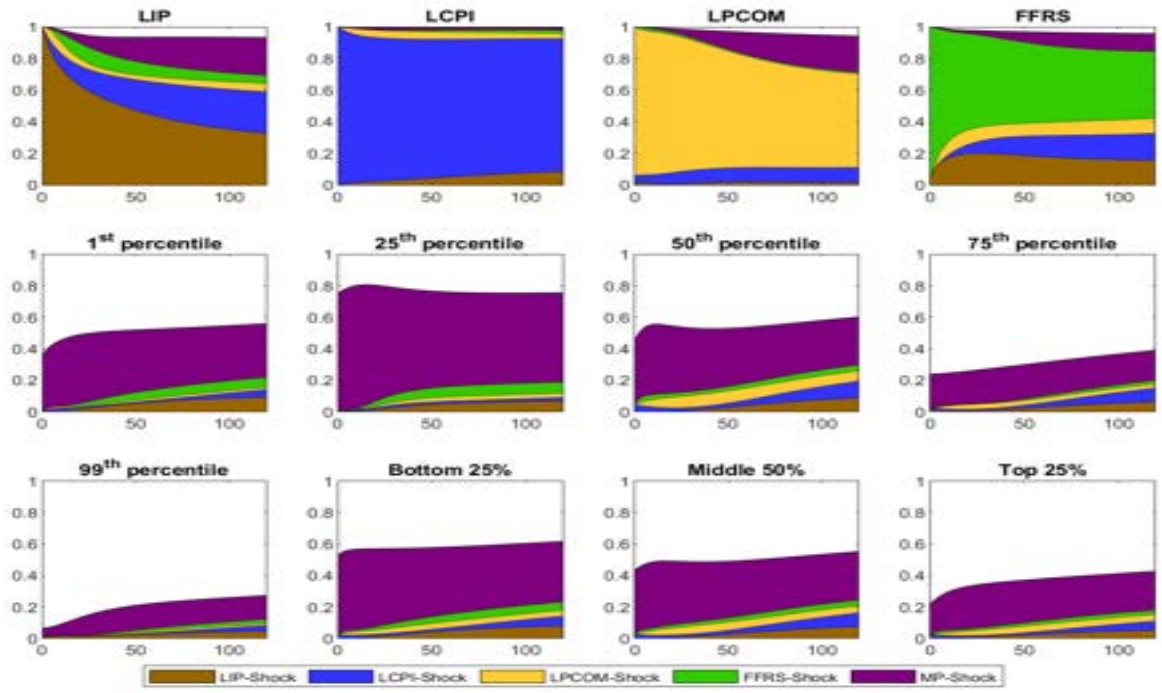

Notes: Presented are the forecast error variance decomposition (FEVD) of the variables in the MAR model attributable to four aggregate shocks and the interest rate-maximizing PM-shock. The contribution from each shock is color-coded, and the color codes are given in the legend box at the bottom of them figure. The four panels in the first row present the FEVDs for four aggregate variables. The four panels in the second row and the first panel in the third row present the FEVDs for the proportion of people with income levels in the neighborhood around the first, 25th, 50th, 75th and 99the percentiles of the most recent income distribution, December 2015. The remaining three panels of the third row presents the FEVDs for the bottom 25%, middle 50% and top 25% income groups computed from the average income distribution.

Figure B.5: Impulse Response Functions and Surfaces to PM-Shock

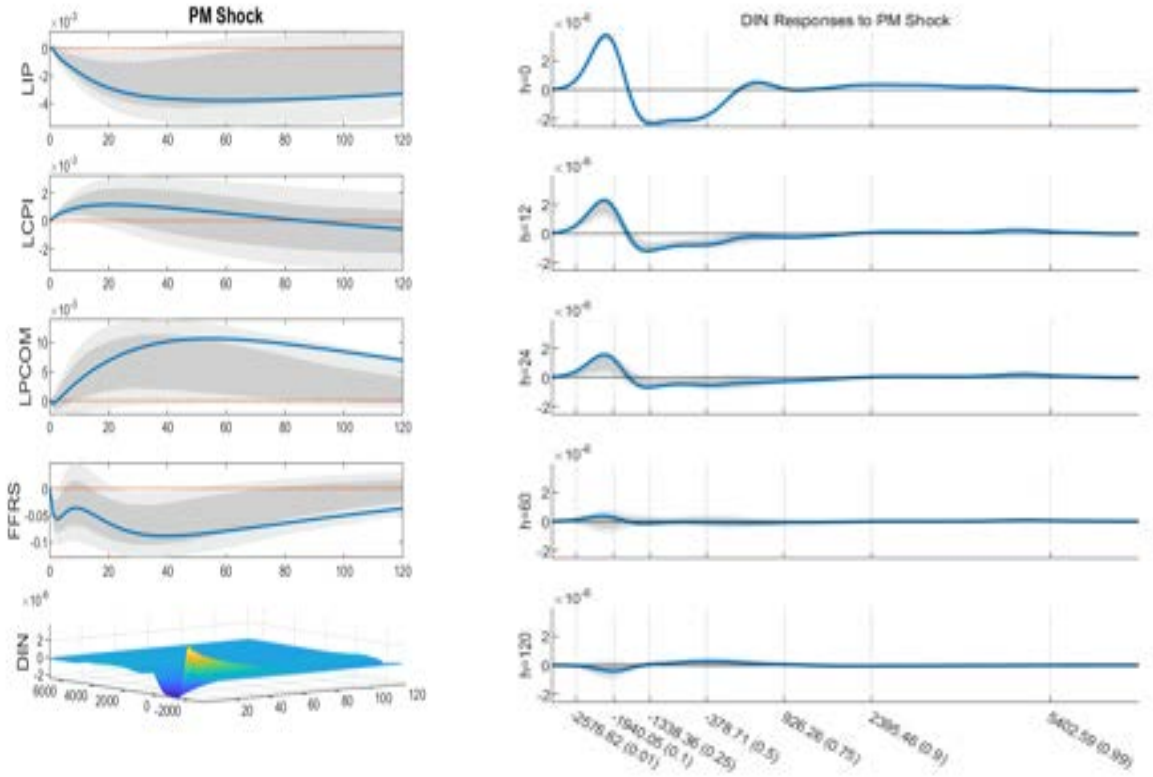

Notes: Presented on the left are IRFs of the aggregate variables and impulse response surfaces of the income distribution to price-maximizing PM-shock. On the right, presented are the functional impulse response functions - two dimensional slices of the response surface - for the horizons $h = 0, 12, 24, 60$ and 120 months.

we set the target horizon at five years to identify the income distribution shock that has most impact on aggregate price level, as we did to identify the interest-rate maximizing shock. We therefore find the linear combination of the three functional income distribution shocks that leads to most positive cumulative changes in the price level upto five years after the impact date. We refer this price level maximizing income distribution shock as *PM-shock*. The weights used to construct the PM shock are $(-0.54, -0.83, -0.13)$.

Appendix C Appendix: Robustness Checks - Choice of m

In this section, we examine the robustness of our results with respect to the number m of FPCs used to approximate income distributions.

The dimension m of our VAR is determined by the number of the FPCs used to approximate the demeaned density (w_t) with $w_t = (f_t - \overline{f})$. For the choice of m, we simply followed the convention in the literature, which is described in Section 3.2 of Hörmann and Kokoszka (2012) as by finding "a balance between retaining the relevant information in the sample, and the danger of working with the reciprocals of small eigenvalues." Our choice $m = 3$ was made as such. It is important to check the robustness of our results to the choice of m, and we find that our results are quite robust with respect to the choice of m as we show in this section.

We provide explicit evidence on the robustness of our results against the choice of m. We repeat

Figure B.6: DIN Responses to Price-Maximizing PM-Shock

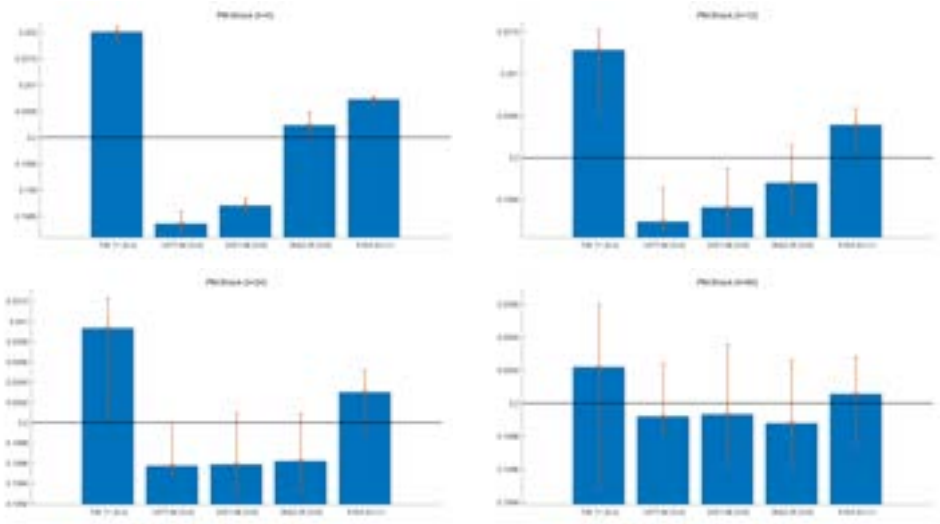

Notes: DIN responses to the Price maximizing PM-shock in histograms for quintile income groups at-impact ($h = 0$, top-left), $h = 12$ months, (top-right), $h = 24$ months (bottom-left) and $h = 60$ months (bottom-right) after the impact. The numbers on the horizontal axis are the quintile values obtained from the income distribution on the month the shock is given. The black horizontal line signifies the benchmark 20% line, and the vertical line at the top center of each bar represents the 90% confidence interval. Mean shift by the aggregate output is not considered when computing the changes in income distribution.

the same analysis on our approximate VAR model with $m = 2$ and $m = 4$, i.e., using two and four FPCs, instead of three FPCs. When $m = 3$ is chosen optimally, using $m = 2$ allows us to assess the bias incurred by omitting the third FPC. Conversely, using $m = 4$ helps evaluate the robustness of the benchmark results with $m = 3$ to the inclusion of an additional, unnecessary FPC component.

We report key results obtained with two FPCs in Section C.1 and those obtained with four FPCs in Section C.2 in the same format as the benchmark results presented in the main text for easy comparisons. As the results show, all qualitative conclusions remain unchanged only with some minor quantitative differences.

C.1 MAR Approximated by Two FPCs

The key results obtained with two FPCs are presented in the figures in this subsection with $m = 2$ in their titles, from Figure C.1 to Figure C.10.

C.2 MAR Approximated by Four FPCs

Similarly, this subsection presents the same set of key results obtained with four FPCs in the figures with $m = 4$ in their titles, from Figure C.11 to Figure C.20.

Appendix D Using Density for a Distributional Variable

There are different ways of representing income distributions and investigating their fluctuations over time. In the paper, we use the density functions of income distributions to empirically analyze the dynamic interactions of income distributions with other aggregate macro variables in our MAR. This is mainly because the density is the most direct and intuitive way of defining a distributional

Figure B.7: DIN Responses to Price-Maximizing PM-Shock with Mean Shift

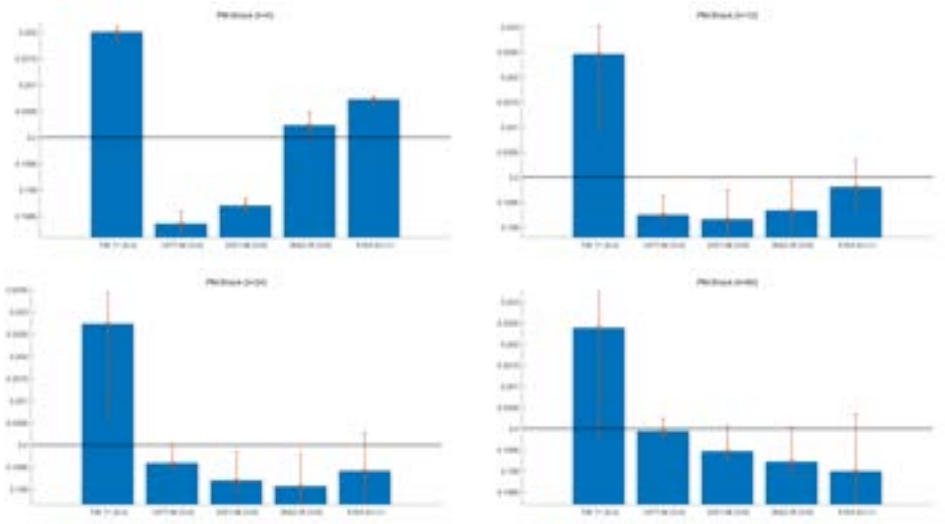

Notes: Responses to the price maximizing PM-shock of income distribution *with* the mean shift by the aggregate output in histograms for quintile income groups at-impact ($h = 0$, top-left), $h = 12$ months, (top-right), $h = 24$ months (bottom-left) and $h = 60$ months (bottom-right) after the impact. The numbers on the horizontal axis are the quintile values obtained from the income distribution on the month the shock is given. The black horizontal line signifies the benchmark 20% line, and the vertical line at the top center of each bar represents the 90% confidence interval. Mean shift by the aggregate output is taken into account.

variable, and using the density makes it possible to nicely relate and compare our results with the conventional approaches based on the indicator basis and the moment basis. Unfortunately, however, the functional data analysis is typically done in the Hilbert space of square integrable functions, which is not most suitable for the analysis of density functions that are subject to two restrictions: non-negativity and unit integral. The set of square integrable density functions is only a subset, *not* a subspace, of the Hilbert space of square integrable functions, which implies that the set of density functions itself is not a Hilbert space. Therefore, it is impossible to use the existing methodology developed for functional data analysis.

However, MARs with constant term for any set of variables including functional variables as well as aggregate variables are equivalent to MARs without constant term defined by the same set of aggregate and functional variables after after they are demeaned. As a result, our functional variable may be effectively analyzed by demeaned density functions in a Hilbert space defined as

$$H = \left\{ f : K \to R \,\middle|\, \int f(r)\, dr = 0, \int f(r)^2 dr < \infty \right\},$$

where we let K be a bounded subset of R, and integrals are defined over K. As discussed earlier, H is a Hilbert space as a subspace of the Hilbert space of square integrable functions. In our empirical analysis, we thus assume that the demeaned densities of income distributions are generated by a functional time series taking values in the Hilbert space H. This allows us to use the standard methodology for functional data analysis to analyze our MAR. Our framework is used by, e.g., Kneip and Utikal (2001) to perform inferences on density functions.

A density recovered by adding an element in H to the mean density or any other reference density has unit integral. However, it may have negative parts. Our empirical analysis focuses not on densities themselves but on demeaned densities, and therefore, this problem does not arise on

Figure B.8: **Variance Decomposition from MAR with PM Shock**

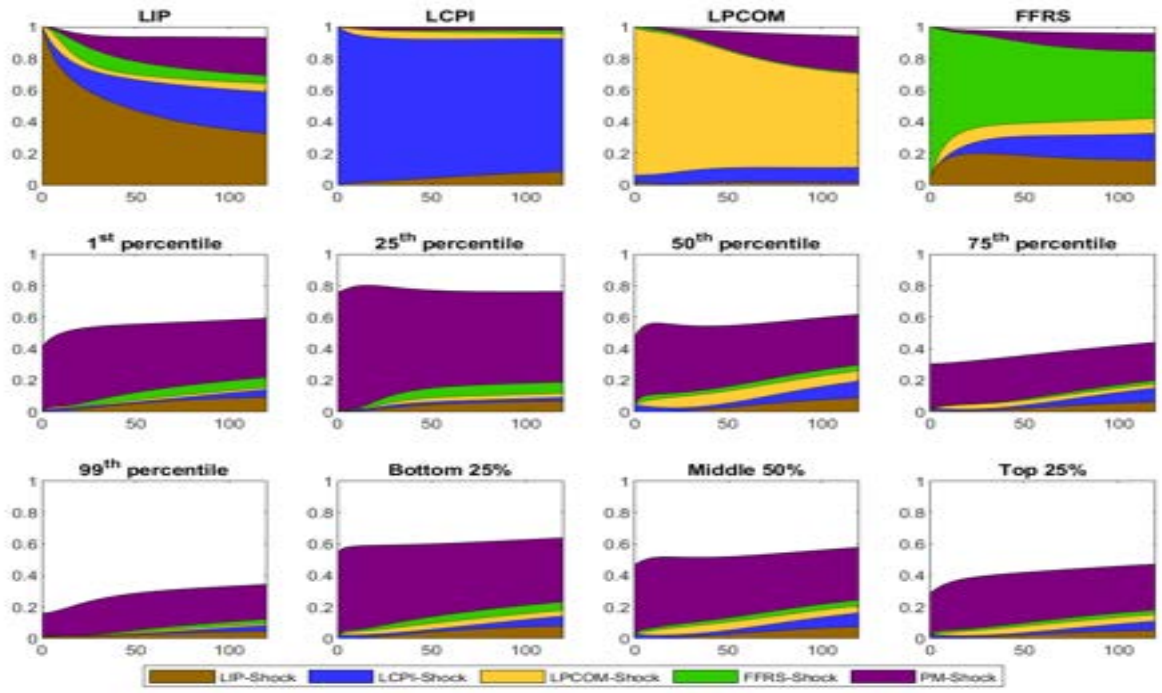

Notes: Presented are the forecast error variance decomposition (FEVD) of the variables in the MAR model attributable to four aggregate shocks and the price-maximizing PM-shock. The contribution from each shock is color-coded, and the color codes are given in the legend box at the bottom of them figure. The four panels in the first row present the FEVDs for four aggregate variables. The four panels in the second row and the first panel in the third row present the FEVDs for the proportion of people with income levels in the neighborhood around the first, 25th, 50th, 75th and 99the percentiles of the most recent income distribution, December 2015. The remaining three panels of the third row presents the FEVDs for the bottom 25%, middle 50% and top 25% income groups computed from the average income distribution.

Figure C.1: Impulse Response Functions and Surfaces to Contractionary Monetary Policy Shocks with $m = 2$

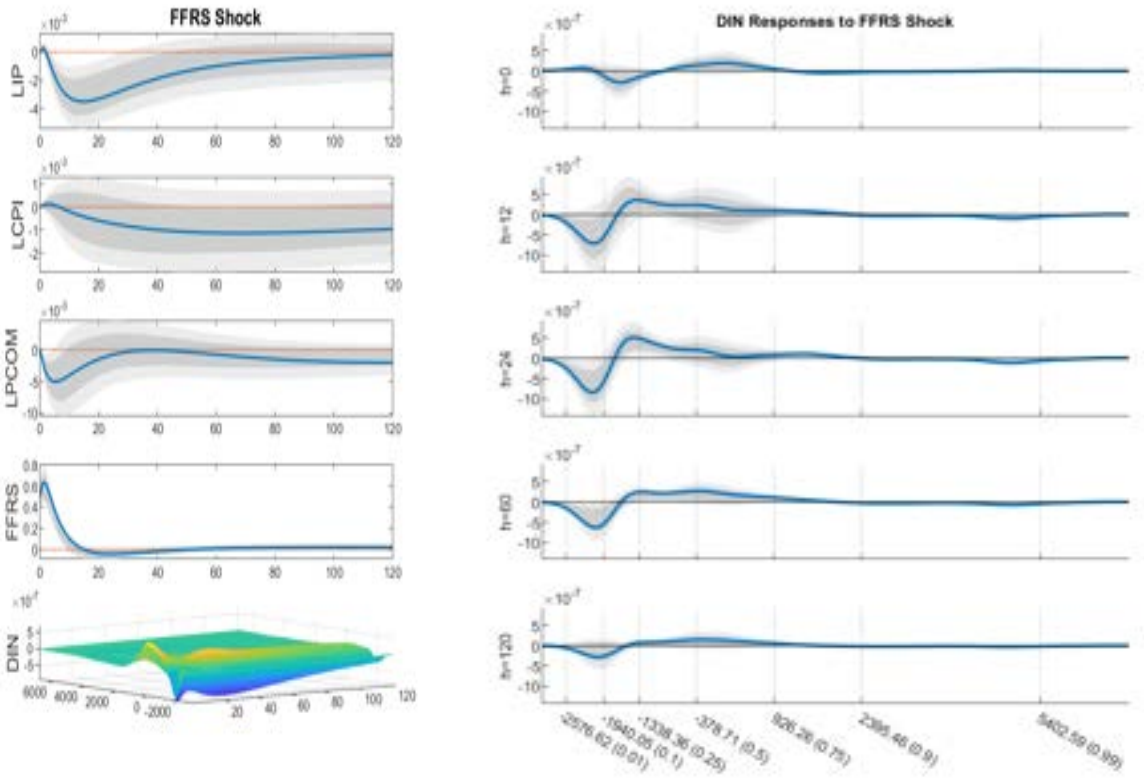

Notes: On the left are IRFs of the aggregate variables and impulse response surface of the income distribution to contractionary monetary policy shocks. On the right, the functional impulse responses of the demeaned income distribution - two dimensional slices of the response surface - are shown for the horizons $h = 0, 12, 24, 60$ and 120 months, with the y-axis indicating the response and the x-axis representing quantile values (1%, 10%, 25%, 50%, 75%, 90% and 99%). Shaded bands represent the 68% and 90% confidence intervals.

the surface. In our structural MAR analysis, negative probabilities may be implied by the reference density and counter-factual functional responses obtained from H. However, we don't think this causes any serious problem. The interested reader is referred to https://en.wikipedia.org/wiki/negative_probability for the use of negative probabilities in various fields. In fact, we didn't have any negative probabilities in our presentations of the responses of income distributions in quintile and decile income groups to various macro shocks. Of course, if necessary, we may just replace negative values of densities by zeros and renormalize them, although this introduces adjustment errors in addition to the errors incurred by approximating infinite dimensional functions to finite dimensional vectors.

As an alternative to density functions for distributional variables, we may use other functions representing the same distributional information in our MAR. The simplest option is to use log-density functions. In this case, the non-negativity is ensured though the unit integral is generally violated. Petersen and Müller (2016) and Horta and Ziegelmann (2018) explore novel frameworks to analyze distributional observations in a Hilbert space not directly relying on density functions. In particular, Petersen et al. (2022) and Zhang et al. (2022), among others, illustrate the use of some concrete transformations of density functions in practical applications. It is certainly possible to use any of these transformations of density functions, instead of density functions themselves, in

Figure C.2: Distributional Effects of Contractionary Monetary Policy Shocks with $m = 2$

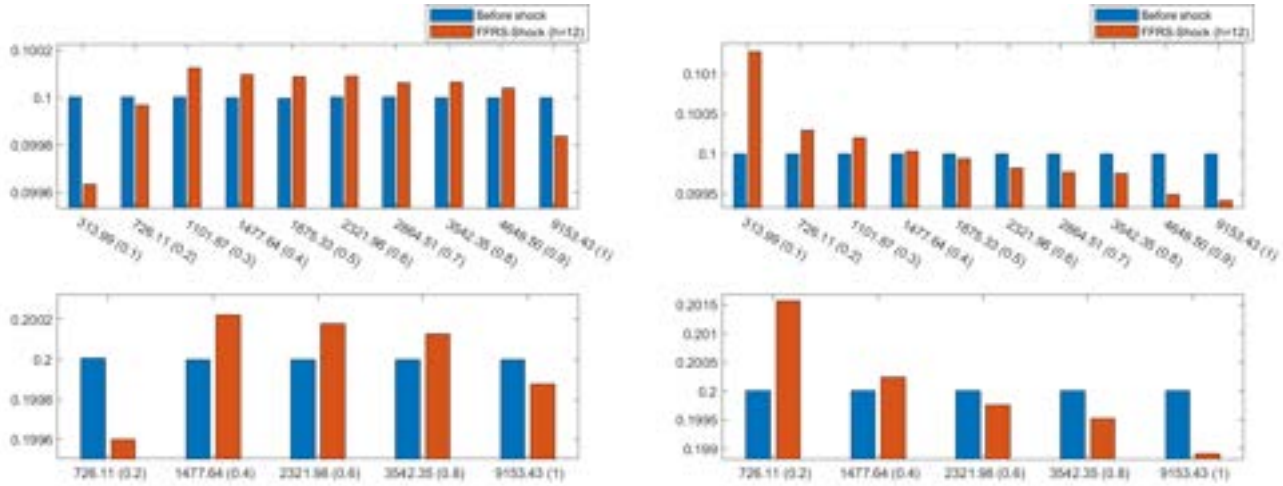

Notes: Presented are the DIN responses to contractionary monetary policy shocks one year after the impact in histograms. The top (bottom) panel on the left shows how the income distribution changes *without* the mean shift for decile (quintile) income groups. Similarly, the top (bottom) panel on the right shows those obtained *with* the mean shift for decile (quintile) income groups.

Figure C.3: IRFs of Gini Index to Contractionary Monetary Policy Shocks with $m = 2$

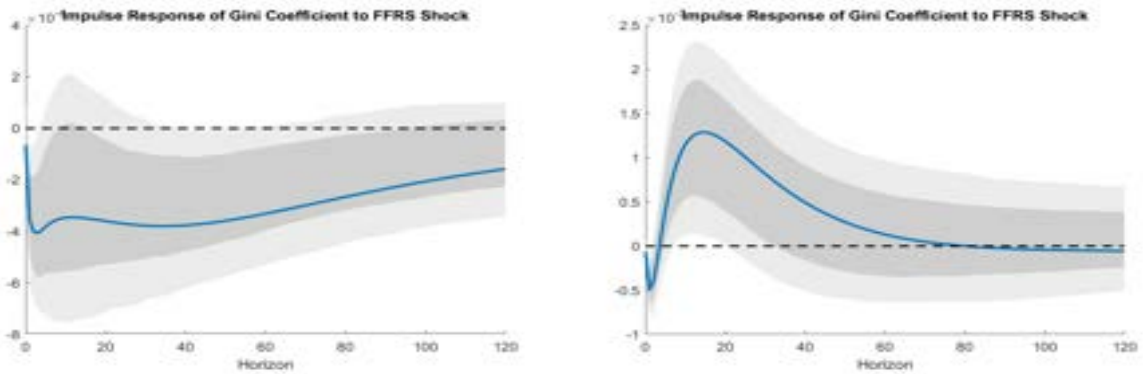

Notes: Presented are the impulse response functions of the Gini index computed from the income distribution over a 10-year horizon, *without* the mean shift (left) and *with* the mean shift (right). Shaded bands represent the 68% and 90% confidence intervals.

Figure C.4: **Variance Decomposition from MAR with DIN Shock with $m = 2$**

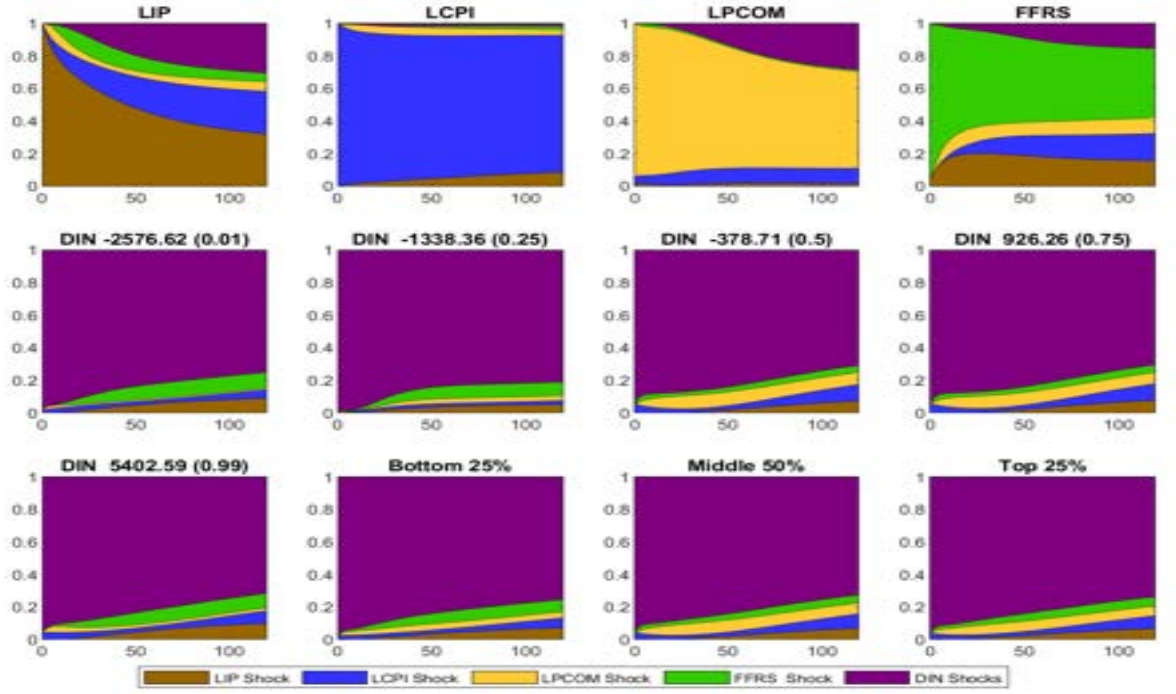

Notes: Presented are the forecast error variance decomposition (FEVD) of the variables in the MAR model attributable to four aggregate shocks and one income distribution shock. Each shock's contribution is color-coded, with the color codes provided in the legend box at the bottom of the figure. The four panels in the first row show the FEVDs for four aggregate variables. The four panels in the second row and the first panel in the third row present the FEVDs for the proportions of the population at income levels around the 1st, 25th, 50th, 75th, and 99th percentiles of the most recent income distribution, December 2015. The remaining three panels in the third row present the FEVDs for the bottom 25%, middle 50%, and top 25% income groups, defined using the historical average income distribution.

our empirical analysis. However, this has not been done in our paper, mainly because of the two reasons. First, we see some clear advantages of using density functions, as discussed above, while there is no such clear advantage of using their transformations. Second, the MAR relying on a transformation of density functions is a different model and not directly comparable with our MAR relying on density functions themselves.

Appendix E Conventional SVAR

This section presents the conventional SVAR as a special case of our MAR with only aggregate variables. If we simply use *Gini* to refer to Gini index for inequality, in place of the income distribution (f_t), our specification of $[B]$ reduces to

$$\begin{pmatrix} \varepsilon_t^{IP} \\ \varepsilon_t^{CPI} \\ \varepsilon_t^{PCOM} \\ \varepsilon_t^{FFRS} \\ \varepsilon_t^{Gini} \end{pmatrix} = \begin{pmatrix} b_{11} & 0 & 0 & 0 & 0 \\ b_{21} & b_{22} & 0 & 0 & 0 \\ b_{31} & b_{32} & b_{33} & 0 & 0 \\ b_{41} & b_{42} & b_{43} & b_{44} & 0 \\ b_{51} & b_{52} & b_{53} & b_{54} & b_{55} \end{pmatrix} \begin{pmatrix} e_t^{IP} \\ e_t^{CPI} \\ e_t^{PCOM} \\ e_t^{FFRS} \\ e_t^{Gini} \end{pmatrix}$$

Figure C.5: Impulse Response Functions and Surfaces to YM Shocks with $m = 2$

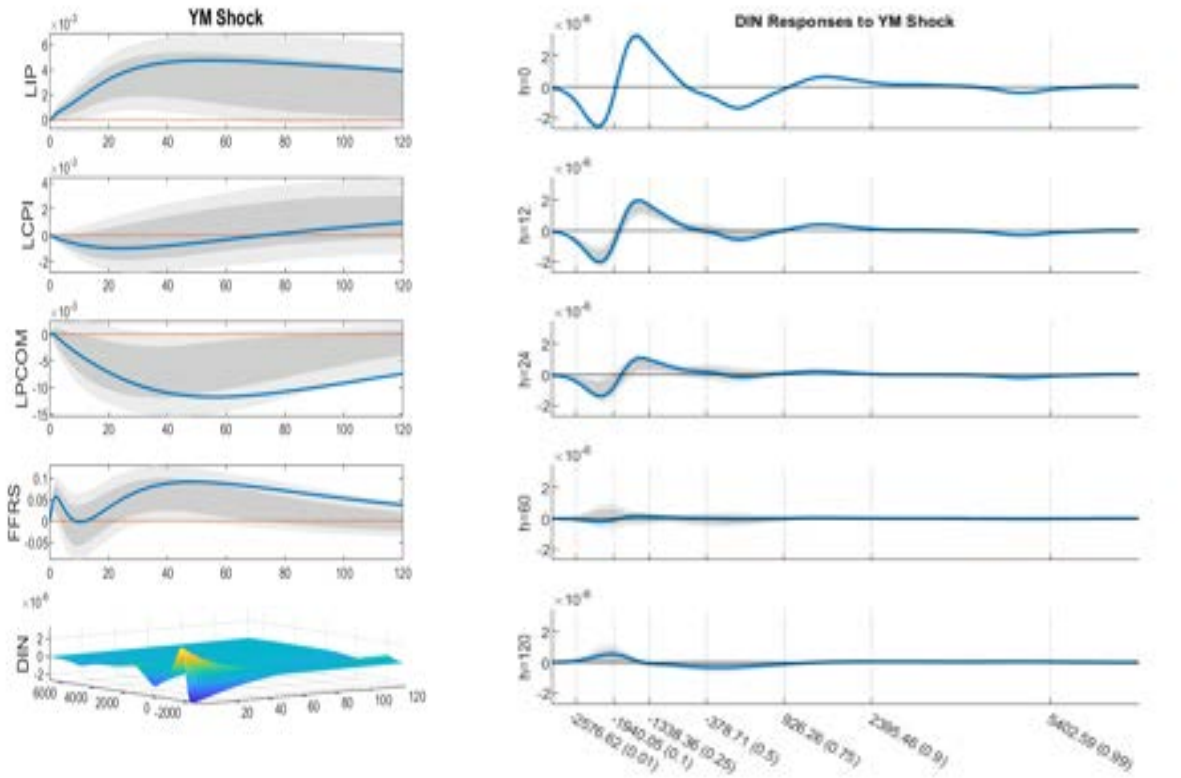

Notes: On the left are IRFs of the aggregate variables and impulse response surface of the income distribution to output maximizing YM shocks. On the right, the functional impulse responses of the demeaned income distribution - two dimensional slices of the response surface - are shown for the horizons $h = 0, 12, 24, 60$ and 120 months, with the y-axis indicating the response and the x-axis representing quantile values (1%, 10%, 25%, 50%, 75%, 90% and 99%). Shaded bands represent the 68% and 90% confidence intervals.

where we only have a 5×5 at-impact matrix, and (e_t^{Gini}) is a usual scalar structural shock.

We perform the conventional structural VAR analysis using these identifying restrictions to compare our results obtained using an MAR with those from taking the conventional approach. Figure E.1 shows the impulse response functions from the conventional aggregate SVAR with Gini index. As in other models, (e_t^{FFRS}) is identified as monetary policy shocks, and (e_t^{Gini}), as a distributional shock, is identified as orthogonal to aggregate shocks.

Figure E.1 and Figure E.2 show the impulse responses and forecast error variance decomposition obtained from the conventional aggregate SVAR model with Gini index. The impulse responses show that the effects of monetary policy shocks on Gini index is qualitatively similar to those in reported in our baseline mixed autoregressive model reported in Figure 8. However, the results of the baseline MAR model are more significant than those of the current model.

Figure C.6: IRFs of Gini Index to YM Shock with $m = 2$

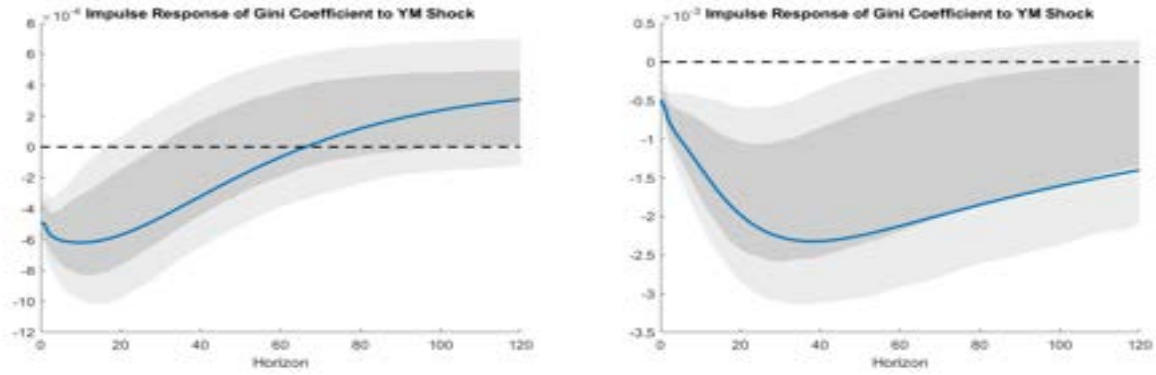

Notes: Presented are the impulse response functions of the Gini index to YM shocks computed from the income distribution over a 10-year horizon, *without* the mean shift (left) and *with* the mean shift (right). Shaded bands represent the 68% and 90% confidence intervals.

Figure C.7: **Variance Decomposition from MAR with YM Shock with** $m = 2$

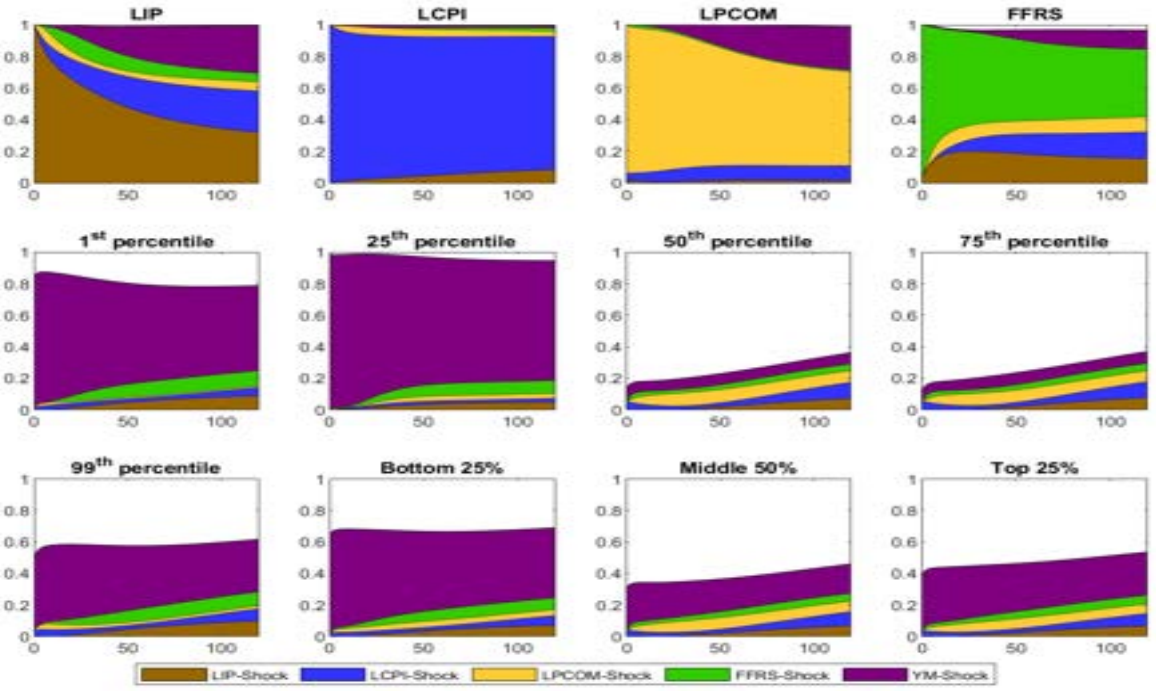

Notes: Presented are the forecast error variance decomposition (FEVD) of the variables in the MAR model attributable to four aggregate shocks and one distributional YM shock. Each shock's contribution is color-coded, with the color codes provided in the legend box at the bottom of the figure. The four panels in the first row show the FEVDs for four aggregate variables. The four panels in the second row and the first panel in the third row present the FEVDs for the proportions of the population at income levels around the 1st, 25th, 50th, 75th, and 99th percentiles of the most recent income distribution, December 2015. The remaining three panels in the third row present the FEVDs for the bottom 25%, middle 50%, and top 25% income groups, defined using the historical average income distribution.

Figure C.8: Impulse Response Functions and Surfaces to GM Shocks with $m = 2$

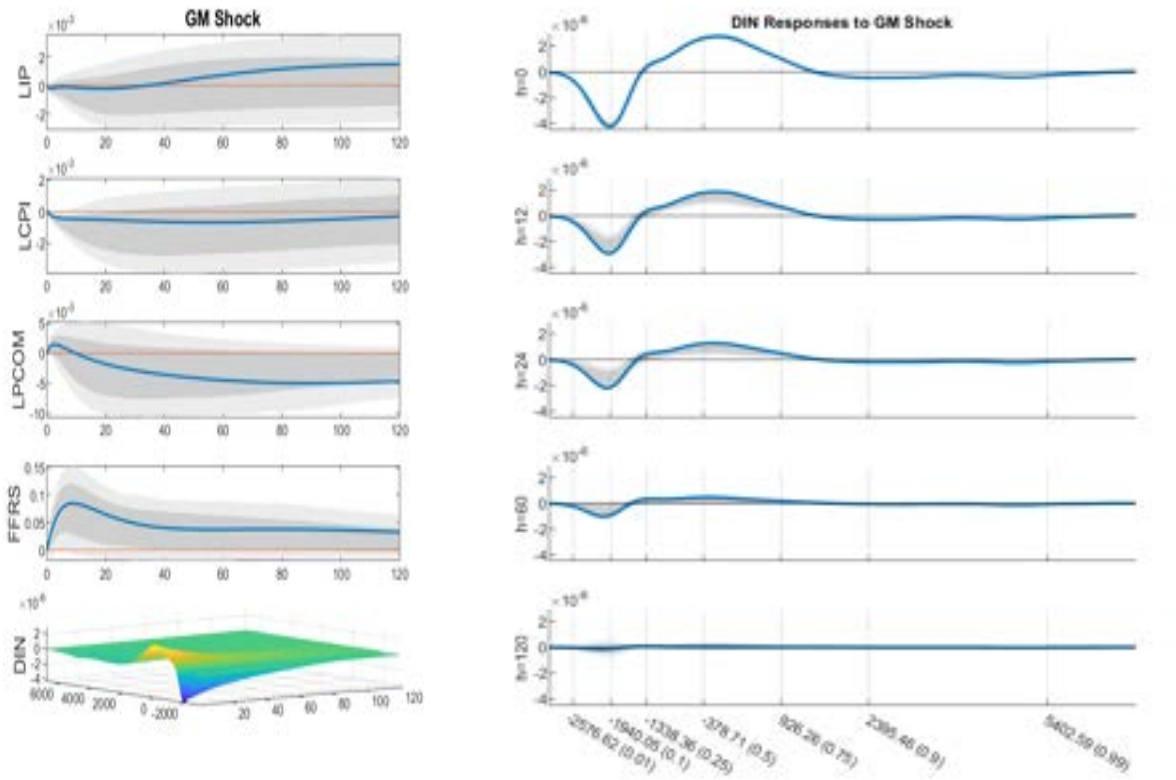

Notes: On the left are IRFs of the aggregate variables and impulse response surface of the income distribution to inequality minimizing GM shocks. On the right, the functional impulse responses of the demeaned income distribution - two dimensional slices of the response surface - are shown for the horizons $h = 0, 12, 24, 60$ and 120 months, with the y-axis indicating the response and the x-axis representing quantile values (1%, 10%, 25%, 50%, 75%, 90% and 99%). Shaded bands represent the 68% and 90% confidence intervals.

Figure C.9: IRFs of Gini Index to GM Shock with $m = 2$

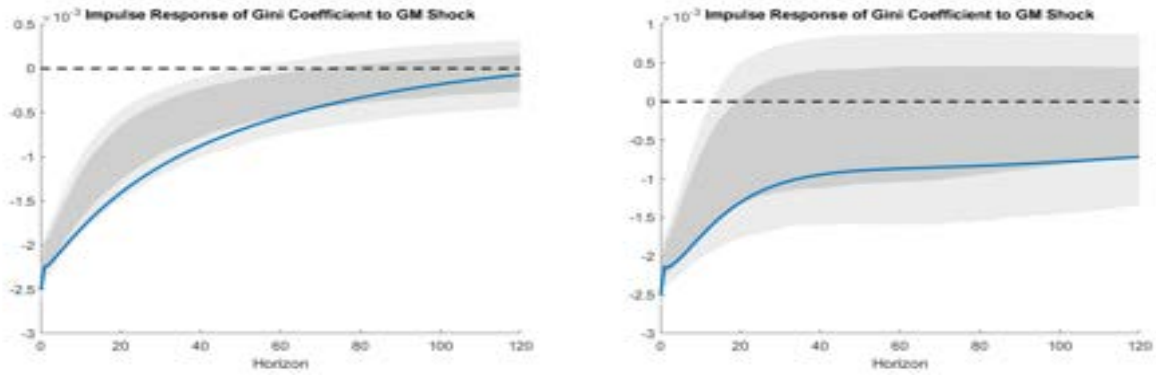

Notes: Presented are the impulse response functions of the Gini index to GM shocks computed from the income distribution over a 10-year horizon, *without* the mean shift (left) and *with* the mean shift (right). Shaded bands represent the 68% and 90% confidence intervals.

Figure C.10: **Variance Decomposition from MAR with GM Shock with** $m = 2$

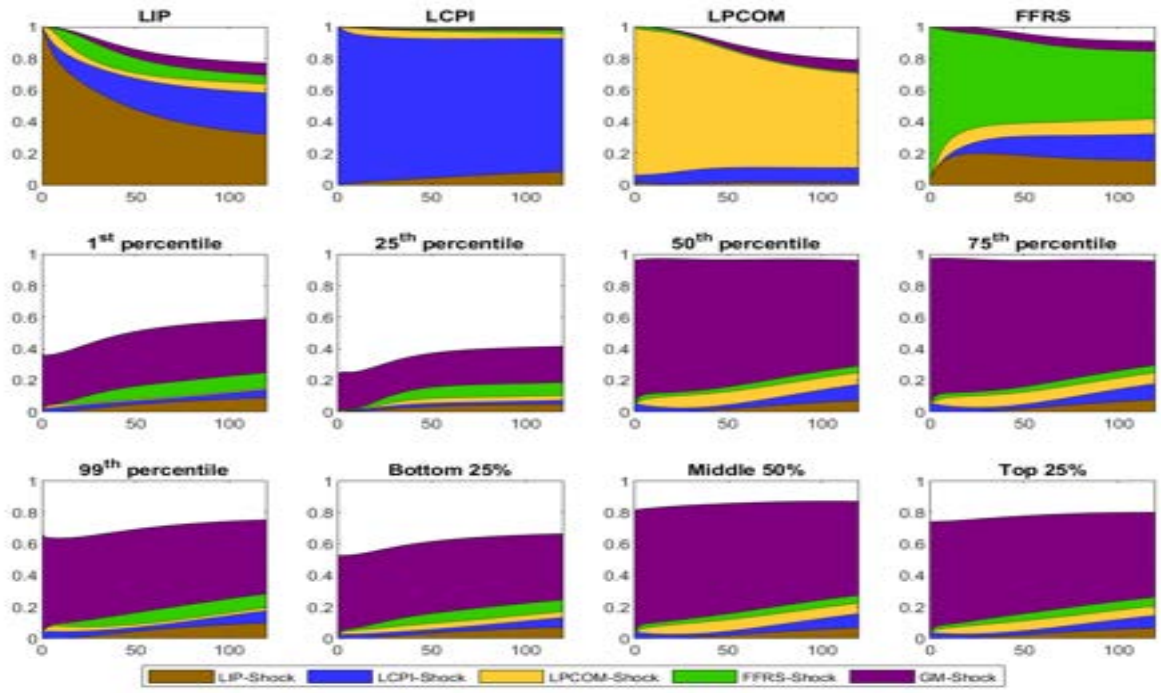

Notes: Presented are the forecast error variance decomposition (FEVD) of the variables in the MAR model attributable to four aggregate shocks and one distributional GM shock. Each shock's contribution is color-coded, with the color codes provided in the legend box at the bottom of the figure. The four panels in the first row show the FEVDs for four aggregate variables. The four panels in the second row and the first panel in the third row present the FEVDs for the proportions of the population at income levels around the 1st, 25th, 50th, 75th, and 99th percentiles of the most recent income distribution, December 2015. The remaining three panels in the third row present the FEVDs for the bottom 25%, middle 50%, and top 25% income groups, defined using the historical average income distribution.

Figure C.11: Impulse Response Functions and Surfaces to Contractionary Monetary Policy Shocks with $m = 4$

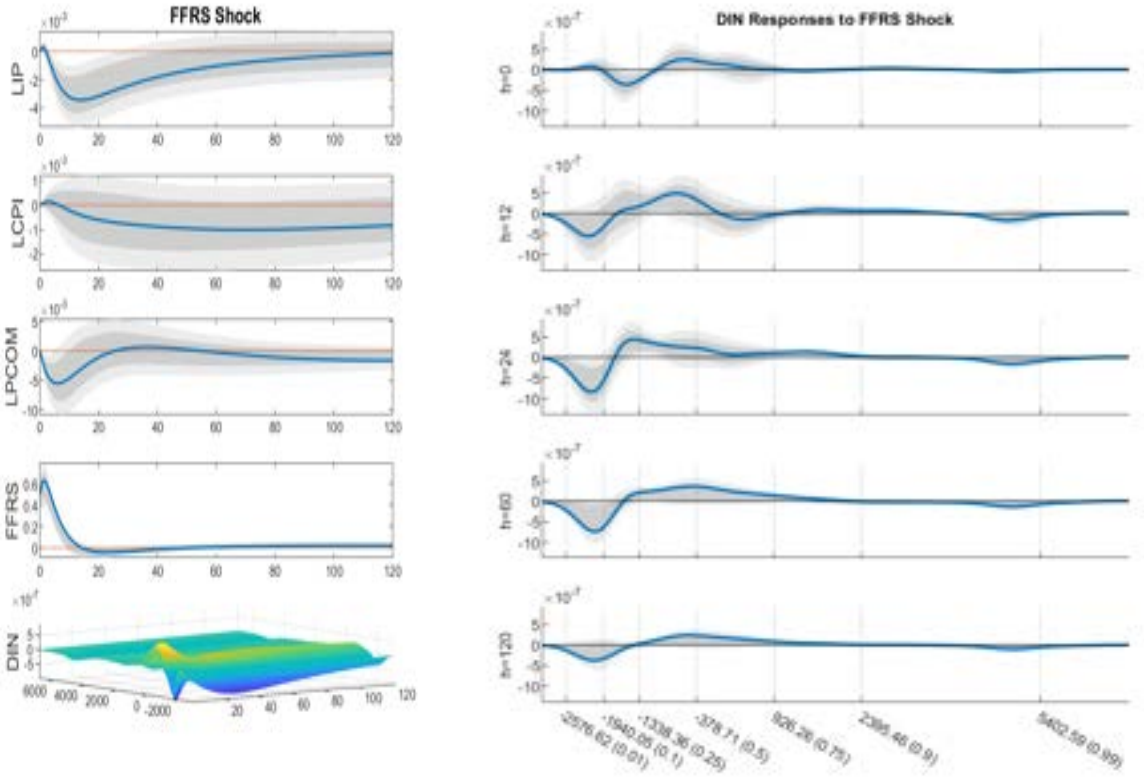

Notes: On the left are IRFs of the aggregate variables and impulse response surface of the income distribution to contractionary monetary policy shocks. On the right, the functional impulse responses of the demeaned income distribution - two dimensional slices of the response surface - are shown for the horizons $h = 0, 12, 24, 60$ and 120 months, with the y-axis indicating the response and the x-axis representing quantile values (1%, 10%, 25%, 50%, 75%, 90% and 99%). Shaded bands represent the 68% and 90% confidence intervals.

Figure C.12: Distributional Effects of Contractionary Monetary Policy Shocks with $m = 4$

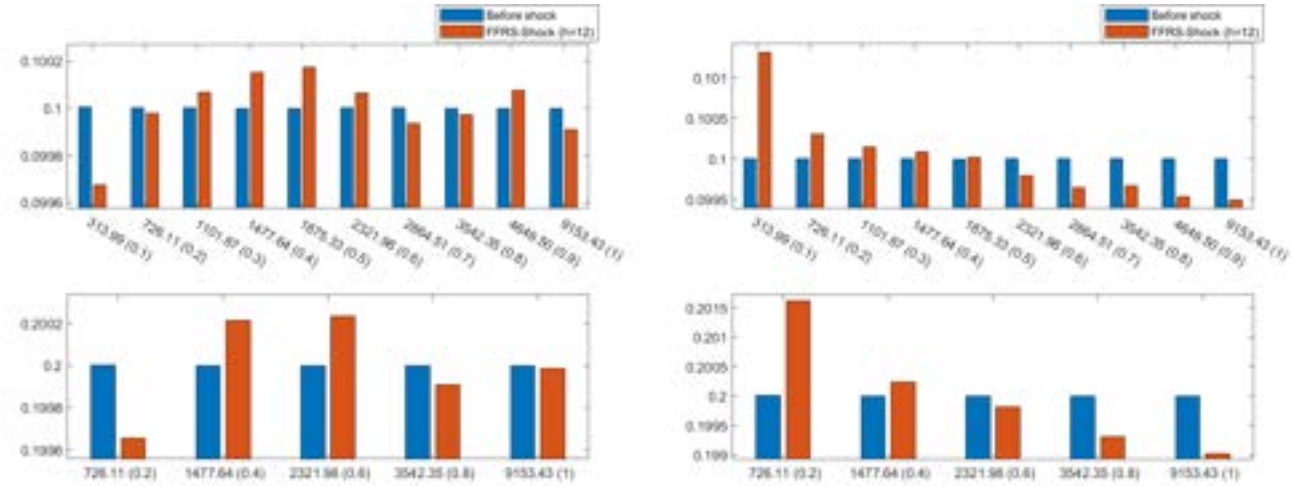

Notes: Presented are the DIN responses to contractionary monetary policy shocks one year after the impact in histograms. The top (bottom) panel on the left shows how the income distribution changes *without* the mean shift for decile (quintile) income groups. Similarly, the top (bottom) panel on the right shows those obtained *with* the mean shift for decile (quintile) income groups.

Figure C.13: IRFs of Gini Index to Contractionary Monetary Policy Shocks with $m = 4$

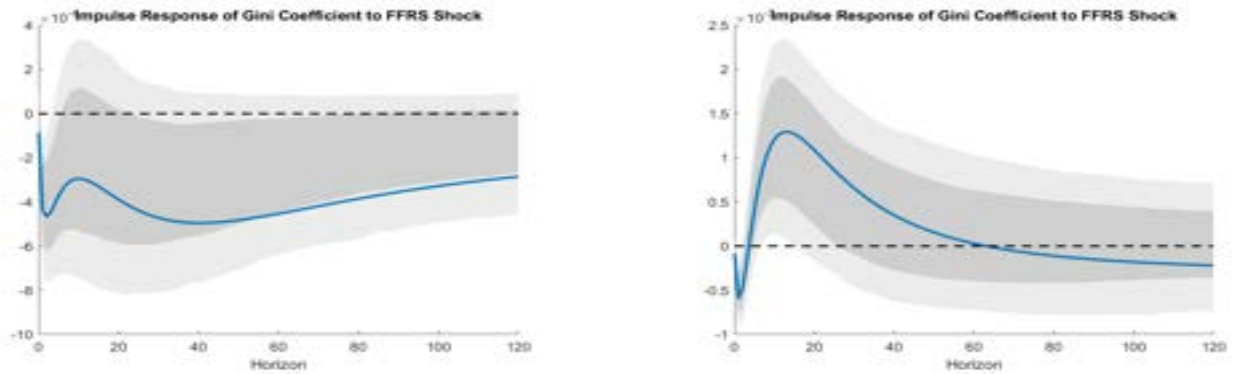

Notes: Presented are the impulse response functions of the Gini index computed from the income distribution over a 10-year horizon, *without* the mean shift (left) and *with* the mean shift (right). Shaded bands represent the 68% and 90% confidence intervals.

Figure C.14: **Variance Decomposition from MAR with DIN Shock with** $m = 4$

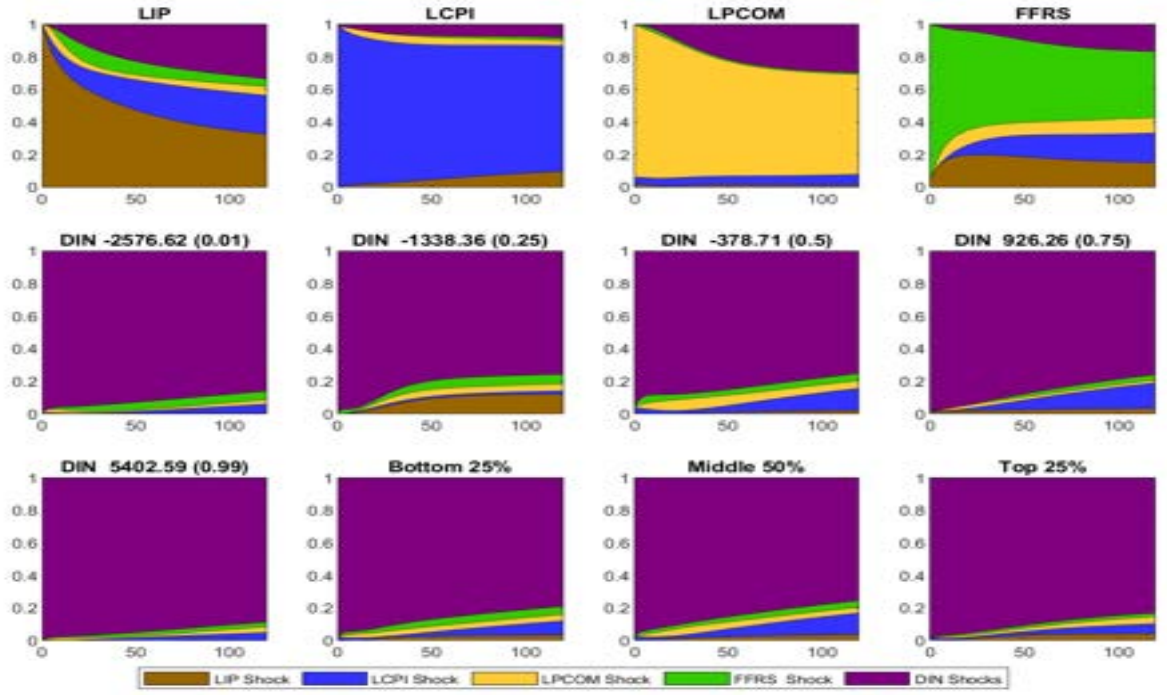

Notes: Presented are the forecast error variance decomposition (FEVD) of the variables in the MAR model attributable to four aggregate shocks and one income distribution shock. Each shock's contribution is color-coded, with the color codes provided in the legend box at the bottom of the figure. The four panels in the first row show the FEVDs for four aggregate variables. The four panels in the second row and the first panel in the third row present the FEVDs for the proportions of the population at income levels around the 1st, 25th, 50th, 75th, and 99th percentiles of the most recent income distribution, December 2015. The remaining three panels in the third row present the FEVDs for the bottom 25%, middle 50%, and top 25% income groups, defined using the historical average income distribution.

Figure C.15: Impulse Response Functions and Surfaces to YM Shocks with $m = 4$

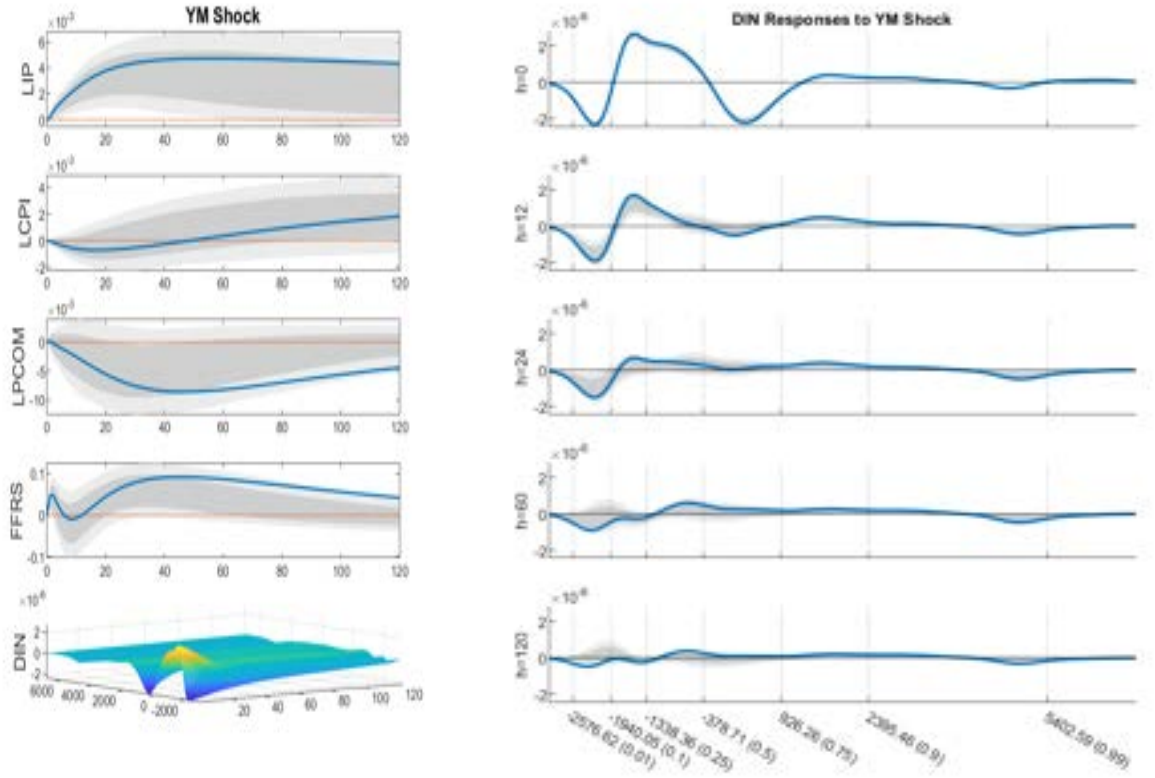

Notes: On the left are IRFs of the aggregate variables and impulse response surface of the income distribution to output maximizing YM shocks. On the right, the functional impulse responses of the demeaned income distribution - two dimensional slices of the response surface - are shown for the horizons $h = 0, 12, 24, 60$ and 120 months, with the y-axis indicating the response and the x-axis representing quantile values (1%, 10%, 25%, 50%, 75%, 90% and 99%). Shaded bands represent the 68% and 90% confidence intervals.

Figure C.16: IRFs of Gini Index to YM Shock with $m = 4$

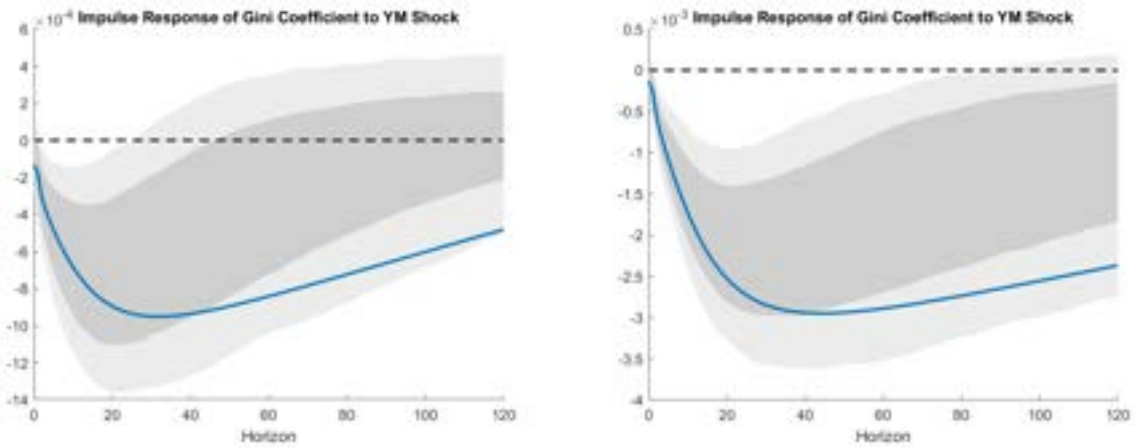

Notes: IRFs of the Gini index to YM shock *without* the mean shift (on the left) and *with* the mean shift (on the right). Shaded bands represent the 68% and 90% confidence intervals.

Figure C.17: **Variance Decomposition from MAR with YM Shock with** $m = 4$

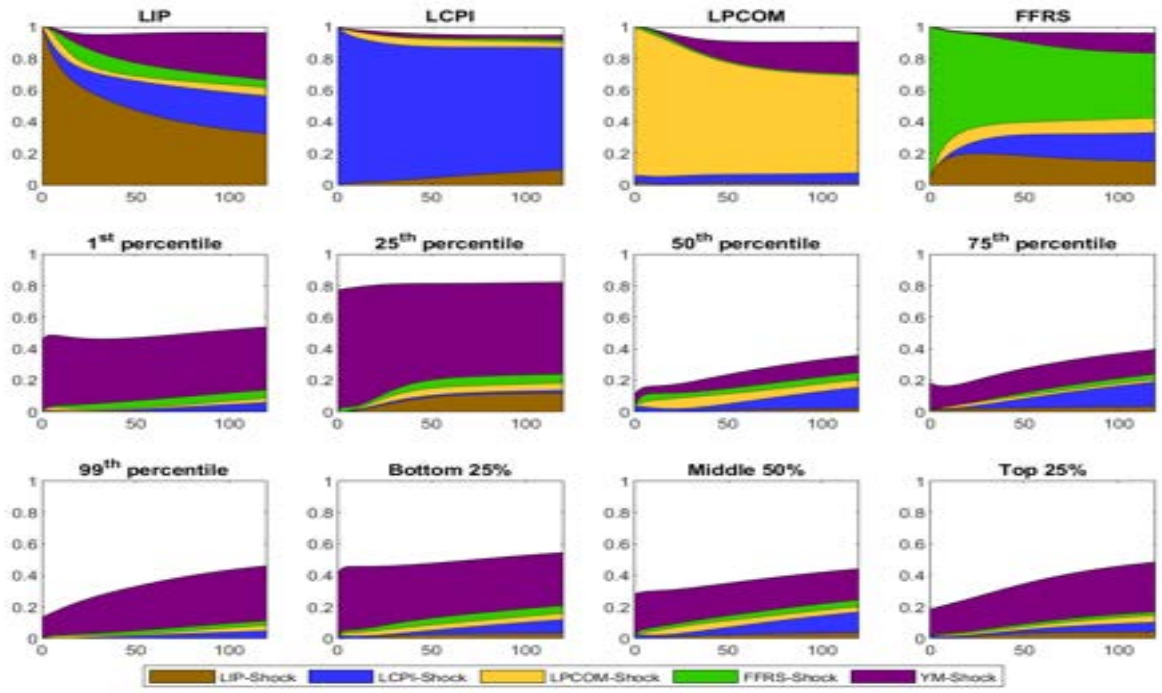

Notes: Presented are the forecast error variance decomposition (FEVD) of the variables in the MAR model attributable to four aggregate shocks and one distributional YM shock. Each shock's contribution is color-coded, with the color codes provided in the legend box at the bottom of the figure. The four panels in the first row show the FEVDs for four aggregate variables. The four panels in the second row and the first panel in the third row present the FEVDs for the proportions of the population at income levels around the 1st, 25th, 50th, 75th, and 99th percentiles of the most recent income distribution, December 2015. The remaining three panels in the third row present the FEVDs for the bottom 25%, middle 50%, and top 25% income groups, defined using the historical average income distribution.

Figure C.18: Impulse Response Functions and Surfaces to GM Shocks with $m = 4$

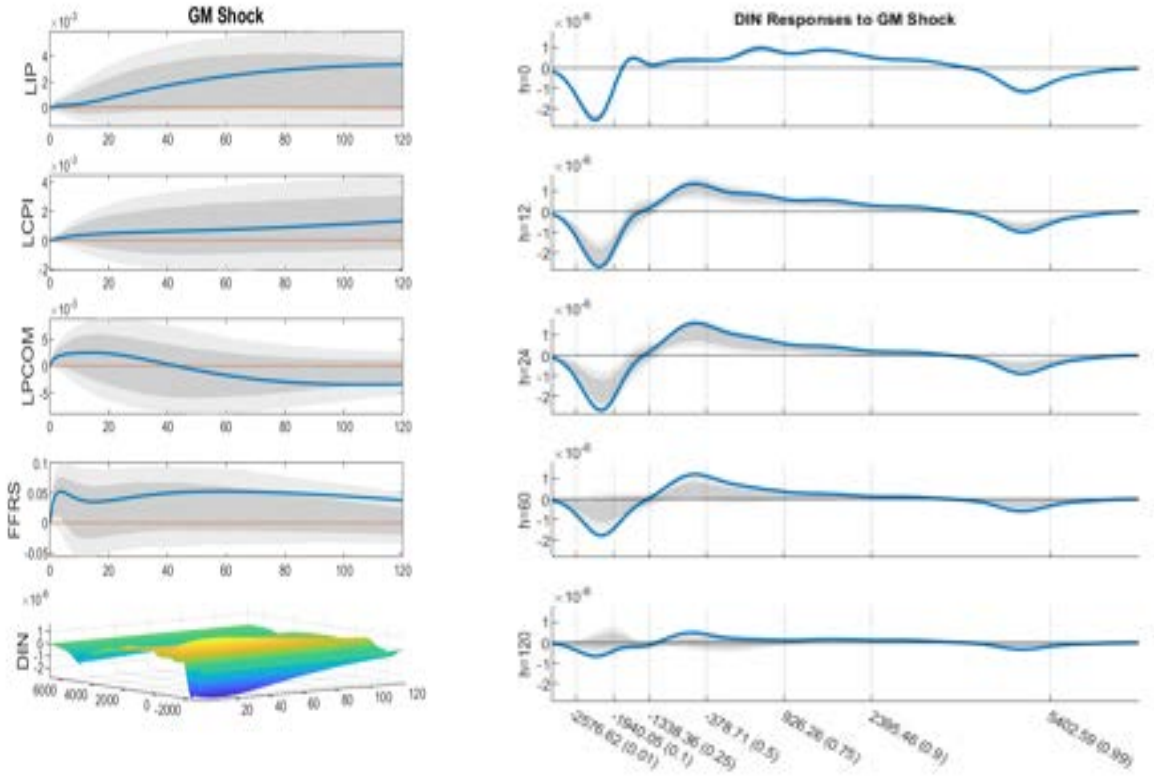

Notes: On the left are IRFs of the aggregate variables and impulse response surface of the income distribution to inequality minimizing GM shocks. On the right, the functional impulse responses of the demeaned income distribution - two dimensional slices of the response surface - are shown for the horizons $h = 0, 12, 24, 60$ and 120 months, with the y-axis indicating the response and the x-axis representing quantile values (1%, 10%, 25%, 50%, 75%, 90% and 99%). Shaded bands represent the 68% and 90% confidence intervals.

Figure C.19: IRFs of Gini Index to GM Shock with $m = 4$

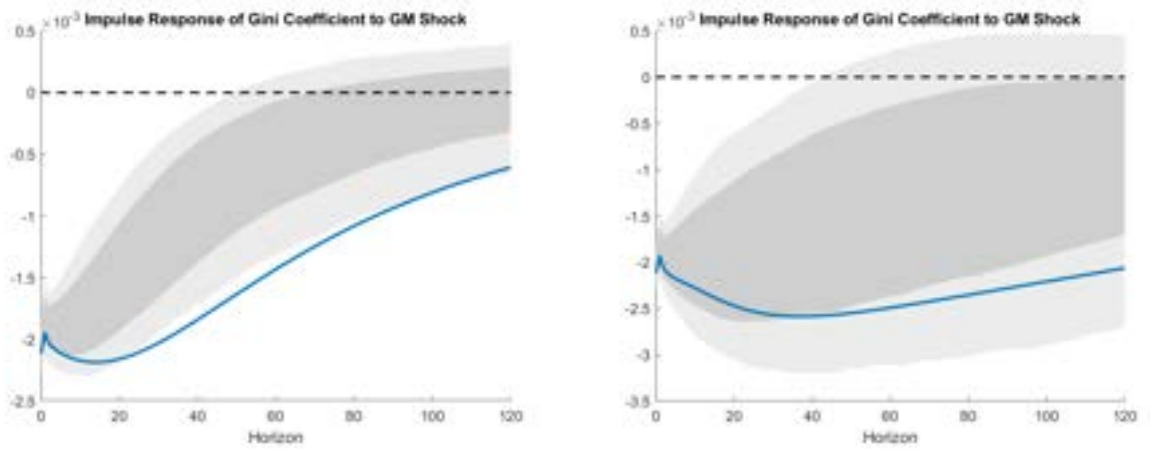

Notes: IRFs of the Gini index to GM shock *without* the mean shift (on the left) and *with* the mean shift (on the right). Shaded bands represent the 68% and 90% confidence intervals.

Figure C.20: **Variance Decomposition from MAR with GM Shock with** $m = 4$

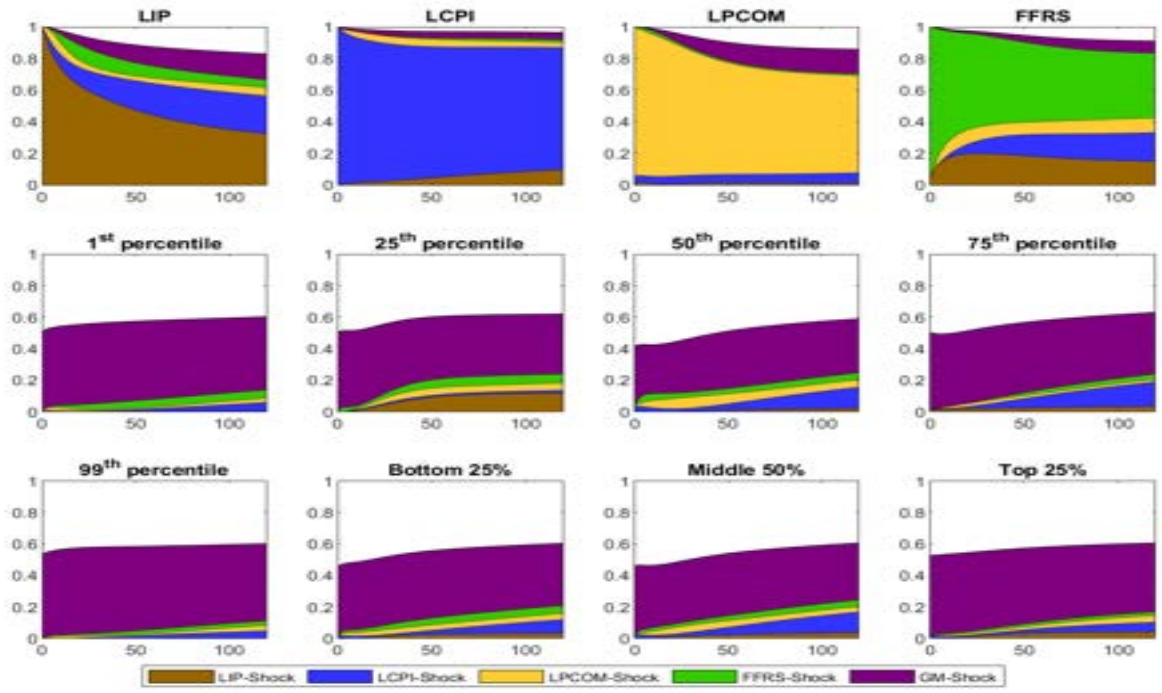

Notes: Presented are the forecast error variance decomposition (FEVD) of the variables in the MAR model attributable to four aggregate shocks and one distributional GM shock. Each shock's contribution is color-coded, with the color codes provided in the legend box at the bottom of the figure. The four panels in the first row show the FEVDs for four aggregate variables. The four panels in the second row and the first panel in the third row present the FEVDs for the proportions of the population at income levels around the 1st, 25th, 50th, 75th, and 99th percentiles of the most recent income distribution, December 2015. The remaining three panels in the third row present the FEVDs for the bottom 25%, middle 50%, and top 25% income groups, defined using the historical average income distribution.

Figure E.1: **Impulse Response Functions from SVAR with Gini Index**

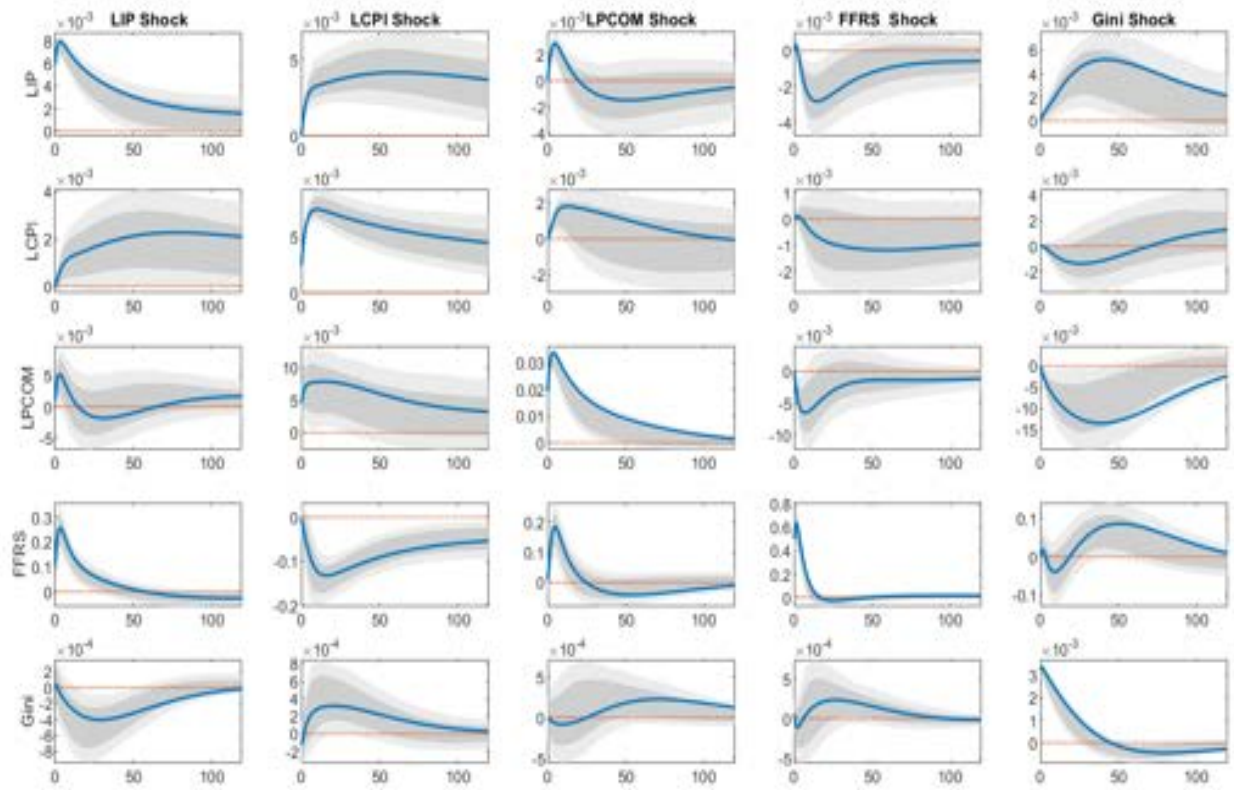

Notes: Presented are full set of impulse response functions from the conventional SVAR model with four aggregate variables in our benchmark model, namely, $IP, CPI, PCOM, FFRS$, and Gini index. Shaded bands represent the 68% and 90% confidence intervals.

Figure E.2: **Variance Decomposition from SVAR with Gini Index**

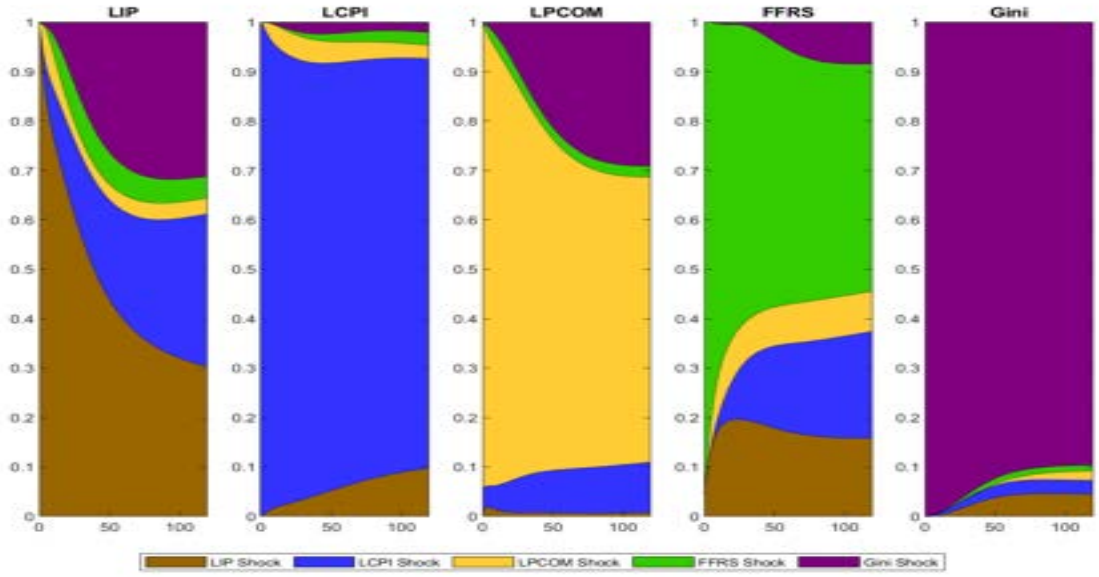

Notes: Each column presents the forecast error variance decomposition of the variables in the conventional aggregate SVAR model, including the Gini index as well as the four aggregate variables in the benchmark model, $IP, CPI, PCOM, FFRS$. Shaded bands represent the 68% and 90% confidence intervals.